Biological conversion of methane and carbon dioxide into methanol using *Methylosinus trichosporium* NCIMB 11131

A Thesis

submitted for the degree of

Doctor of Philosophy

by

Krishna Kalyani Sahoo

(Roll No.: 186106110)

Under the supervision of

Prof. Debasish Das

May 2024

Department of Biosciences & Bioengineering

Indian Institute of Technology Guwahati

Guwahati 781039, Assam, India

INDIAN INSTITUTE OF TECHNOLOGY GUWAHATI

Department of Biosciences and Bioengineering

STATEMENT

I do hereby declare that the content embodied in this thesis is the result of investigations carried out by me in the **Department of Biosciences and Bioengineering, Indian Institute of Technology Guwahati**, Guwahati, Assam, India under the supervision of **Prof. Debasish Das**. In keeping with the general practice of reporting scientific observations, due acknowledgements have been made wherever the work described is based on the findings of other investigators.

Krishna Kalyani Sahoo

May 2024 **Krishna Kalyani Sahoo**

INDIAN INSTITUTE OF TECHNOLOGY GUWAHATI

Department of Biosciences and Bioengineering

CERTIFICATE

It is certified that the work described in this thesis entitled "**Biological conversion of methane and carbon dioxide into methanol using *Methylosinus trichosporium* NCIMB 11131**" by **Ms. Krishna Kalyani Sahoo** for the award of degree of **Doctor of Philosophy** is an authentic record of the results obtained from the research work carried out under my supervision in the **Department of Biosciences and Bioengineering, Indian Institute of Technology Guwahati**, Guwahati, Assam, India. The work embodied in this thesis has not been submitted elsewhere for a degree.

Debasish Das

Prof. Debasish Das
(Thesis Supervisor)
Department of Biosciences & Bioengineering
Indian Institute of Technology Guwahati
Guwahati 781039, Assam, India

Acknowledgements

I deeply express my heartiest gratitude to my thesis supervisor, ***Prof. Debasish Das****, Department of Biosciences and Bioengineering, IIT Guwahati, for providing me the opportunity to be a part of* ***Bioprocess Development Laboratory*** *and pursue this research work. I must acknowledge the freedom of thinking, planning, execution and expression which was given by him in every step of my research work, while keeping faith and confidence in my capabilities. His valued lessons in matters of science and most importantly life, will prove to be helpful in my future endeavours as well.*

I am also highly obliged to my doctoral committee members, ***Prof. S. Senthilkumar****,* ***Dr. Selvaraju Narayanasamy*** *and* ***Prof. Vaibhav V. Goud*** *for their careful evaluation, unbiased opinions and constructive suggestions, which have helped me to improve my work pertaining to Ph.D. Thesis.*

I owe my thanks to the ***Department of Biosciences and Bioengineering****,* ***School of Energy Science and Engineering****, and* ***Department of Chemical Engineering****,* ***IIT Guwahati*** *for providing the necessary research facilities to accomplish my Ph.D. thesis objectives. I would also like to particularly acknowledge* ***Department of Mechanical Engineering****,* ***IIT Guwahati*** *for providing technical expertise and support related to engine testing experiments. I am thankful to* ***Ministry of Education, Government of India*** *for the financial assistance provided throughout the course of my Ph.D. work.*

I am immensely grateful to my lab alumni-cum-seniors, ***Dr. Mayurketan Mukherjee****,* ***Dr. Bidhu Bhusan Makut, Dr. Payel Sarkar, Dr. Dineshbabu Gnanasekaran, Dr. Gargi Goswami, Dr. Chandan Mukherjee, Dr. Ankan Sinha*** *and* ***Dr. Ratan Kumar*** *for their valuable feedback, guidance and support whenever needed. Moreover, it was my pleasure*

working with ***Pavan, Boudhnath, Rashid, Gobindo, Kumar Sarvesh***, ***Sarvesh Singh*** *and* ***Sagar***. *A special thanks to* ***Swagata*** *for temporarily assisting me with my research work.*

I would like to extend sincere thanks to my current labmates, ***Mr. Noor Mohammed, Ms. Anupriya*** *and* ***Mr. Ujjal,*** *who have made this journey worthwhile. I firmly express my gratefulness to my senior-cum-friend* ***Mr. John Kiran Katari*** *for his constant motivation and immeasurable support without which this journey would have been incomplete. Overall,* ***Bioprocess Development Laboratory*** *will always remain close to my heart, and each of the moments I have spent herein are going to be cherished forever.*

My heartfelt credit further goes to my best friends, ***Rumela*** *and* ***Sampriti****, who have been the pillars of enormous strength throughout these years. No wonder, you two have always cheered me up and made my life eventful at IIT Guwahati. I am also thankful to* ***Shaona, Meenakshi*** *and* ***Chitra*** *for their companionship.*

I am highly indebted to my beloved parents, ***Mr. Chaitanya Sahoo*** *and* ***Mrs. Pravati Sahoo*** *for their blessings, encouragement, understanding and unconditional love throughout my life. I thank my dearest sister* ***Soumyashree*** *for always being there to calm and comfort me during my tough moments. Finally, I humbly thank the* ***Almighty God*** *who made everything possible.*

Krishna Kalyani Sahoo

May 2024 **Krishna Kalyani Sahoo**

ABSTRACT

The emission of greenhouse gases, such as methane and carbon dioxide, has been increasing globally at an alarming rate. Conventional chemical methods to transform methane and carbon dioxide into useful chemicals are plagued by the requirement for expensive catalysts and extreme operating conditions. The exploitation of microorganisms as biocatalysts is an attractive alternative to sequester these greenhouse gases and convert them into value-added chemicals or liquid fuels through their inherent metabolic pathways. Microbial biocatalysts are advantageous over chemical processes as they require mild-operating conditions and do not release any toxic by-products. From a contextual perspective, methanotrophs, a class of Gram-negative, methane oxidizing bacteria, are being explored as novel platform to produce methanol – a potential fuel. Methanotrophs uptake methane as an obligate source for the derivation of carbon and energy. Besides, methanotrophs are capable of capturing carbon dioxide and enzymatically reducing it into methanol under specific conditions. However, the state-of-the-art technology of methanotrophic methanol production is primarily constrained by: (i) low titer of methanotrophic biomass and methanol owing to (ii) limited mass transfer and solubility of methane and CO_2 in liquid medium. Current rising energy demand and rapid depletion of non-renewable fossil fuel reserves have shifted the research focus towards exploring non-petroleum based cleaner and renewable alternate transportation fuels. To that end, oxygenated fuels (or alcohols) such as methanol, are advantageous in terms of improving the combustion, emission and performance characteristics of engine. However, a major concern is the dependency of alternative fuel technology on chemical methods for methanol synthesis which are energy-intensive, as well as economically and environmentally non-sustainable. The present study was designed to address the existing

challenges and gaps through the development of a sustainable bioprocess for methanol production.

The present study demonstrates a two-stage integrated process for bio-methanol production using *Methylosinus trichosporium* NCIMB 11131, coupled with the sequestration of methane and carbon dioxide. The first stage involved generation of methanotrophic biomass via sequestration of methane, which was utilized as biocatalyst in the second stage to reduce CO_2 into methanol. At the onset of the study, the organism was characterized under various physicochemical parameters, to identify the optimum conditions for obtaining high biomass titer, biomass productivity, methane fixation rate and methanol titer. Maximum biomass titer of 4.45 g L^{-1} and productivity of 0.872 g L^{-1} d^{-1} were achieved in a semi-batch stirred tank reactor, with methane concentration in the inlet gas mixture of 2.5% v/v, gas flow rate of 0.5 vvm, in optimized medium containing 0.75X unit concentration of trace metals, in the first stage. The corresponding methane fixation rate was estimated to be 0.476 g L^{-1} d^{-1}. Maximum methanol titer of 0.58 g L^{-1} was achieved at headspace carbon dioxide concentration of 50% v/v and liquid to headspace volume ratio 10:90 in an air-tight batch reactor in the second stage.

Furthermore, process engineering strategies were developed to address the key challenges associated with inferior mass transfer rates and limited solubility of methane and CO_2 in liquid media leading to lower titers of biomass and methanol. In the first stage, combinatorial process engineering approach of design of micro-sparger, engagement of draft tube and addition of mass transfer vector was employed to enhance production of biomass. Maximum biomass titer of 7.68 g L^{-1} and productivity of 1.459 g L^{-1} d^{-1} were achieved in an airlift reactor equipped with a micro-sparger of 5 µm pore size, in the presence of draft tube and 10% v/v silicone oil as mass transfer vector. Maximum methane fixation rate was estimated to be 0.795 g L^{-1} d^{-1}. Process engineering strategy for the second stage involved customization

of a high-pressure stirred tank reactor to enhance the solubility of CO_2 under elevated operating pressure for consequent increase in methanol titer. Maximum methanol titer of 1.98 g L^{-1} was achieved under headspace pressure of 4 bar, which was an increment of 235.6% relative to atmospheric pressure. Subsequently, methanol production was demonstrated through recycling of *Methylosinus trichosporium* biomass to curtail time and resources incurred towards recurrent biomass generation. Following three cycles of biomass reutilization, a maximum cumulative methanol titer of 3.6 g L^{-1} was achieved, a value significantly higher than other studies reported in literature. Methanol was recovered from cultivation medium using distillation attaining a maximum purity of 94.74%.

Eventually, different blends of methanol (0-20% v/v) with diesel were evaluated for their suitability as alternate transportation fuel. Physicochemical properties of diesel-methanol blends either improved or exhibited equivalence relative to pure diesel, as control. The blends were investigated for their effect on emission and performance characteristics of four-stroke internal combustion engine under varying engine loads (25, 50, 75 and 100%). Emissions of carbon monoxide, hydrocarbon and SO_x, and opacity of smoke decreased with increasing methanol content in the blend, attaining maximum decrements of 38.8-48.4%, 39.8-61.6%, 79.6-91.0%, and 21.0-27.5%, respectively, with 20% methanol-containing blend (M20) under varying load conditions. Superior performance parameters *e.g.*, brake specific fuel consumption (0.29 kg kW^{-1} h^{-1}) and brake thermal efficiency (28%) were achieved using M20, while brake power and mechanical efficiency exhibited equivalence with pure diesel. To the best knowledge of the author, this is the first study unveiling the potential of methanotroph-derived bio-methanol as a renewable alternative transportation fuel.

Contents

List of Figures

List of Tables

CHAPTER 1

Introduction

1.1. Background and motivation

There has been a tremendous increase in the emission of greenhouse gases from various anthropogenic sources; the global energy sector being the primary contributor, is responsible for the release of 36.8 billion tonnes of carbon dioxide and 135 million tonnes of methane into the atmosphere (International Energy Agency, 2023; Global Methane Tracker, 2023). There are ongoing efforts to transform these greenhouse gases into various value-added chemicals and liquid fuels, *e.g.*, methanol. Methanol is a widely used industrial solvent, and a precursor for synthesis of other chemicals, such as formaldehyde, acetic acid, dimethyl ether and methyl tert-butyl ether (Dalena et al., 2018). Further, methanol is being regarded as a potential alternative to petroleum-based fuels attributed to high oxygen content which causes clean combustion, and reduced soot and smoke emissions (Verhelst et al., 2019). Conventional chemical methods for methanol production including catalyst-driven hydrogenation of CO_2, oxidation of methane, or thermal gasification of agricultural biomass, are limited by requirement for expensive catalysts (*e.g.,* $CuO/ZnO/Al_2O_3$, MoO_3/SiO_2, MoO_3/Ga_2O_3, V_2O_5/SiO_2, NiO and FeO_x/ZrO_2), high temperature (~850 °C) and pressure (~100 bar), and generation of carbon monoxide as byproduct (Ali et al., 2020; Keller and Sharma, 2022; Sahoo et al., 2022; Li et al., 2023).

Alternatively, biological methods are being explored to produce methanol from methane and CO_2, utilizing methanotrophic microorganisms as biocatalyst. Microbial biocatalyst-based processes are advantageous over chemical methods as they require milder operating conditions and do not release any toxic by-products (Sahoo et al., 2021).

Methanotrophs are Gram-negative proteobacteria which utilize methane as the sole source of carbon and energy for growth (Fei et al., 2014). Methane utilized by methanotrophs is further oxidised into methanol, formaldehyde, formic acid and CO_2, through sequential catalysis by intracellular enzymes namely, methane monooxygenase (MMO), methanol dehydrogenase (MDH), formaldehyde dehydrogenase and formate dehydroagenase, respectively (Xin et al., 2007). Except MMO, the set of other three dehydrogenase enzymes are reversible in nature. A fraction of the intermediately produced formaldehyde or formate gets assimilated into the biomass as carbon source through RuMP (ribulose monophosphate) or serine pathway (Park and Kim, 2019). Although, methanol can directly be produced through MMO-catalysed methanotrophic methane oxidation, the method is limited by requirement for MDH inhibitors (to prevent further oxidation of methanol) and formate as a source of reducing equivalent, NADH (necessary for the activity of MMO in presence of MDH inhibitors), which increase the overall cost of production (Xin et al., 2004). Alternatively, methanol can be produced through methanotrophic reduction of CO_2. CO_2 being the end-product in the methanotrophic metabolism, when fed to the cells in excess concentration, drive the equilibrium in reverse direction (Xin et al., 2004, 2007). The reduction reaction is catalysed by endogenous formate dehydrogenase, formaldehyde dehydrogenase and methanol dehydrogenase enzymes. Since the activity of MMO is irreversible, the process results in the accumulation of methanol as an extracellular end-product (Xin et al., 2007). Different metabolic pathways adopted by methanotrophs for methanol production will be discussed in detail in Chapter 2.

Researchers have relied on concomitant application of multiple process engineering approaches such as, co-cultivation, cell immobilization, methane vector supplementation and repeated-batch cultivation to improve methanol production (Patel et al., 2020, 2023). Despite these attempts, the maximum methanol titer achieved using pure methane or methane-containing mixed feed (*e.g.*, biogas) is limited to 70.74 mM (2.27 g L^{-1}) (Patel et al., 2020,

2022); while from that of pure CO_2 it is confined to a value of 0.52 mM (0.017 g L^{-1}) (Xin et al., 2007; Patel et al., 2018). Lower mass transfer and limited solubility of methane and CO_2 in methanotrophic gas fermentation present a major bottleneck, exerting limiting impact on the titers and productivities of biomass and methanol (Sahoo et al., 2023). Reactor configuration is a fundamental aspect of any fermentation process design, which to a greater extent can regulate the mass transfer phenomena inside the cultivation system. For instance, airlift reactors are considered to be advantageous over other cultivation systems attributed to better mixing and mass transfer, greater liquid recirculation and gas hold-up (Doran, 1995). Reactor design aspects, especially from the point of view of design of sparger and configuration of draft tube hold significant importance in defining the reactor performance characteristics. Moreover, mass transfer vectors, a class of organic solvents are reported to enhance the solubility of gaseous substances in the liquid medium (Han et al., 2009). Furthermore, elevated operating pressure has been reported to be a suitable strategy towards enhancing the solubility of gaseous substrates in various microbial gas fermentation systems (Van Hecke et al., 2019). To that end, development of process engineering strategies from the perspective of suitable reactor configuration and design, supplementation of exogenous mass transfer vectors, and elevation of operating pressure, possess potential scope towards combating the hurdles associated with limited mass transfer and solubility.

Rising energy demand, rapid depletion of non-renewable fossil fuel reserves, surging fuel prices, and environmental pollution, have driven the research focus towards exploring non-petroleum based cleaner and renewable alternatives. Blending of alcohols with diesel has been reported to improve engine performance, combustion and emission characteristics (Zhang et al., 2022). Furthermore, methanol as a diesel fuel additive is considered to be superior over ethanol and butanol owing to: lower viscosity which facilitates easier injection, spraying and atomization; higher O_2 content (50%) which improves combustion characteristics; and

improved combustion leading to increased thermal efficiency, and reduced emissions of soot, hydrocarbon and CO (Zhang et al., 2022). Although many studies have reported the effect of diesel-methanol blends on the emission and performance characteristics of internal combustion (IC) engine, these are limited to commercially available chemically synthesized methanol (Hasan et al., 2021; Vargün et al., 2022). Given the drawbacks associated with chemical methods of methanol production, it is imperative to explore the potential of bio-methanol, produced through a completely biological methanotroph-based gas fermentation process, as a renewable alternative fuel.

1.2. Objectives of the study

The present study was carried out with the following objectives formulated based upon the current bottlenecks in methanotrophic methanol production:

- **Characterization of *M. trichosporium* NCIMB 11131 for growth and methanol production using methane and CO_2, respectively.**
- **Process engineering strategy for improved methanotrophic biomass production through enhanced mass transfer and solubility of methane.**
- **Process engineering strategy for enhanced methanol production from CO_2 and subsequent recovery using distillation.**
- **Evaluation of methanol as a potential diesel fuel blend for fuelling four-stroke internal combustion engine.**

1.3. Approach of the thesis

The state-of-the-art technology of methanotrophic methanol production is primarily constrained by: (i) low titer of methanotrophic biomass and methanol owing to (ii) limited mass transfer and solubility of methane and CO_2 in liquid medium. Another major concern is the dependency of alternative fuel technology on chemical methods for methanol synthesis which

are energy-intensive, as well as economically and environmentally non-sustainable. The present study was designed to address the existing challenges and gaps in a systematic manner, which will be discussed in-depth in the subsequent thesis chapters.

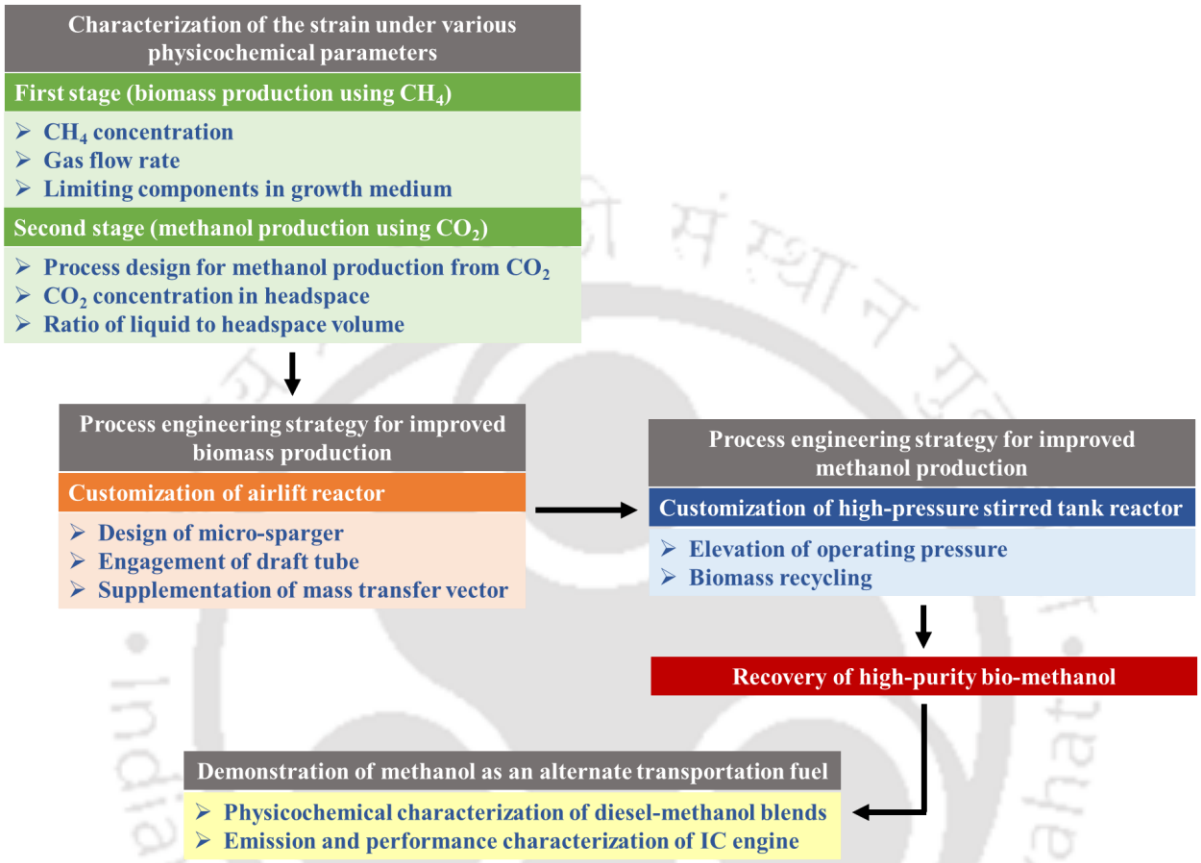

Fig. 1.1. Approach of the thesis towards development of a two-stage integrated process for bio-methanol production.

The present study demonstrates a two-stage integrated process for bio-methanol production using *Methylosinus trichosporium* NCIMB 11131, coupled with the sequestration of methane and carbon dioxide. The first stage involved generation of methanotrophic biomass via sequestration of methane, which was utilized as biocatalyst in the second stage to reduce CO_2 into methanol. At the onset of the study, the organism was characterized under varying methane concentrations, gas flow rates, and composition of other limiting nutrients in the growth medium, to identify the optimum conditions for obtaining high biomass titer and improved methane sequestration in the first stage. Further, to achieve an improved methanol

titer, selection of appropriate process design for methanol production from CO_2, and optimization of CO_2 concentration in the headspace and liquid to headspace volume ratio were carried out in an air-tight batch reactor in the second stage.

Subsequently, process engineering strategies were developed to address the key challenges associated with inferior mass transfer rates and limited solubility of methane and CO_2 in liquid media leading to lower titers of biomass and methanol. In the first stage, a combinatorial approach of design of micro-sparger, engagement of draft tube and use of mass transfer vector was employed in a customized airlift reactor to achieve improved mass transfer and solubility of methane and in turn, increased biomass titer. Process engineering strategy for the second stage involved customization of a high-pressure stirred tank reactor to enhance the solubility of CO_2 under elevated operating pressure, and consequent increase in methanol titer. Moreover, in order to cut-down the time and cost expended towards recurrent biomass production in the first stage, biomass recycling strategy was employed to reuse the biomass for multiple cycles of second stage and achieve a high cumulative methanol titer. Subsequently, distillation was carried out to recover high-purity bio-methanol from the cultivation medium. Eventually, bio-methanol was evaluated for its suitability for blending with diesel as an alternate transportation fuel, through analysis of physicochemical properties, and characterization of emission and performance in a four-stroke internal combustion engine.

1.4. Thesis organization

The thesis consists of **seven chapters** encompassing introduction to conclusions. **Chapter 1** primarily establishes the background and motivation for the current study with detailed emphasis on the existing gaps in present research, steps towards understanding hurdles to fill gaps and the futuristic objectives to resolve the problems in the current state-of-the-art technology. It highlights the approach employed in the present study to address the major bottlenecks assessed from existing methanotrophic methanol production and its application as

an alternate transportation fuel. **Chapter 2** presents a detailed survey of literature depicting the current global need for sustainable greenhouse gas sequestration technology in view of rapidly increasing methane and CO_2 concentrations in the atmosphere. Further, the chapter highlights the major limitations associated with the existing chemical methods for methane and CO_2 sequestration towards their conversion into value-added products, such as methanol; and the significance of methanol as a liquid chemical and a potential fuel. The chapter delves in establishing the importance of methanotrophic microorganisms as sustainable alternative biological platform for methanol production coupled with the sequestration of methane and CO_2. It provides an insight into the biology of methanotrophs, including metabolic pathways adopted by them for the utilization of methane and CO_2, and production of methanol thereof. The chapter reviews the existing process engineering strategies employed towards achieving improvements in methanol production. It also discusses different reactor configurations used for methanol production towards combating the mass transfer and solubility limitations encountered in methanotrophic gas fermentation systems. Finally, recent studies on the application of methanol as an alternate transportation fuel have also been reviewed. **Chapter 3** reports a two-stage integrated process for bio-methanol production using *Methylosinus trichosporium* NCIMB 11131, coupled with the fixation of methane and CO_2. The first stage involved sequestration of methane to produce methanotrophic biomass, which was used as biocatalyst to convert CO_2 into methanol in the second stage. Further, this chapter deals with the characterization of the strain under different physicochemical parameters to identify the optimum conditions for achieving high titers of biomass and methanol in the first and second stages, respectively. **Chapter 4** addresses the key challenge of limited mass transfer and solubility of methane, in the first stage, towards improving its bioavailability to methanotrophic bacteria for growth and biomass generation. It demonstrates a combinatorial process engineering approach of design of micro-sparger, engagement of draft tube and

supplementation of mass transfer vector in an airlift reactor towards achieving enhanced mass transfer, leading to consequent improvements in biomass titer, biomass productivity and methane fixation rate. **Chapter 5** describes a process engineering strategy comprising elevation of operating pressure to enhance the solubility of CO_2, thereby increasing its conversion into methanol; and recycling of biomass towards achieving a high cumulative methanol titer, thus curtailing the time and resources expended towards recurrent biomass generation. This is followed by distillation to recover high-purity bio-methanol. **Chapter 6** demonstrates the application of methanotroph-derived bio-methanol as a potential diesel fuel blend for fuelling four-stroke internal combustion engine, thereby establishing its suitability as a non-petroleum based renewable alternate transportation fuel. **Chapter 7** comprises the overall conclusion and summarizes key research highlights obtained from the present study. The conclusion section is followed by scope for further investigation based on the outcomes of the current thesis work.

1.5. References

1. Ali, S., Sørensen, K., & Nielsen, M. P. (2020). Modeling a novel combined solid oxide electrolysis cell (SOEC)-Biomass gasification renewable methanol production system. *Renewable Energy*, *154*, 1025-1034.
2. Dalena, F., Senatore, A., Marino, A., Gordano, A., Basile, M., & Basile, A. (2018). Methanol production and applications: an overview. *Methanol*, 3-28.
3. Doran, P. M. (1995). *Bioprocess engineering principles*. Elsevier.
4. Fei, Q., Guarnieri, M. T., Tao, L., Laurens, L. M., Dowe, N., & Pienkos, P. T. (2014). Bioconversion of natural gas to liquid fuel: opportunities and challenges. *Biotechnology Advances*, *32*(3), 596-614.
5. Global Methane Tracker (2023). International Energy Agency. https://www.iea.org/news/methane-emissions-remained-stubbornly-high-in-2022-

even-as-soaring-energy-prices-made-actions-to-reduce-them-cheaper-than-ever. (Accessed 30 September 2023).

6. Han, B., Su, T., Wu, H., Gou, Z., Xing, X.H., Jiang, H., Chen, Y., Li, X., & Murrell, J.C. (2009). Paraffin oil as a "methane vector" for rapid and high cell density cultivation of *Methylosinus trichosporium* OB3b. *Applied microbiology and biotechnology*, *83*, 669-677.
7. Hasan, A.O., Osman, A.I., Ala'a, H., Al-Rawashdeh, H., Abu-jrai, A., Ahmad, R., Gomaa, M.R., Deka, T.J., & Rooney, D.W. (2021). An experimental study of engine characteristics and tailpipe emissions from modern DI diesel engine fuelled with methanol/diesel blends. *Fuel Processing Technology*, *220*, 106901.
8. International Energy Agency (2023). https://www.iea.org/news/global-co2-emissions-rose-less-than-initially-feared-in-2022-as-clean-energy-growth-offset-much-of-the-impact-of-greater-coal-and-oil-use. (Accessed 30 September 2023).
9. Keller, M., & Sharma, A. (2022). Reverse Boudouard reforming produces CO directly suitable for the production of methanol from CO_2 and CH_4. *Chemical Engineering Journal*, *431*, 134127.
10. Li, Y., Hu, Y., Chu, J., Yao, Y., Lv, H., & Xu, C. (2023). Investigation of renewable methanol production from CO_2 hydrogeneration based on spectral splitting and heat integration. *Fuel*, *352*, 129041.
11. Park, S. Y., & Kim, C. G. (2019). Application and development of methanotrophs in environmental engineering. *Journal of Material Cycles and Waste Management*, *21*, 415-422.
12. Patel, S. K., Gupta, R. K., Kalia, V. C., & Lee, J. K. (2022). Synthetic design of methanotroph co-cultures and their immobilization within polymers containing

magnetic nanoparticles to enhance methanol production from wheat straw-based biogas. *Bioresource Technology*, *364*, 128032.

13. Patel, S. K., Kalia, V. C., & Lee, J. K. (2023). Integration of biogas derived from dark fermentation and anaerobic digestion of biowaste to enhance methanol production by methanotrophs. *Bioresource Technology*, *369*, 128427.
14. Patel, S. K., Kalia, V. C., Joo, J. B., Kang, Y. C., & Lee, J. K. (2020). Biotransformation of methane into methanol by methanotrophs immobilized on coconut coir. *Bioresource Technology*, *297*, 122433.
15. Patel, S.K., Kondaveeti, S., Otari, S.V., Pagolu, R.T., Jeong, S.H., Kim, S.C., Cho, B.K., Kang, Y.C., & Lee, J.K. (2018). Repeated batch methanol production from a simulated biogas mixture using immobilized *Methylocystis bryophila*. *Energy*, *145*, 477-485.
16. Sahoo, K. K., Datta, S., Goswami, G., & Das, D. (2022). Two-stage integrated process for bio-methanol production coupled with methane and carbon dioxide sequestration: kinetic modelling and experimental validation. *Journal of Environmental Management*, *301*, 113927.
17. Sahoo, K. K., Goswami, G., & Das, D. (2021). Biotransformation of methane and carbon dioxide into high-value products by methanotrophs: current state of art and future prospects. *Frontiers in Microbiology*, *12*, 636486.
18. Sahoo, K. K., Sinha, A., & Das, D. (2023). Process engineering strategy for improved methanol production in *Methylosinus trichosporium* through enhanced mass transfer and solubility of methane and carbon dioxide. *Bioresource Technology*, *371*, 128603.
19. Van Hecke, W., Bockrath, R., & De Wever, H. (2019). Effects of moderately elevated pressure on gas fermentation processes. *Bioresource technology*, *293*, 122129.

20. Vargün, M., Yılmaz, I. T., & Sayın, C. (2022). Investigation of performance, combustion and emission characteristics in a diesel engine fueled with methanol/ethanol/nHeptane/diesel blends. *Energy*, *257*, 124740.
21. Verhelst, S., Turner, J. W., Sileghem, L., & Vancoillie, J. (2019). Methanol as a fuel for internal combustion engines. *Progress in Energy and Combustion Science*, *70*, 43-88.
22. Xin, J. Y., Cui, J. R., Niu, J. Z., Hua, S. F., Xia, C. G., Li, S. B., & Zhu, L. M. (2004). Production of methanol from methane by methanotrophic bacteria. *Biocatalysis and Biotransformation*, *22*(3), 225-229.
23. Xin, J. Y., Zhang, Y. X., Zhang, S., Xia, C. G., & Li, S. B. (2007). Methanol production from CO_2 by resting cells of the methanotrophic bacterium *Methylosinus trichosporium* IMV 3011. *Journal of basic microbiology*, *47*(5), 426-435.
24. Zhang, Z., Tian, J., Li, J., Lv, J., Wang, S., Zhong, Y., Dong, R., Gao, S., Cao, C., & Tan, D. (2022). Investigation on combustion, performance and emission characteristics of a diesel engine fueled with diesel/alcohol/n-butanol blended fuels. *Fuel*, *320*, 123975.

CHAPTER 2

Review of Literature

2.1. Global status of methane and CO_2 emissions

Overpopulation and economic development have led to increased greenhouse gas emissions since the beginning of the pre-industrial era, resulting in unprecedented levels of atmospheric methane and carbon dioxide concentrations. The consequent effect has been reflecting through global climate change and enhanced global warming since the mid-20th century. According to National Oceanic and Atmospheric Administration-Earth System Research Laboratories (NOAA-ESRL), the global average atmospheric concentration of methane has increased by 7.85% in last 20 years, reaching 1911.82 ppb in 2022 (Fig. 2.1). Similarly, as of the year 2022, the global average atmospheric concentration of CO_2 has reached 418.53 ppm, which is an increment of 12.1% over the last two decades. As per the data from the Global Monitoring Laboratory (NOAA-ESRL, 2023), the global atmospheric concentrations of methane and CO_2 have been rising annually at an average rate of 7 ppb and 2.2 ppm, respectively, over the past twenty years. The global energy sector itself has resulted in the emission of 36.8 billion tonnes of CO_2, and 135 million tonnes of methane, which accounts for only 40% of the total anthropogenic methane emission (International Energy Agency, 2023; Global Methane Tracker, 2023).

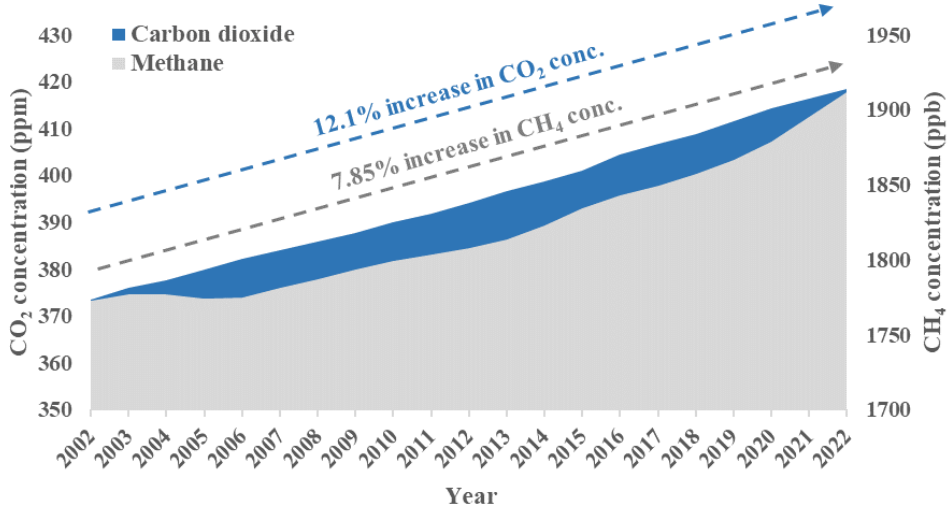

Fig. 2.1. Globally averaged atmospheric concentrations of methane and carbon dioxide in the last two decades (NOAA-ESRL, 2023).

Moreover, methane has a global warming potential 27-30 times that of CO_2 over a 100-year-timescale (US EPA, 2023). The carbon dioxide emitted today possess the potential to last for thousands of years in the atmosphere, while the emitted methane persists for almost a decade. Despite the shorter lifetime, the energy absorbed by methane during the given time span is relatively much higher than CO_2, bestowing greater global warming potential (US EPA, 2023). Owing to the past as well as ongoing anthropogenic emissions, global warming is increasing at the rate of 0.2 °C per decade (IPCC, 2018). If the given rate continues until 2030 to 2052, the global warming which already stands at 1 °C beyond the pre-industrial level, is estimated to hit 1.5 °C. IPCC regards "1.5 °C" as the threshold, crossing which is predicted to unleash harsh impacts on the climate, including severe rainfall, heatwaves and droughts. Contextually, the Paris Agreement (2016) aimed to restrict the global warming to 1.5 °C, and curb it from reaching 2 °C beyond the pre-industrial level, which mandates cutting down the greenhouse gas emissions up to 43% by 2030. Moreover, there are is an ongoing global effort to achieve "net-zero" emissions by 2050 (United Nations Climate Action, 2022).

2.2. Conventional chemical methods for methane and CO_2 sequestration, and conversion into methanol: a value-added product

Owing to the current global urgency to mitigate the major greenhouse gases (*viz.*, methane and CO_2), researchers are striving to sequester these gases, and transform them into various value-added chemicals and liquid fuels such as formaldehyde, methanol, ethanol, propanol, butanol, acetic acid and formic acid (Wang et al. 2017). Methanol, a widely used industrial solvent, is also known to be a precursor for synthesizing other chemicals like acetic acid, formaldehyde, methylamine, dimethyl ether, and methyl tert-butyl ether (MTBE) (Dalena et al. 2018). Moreover, methanol is being considered as a potential transportation fuel owing to its high specific energy ratio, high heat of vaporization, high flame speed, low combustion temperature, low stoichiometric air to fuel ratio, low carbon to hydrogen ratio, clean burning characteristics and so on (Verhelst et al. 2019). Although CH_4 is also used as a fuel, methanol stands superior to CH_4 in several ways such as: (i) methanol is a liquid at STP, which facilitates easy and safe storage and transportation with minimum product loss; and (ii) methanol possesses 488-times greater volumetric energy content (15871 MJ m^{-3}) as compared to CH_4 (32.50 MJ m^{-3}) (Verhelst et al. 2019).

Conventional chemical methods for sequestration of methane and CO_2, and conversion into methanol, include catalyst-driven hydrogenation of CO_2 (Chang et al. 2017; Frei et al. 2019) and oxidation of methane (Kim et al. 2017; Bozbag et al. 2018). Methanol synthesis has also been reported through thermochemical gasification of agricultural biomass (Bai et al. 2019). However, the chemical routes are mainly constrained by the requirement of: (i) expensive catalysts, *e.g.*, $CuCeTiO_x$, Pd/In_2O_3, $CuO/ZnO/Al_2O_3$, $Fe_2O_3(MoO_3)_3$, MoO_3/SiO_2, MoO_3/Ga_2O_3, V_2O_5/SiO_2, NiO and FeO_x/ZrO_2; (ii) extreme process conditions such as, temperature and pressure as high as 850 °C and 100 bar, respectively; and (iii) generation of toxic byproducts, *e.g.*, carbon monoxide (Kumar et al. 2014; Han et al. 2016; Chang et al. 2017;

Frei et al. 2019; Ali et al. 2020; Keller and Sharma 2022; Li et al. 2023). The enumerated drawbacks make the overall process cost-intensive and non-sustainable.

2.3. Biological method for methane and CO_2 sequestration and methanol production using methanotrophs

In order to overcome the constraints associated with conventional chemical methods, researchers are investigating alternate biological routes for carbon sequestration and methanol production. To that end, methanotrophic microorganisms are being explored as potential biocatalysts for the sequestration of methane and CO_2, and production of methanol thereof.

2.3.1. Overview of methanotrophs

Methanotrophs are a class of Gram-negative Proteobacteria, reported to be suitable candidates for methanol production (Fei et al. 2014; Ge et al. 2014). Methanotrophs can grow utilizing methane as the exclusive source of carbon and energy (Xin et al. 2007). Methane fixed by methanotrophs gets sequentially oxidized into methanol, formaldehyde, formate and CO_2, catalysed by an endogenous cascade of four enzymes *viz.*, methane monooxygenase (MMO), methanol dehydrogenase (MDH), formaldehyde dehydrogenase (FaDH), and formate dehydrogenase (FDH), respectively (Patel et al. 2020c) (Fig. 2.2). Except MMO, the other three enzymes have reversible activity (Xin et al. 2007). A portion of intermediately generated formaldehyde/formate gets integrated into biomass as carbon source through serine or RuMP (ribulose monophosphate) cycle (Park and Kim 2019). MMO is differentiated into two categories: soluble (sMMO) and particulate (pMMO). sMMO occurs in the cytoplasm, with upregulated expression under high concentration of iron ions and lower ratio of copper to biomass; while pMMO occurs embedded on the membrane, expressing elevated activity under higher copper to biomass ratio (Chidambarampadmavathy et al. 2015). In fact, high copper to biomass ratio inhibits the activity of sMMO, in turn resulting in pMMO expression (in plasma membrane) for the catalysis of methane oxidation in the periplasmic space. This mechanism

wherein copper acts as a metabolic activator for inducing pMMO expression is known as the "copper switch" (Chidambarampadmavathy et al. 2015). Abundance of copper results in the formation of surplus intracytoplasmic membranes, and consequently the pMMO-linked membrane proteins (Fei et al. 2014). Owing to the synthesis of excess intracytoplasmic membranes, methanotrophs possessing pMMO have higher lipid content relative to other methanotrophs. The metal-driven regulation of the enzyme activities could be attributed to their structural design. pMMO has a trimeric structure characterized by the presence of a mono-nuclear or di-nuclear copper centre in each of the monomers (Ge et al. 2014). On the other hand, sMMO possesses a dimeric structure, wherein each monomer contains a di-iron centre. Only a subset of methanotrophs possess sMMO, while pMMO occurs in all the known methanotrophs except a handful of *Methyloferula* and *Methylocella* species which express only sMMO (Kalyuzhnaya et al. 2015; Koo and Rosenzweig 2021). Although, methane is presumed to be easily accessible to pMMO owing to membrane localization, however, sMMO is reported to catalyse quicker oxidation of methane relative to pMMO (Ge et al. 2014).

Methanotrophs are broadly categorized into three types (Type I, Type II and Type X) based on the C1 assimilation pathway, intracytoplasmic membrane (ICM) morphology, membrane phospholipid composition, and other physiological traits (Hanson and Hanson 1996). For example, with respect to the assimilation of C1-carbon source, Type I and Type X methanotrophs uptake formaldehyde using RuMP pathway, whereas, Type II methanotrophs uptake formate using serine pathway (Hanson and Hanson 1996; Park and Kim 2019). Type X methanotrophs differ from Type I owing to: (a) slight expression of enzymes pertaining to serine pathway and, (b) ribulose-bisphosphate carboxylase, an enzyme in Calvin-Benson-Bassham (CBB) pathway. Moreover, they require higher growth temperature, relative to Type I and Type II methanotrophs. Type X methanotrophs can reportedly assimilate CO_2 into biomass via CBB pathway (Baxter et al. 2002; Park and Kim 2019). Further, in terms of ICM

arrangement, Type I and Type X species are characterized by the presence of vesicular disk bundles, while Type II species contain paired membranes oriented along the cell's periphery (Hanson and Hanson 1996). From the perspective of membrane phospholipid fatty acid (PLFA) content, species of Type I and Type X mainly contain 14-16 and 16-carbon PLFAs, respectively, whereas, Type II species primarily possess 18-carbon PLFAs. Later, Dedysh et al. (2001) isolated *Methylocapsa acidophila* B2, with a novel arrangement of ICM and PmoA peptide sequence, distantly identical to Type I and II, and hence was designed as Type III methanotroph. The strain was reported to utilize serine pathway for assimilating C1-carbon source (Dedysh et al. 2002). On the basis of 16S rRNA gene sequences, aerobic methanotrophs are classified into three primary groups (Kalyuzhnaya et al. 2015). Group I (Gammaproteobacteria) comprise of the Type I and Type X methanotrophs, which include the genera *Methylobacter*, *Methylomicrobium*, *Methylohalobius*, *Methylomonas*, *Methylosarcina*, *Methylosphaera*, *Methylosoma*, *Methylothermus*, *Methyloglobus, Methyloprofundus, Methylogaea, Methylomarinum, Methylovulum, Methylomarinovum, Methylorubrum, Methyloparacoccus, Methylocaldum* and *Methylococcus*. Group II (Alphaproteobacteria) consists of the Type II and Type III methanotrophs, namely the genera *Methylosinus*, *Methylocella*, *Methylocystis, Methyloferula* and *Methylocapsa*. Group III comprises of the lately discovered phylum, Verrucomicrobia (*viz.*, the *Methylacidiphilum* and *Methylacidimicrobium* genera), which are thermoacidophilic methanotrophs, capable of assimilating CO_2 through CBB pathway (Fei et al. 2014; Kalyuzhnaya et al. 2015; Koo and Rosenzweig 2021).

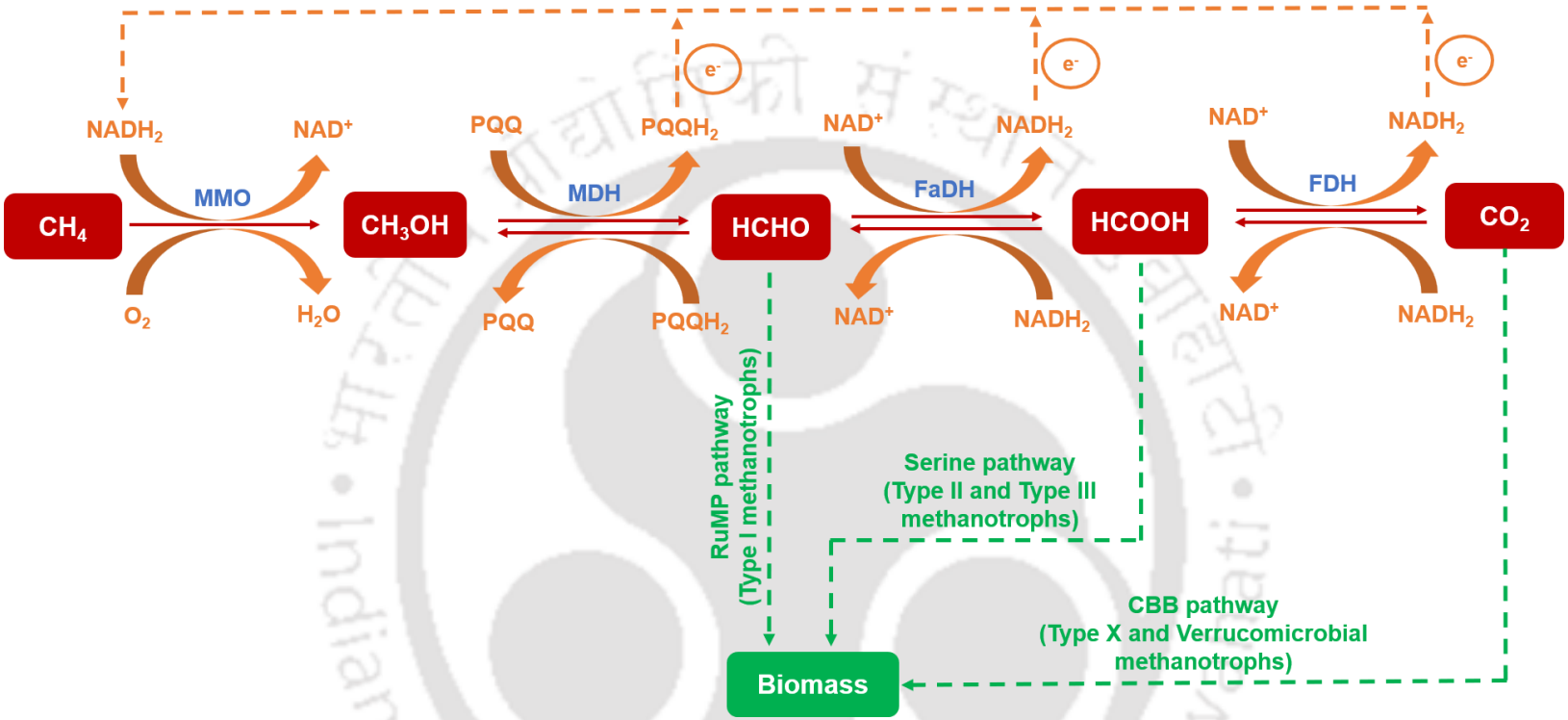

Fig. 2.2. Metabolic pathway for the utilisation of methane and carbon dioxide by methanotrophs to produce biomass and methanol (adapted from Sahoo et al. 2021). MMO: methane monooxygenase; MDH: methanol dehydrogenase; FaDH: formaldehyde dehydrogenase; FDH: formate dehydrogenase; PQQ: pyrroloquinoline quinone; $PQQH_2$: pyrroloquinoline quinol; NADH: nicotinamide adenine dinucleotide hydrogen; RuMP: ribulose monophosphate; CBB: Calvin-Benson-Bassham.

2.3.2. Substrate-dependent metabolic pathways adopted for microbial methanol production

Methanol can be produced through oxidation of methane catalysed by MMO. During oxidation of methane to methanol, MMO requires two units each of electrons and protons, to disrupt the double bond in O_2 (Kalyuzhnaya 2016). While one atom of oxygen is utilized for oxidizing methane, the second one undergoes hydrogenation to form water (Xin et al. 2007). sMMO utilizes NADH as electron donor, while for pMMO the physiological reducing equivalents are assumed to be NADH or QH_2 (ubiquinol), which are produced in the course of formaldehyde/formate oxidation (Kalyuzhnaya 2016). pMMO activity has also been attained *in vitro* through the supplementation of duroquinol as reductant, which is presumed to mimic the native ubiquinol occurring in the membranes (Koo and Rosenzweig 2021). While the further oxidation of methanol catalysed by MDH requires PQQ (pyrroloquinoline quinone), the sequential oxidations of formaldehyde into formate and CO_2 liberate NADH (Fig. 2.2). NADH released get utilized by MMO to oxidise methane into methanol (Xin et al. 2007). Methanotrophs have been extensively studied for methanol production through MMO-catalysed oxidation of pure methane (Patel et al. 2016c, 2020b, c; Taylor et al. 2018). However, the produced methanol tends to get sequentially oxidised into formaldehyde, formate and CO_2, by MDH, FaDH and FDH, respectively, yielding lower methanol titer. To obtain methanol directly from methane, researchers have reported supplementation of medium with various MDH inhibitors (*e.g.*, NH_4Cl, NaCl, $MgCl_2$, EDTA, phosphate, and cyclopropanol) to block MDH from catalysing subsequent oxidation of methanol (Patel et al. 2020c, d). However, inhibition of MDH activity causes interruption in supply of NADH, an essential co-factor for MMO activity. In order to prevent interruption in oxidation of methane to methanol, MMO activity is maintained by exogenously supplementing the medium with formate, as a source for regenerating NADH (Patel et al. 2022). But the use of MDH inhibitors and formate increase

the overall cost of production. Researchers have reported maximum methanol production up to 52.9 mM (1.69 g L^{-1}) using pure methane as substrate in *Methylocystis bryophila* in the presence of $MgCl_2$ and phosphate as MDH inhibitors, and formate as NADH source (Patel et al. 2020c).

Studies have also reported utilization of pure CO_2 as a substrate for methanol production (Xin et al. 2007; Patel et al. 2016a, 2018a). CO_2, the end-product of methanotrophic metabolism, when supplied to the cells in excess concentration, shift the equilibrium in backward direction, causing reduction of CO_2. CO_2 is sequentially reduced by reversible enzymes FDH, FaDH and MDH, resulting in extracellular accumulation of methanol (Fig. 2.2). Irreversible activity of MMO averts further conversion of methanol. Reduction of CO_2 into methanol requires surplus reducing equivalents to drive the equilibrium against the laws of energy. NADH is required for sequential reductions of CO_2 into formate and formaldehyde; while $PQQH_2$ is required for reduction of formaldehyde into methanol. Further deficit in reducing equivalents, beyond the intrinsic NADH production capability of the cell, is offset by endogenous poly-β-hydroxybutyrate (PHB) reserves. NAD+-linked β-hydroxybutyrate dehydrogenase degrades PHB into acetoacetic acid, causing generation of reducing equivalents (Xin et al. 2007; Sahoo et al. 2021). Studies have reported maximum methanol titer up to 0.52 mM (0.017 g L^{-1}) using pure CO_2 as feed in covalently immobilized cells of *Methylocystis bryophila* on chitosan (Patel et al. 2018a).

Moreover, researchers have demonstrated use of biogas, a low-cost alternative to pure gases (CH_4 and CO_2), as feed for microbial methanol production. Biogas derived from anaerobic digestion of various types of wastes *e.g.*, wheat straw, potato peels, and rice straw, containing around 65.3-67.2% CH_4, have been utilized for methanotrophic methanol production (Patel et al. 2020a, 2021a, 2022, 2023b). Studies have also reported methanol production using biogas (~67.7- 68.9% CH_4) obtained from commercial anaerobic digestor and

municipal sewage treatment plant (Sheets et al. 2017; Kim et al. 2018). Methane solubility is a key challenge during methanol production through methane oxidation pathway, owing to its extremely low diffusion coefficient (1.5×10^{-5} cm^2 s^{-1}) (Patel et al. 2021b). Contextually, certain studies have demonstrated alteration of feed through supply of raw biogas, simulated biogas or synthetic gas mixture, instead of pure methane, as a suitable approach for enhancing methanol production. For instance, Patel et al. (2021a) reported 39.2% and 21.5% improvement in methanol production from *M. tundrae* and *M. stellata*, respectively, using raw biogas as feed, relative to pure methane. In another study, feeding of simulated biogas resulted in 167 and 149% higher methanol titer as compared to pure methane in cultures of *M. bryophila* and *M. stellata*, respectively, grown using nanoparticle-containing medium (Patel et al. 2023a). Similarly, *M. sporium* yielded higher methanol titer utilizing synthetic gas mixture than that from pure methane (Patel et al. 2016c). Another study reported 3.5-fold improvement in methanol production through supplementation of hydrogen in raw biogas (Patel et al. 2016a). These improvements have been attributed to differential response of the methanotrophic strains towards mixed feed and pure methane. However, owing to the predominance of methane content in biogas, methanotrophic methanol production from biogas is accomplished through typical MMO-catalysed methane oxidation, thereby requiring the supplementation of MDH inhibitors and formate. Highest methanol titer of 70.74 mM (2.27 g L^{-1}) was reported in a methanotrophic co-culture fed with wheat straw-derived biogas (Patel et al. 2022).

2.4. Metabolic engineering approaches towards microbial methanol production

Methanotrophs have been genetically engineered to produce a range of value-added products using methane, such as lysine, cadaverine, 2-hydroxyisobutyric acid and 1,3-butanediol from *Methylosinus trichosporium* OB3b (Nguyen et al. 2020; Mai et al. 2021); muconic acid and mevalonate from *M. capsulatus* Bath (Henard et al. 2019; Jeong et al. 2023); and 2, 3-butanediol, ectoine and putrescine from *Methylomicrobium alcaliphilum* 20Z (Nguyen

et al. 2018; Nguyen and Lee 2019; Cho et al. 2022). In addition to these, metabolic engineering strategies are being employed to exploit the native methanotrophs beyond their innate methanol production potential. One such strategy involves multi-carbon substrate utilization. For instance, an improved methanol titre (11.6 mM) was reported in methanotrophic strain *M. alcaliphilum* 20Z, where one step conversion of methane to methanol was achieved with co-utilization of methane and glycerol, and knock out of *mxaFI* (calcium-dependant MDH) and *xoxF* (lanthanum-dependant MDH), without the requirement for MDH inhibitor and exogenous formate supplementation (Le et al. 2021). Secondly, development of metabolic flux balance-based models has been useful in predicting the exact mechanisms underlying various pathways. For example, genome scale metabolic model was developed for *M. buryatense* 5G(B1), where three possible modes of methane oxidation were predicted (Torre et al. 2015). The flux balance simulations predicted that: (i) the process of methane/oxygen utilization that results in growth, is supported only by the supply of electrons from the methanol oxidation step to the methane oxidation step; (ii) pMMO activity is mostly supported by direct coupling between the steps of methanol oxidation and methane oxidation, which otherwise cannot be accomplished by feeding NADH as electron donor (Since, NADH-derived electrons can drive only about 20% of the methane oxidation); and (iii) the effectiveness of direct coupling is enhanced through the input of additional NADH, which is supposed to compensate for possible electron loss, and to maintain methane oxidation even during genetic or nutritional perturbations, or to facilitate uphill transfer of electrons (Torre et al. 2015). Moreover, genetic engineering tools are being used for the development of methanotrophic transformants or mutants. For example, Yan et al. (2016) developed electroporation protocols for three methanotrophic strains *viz., Methylomicrobium buryatense* 5GB1C, *Methylobacter tundripaludum* 21/22 and *Methylomonas* sp. strain LW13, with high transformation efficiencies. With respect to genetic engineering tools for developing synthetic methanotrophs or introducing methanotrophy in

model hosts, conjugation and electroporation methods are being widely used (Crombie and Murrell 2011). However, studies are also required to be carried out in the direction of engineering suitable methanotrophic strains for over-expression of the native enzymes namely, formate-, formaldehyde- and methanol dehydrogenase, towards obtaining enhanced methanol production through CO_2 reduction pathway.

Additionally, transfer of methanotrophic genes and their functional expression in model organisms, is used as an alternative to engineering native methanotrophs for methanol production. Contextually, there are a few reports of introducing methanotrophy in platform organisms such as *E. coli*. For instance, pMMO was first expressed in *E. coli* (*in vitro*) by reassembly of catalytic domains of the enzyme on apoferritin, which resulted in comparable enzyme activities as that of its native form (Kim et al. 2019). Using the purified enzyme, the highest *in vitro* methanol production obtained was 1350 mol mol^{-1} pMMO (mimic type-m3). Bennett et al. (2021) developed a synthetic *E. coli* strain for methanotrophy by transfer of soluble methane monooxygenase (sMMO) from *Methylococcus capsulatus* and achieved a productivity of 85 ± 2 mg methanol g CDW^{-1} h^{-1}. However, the methanol titres and the productivities achieved are not so encouraging despite the successful application of metabolic engineering strategies. While a significant metabolic level progress is evident in developing platform chemicals from methane and methylotrophic methanol utilization, there is much need and scope for developing metabolic engineering strategies towards further improving methanol production using methane or CO_2 as substrate.

Strain engineering for methanotrophs is cumbersome attributed to the involvement of complex methods like homologous expression, given the fact that understanding on their metabolism is still inadequate. Moreover, heterologous expression of methanotrophic enzymes in model hosts, such as *E. coli*, has not been successful enough to realize their industrial potential, attributed either to the failure to accomplish *in vivo* methane oxidation, or

dependence on co-utilization of sugar substrate (*e.g.*, glucose) in addition to methane (Kim et al. 2019; Bennett et al. 2021; Gregory et al. 2022). Thus, extensively rigorous research is required in the direction of metabolic engineering to bring synthetic methanotrophs up to the mark of industrial feasibility. In contrast to metabolic engineering, process engineering strategies are proving to be more efficient in terms of the overall output.

2.5. Bioprocess engineering strategies for improved methanol production

The current state-of-the-art of methanol production from methanotrophs is plagued by: (i) limited mass transfer and solubility of gaseous substrates, (ii) low substrate uptake efficiency, (iii) slow growth rate, and (iv) low methanol titer. The current section discusses various process engineering strategies adopted by researchers to address the above challenges towards obtaining improved methanol production.

2.5.1. Cell immobilization

Cell immobilization is a prevalent method for improving stability of cells. Immobilization aids in preserving biocatalytic activity of the cells for longer incubation periods as compared to free cells (Patel et al. 2020d). Different types of materials, *e.g.*, alginate, polyvinyl alcohol (PVA), chitosan, groundnut shell, silica gel, Amberlite, Duolite, polyethyleneimine, 3-aminopropyltriethoxysilane and glutaraldehyde, have been used as support for immobilization of methanotrophs to produce methanol (Razumovsky et al. 2008; Patel et al. 2017, 2018a, b, 2020a; Taylor et al. 2018). Immobilized cells are reported to exhibit reduced MDH activity, greater retention of residual sMMO activity, and consequent higher residual methanol production efficiency relative to free cells, even after multiple cycles of biomass reuse (Patel et al. 2020a, d). For instance, encapsulation of *M. album* cells in PVA and alginate resulted in MDH activities of 22.8 and 23.4%, residual sMMO activity of 65.6 and 44.9%, and residual methanol production efficiency of 56.4 and 38.2%, respectively, relative to free cells exhibiting values of 49.5, 5.3 and 4.5%, for corresponding parameters (Patel et al.

2020d). Immobilization promotes various degrees of interactions between the cells and the support, leading to reduction in leaching out of immobilized cells, and consequent improvement in methanol production stability (Patel et al. 2020a). Further, the application of a unique range of supports varying from macroporous carbon particles to magnetic nanoparticle-doped polymers, for immobilization of methanotrophs, has resulted in 18.1 to 25-fold increment in methanol production stability (Patel et al. 2019, 2022). Moreover, lignocellulosic biowastes, such as, coconut coir and banana leaves, have also been demonstrated as support for methanotrophic immobilization (Patel et al. 2020c, 2021a). Researchers have also compared methanol yields from different immobilization methods. For instance, covalent mode is reported to yield more methanol (52.9 mM), relative to adsorption method (31.8 mM), attributed to 5.4-fold reduced cumulative leaching and 2.8-fold improved residual sMMO activity retention in cells immobilized through covalent method as compared to adsorption method (Patel et al. 2020c). Given the influence of iron and copper on methanotrophic growth and activity of MMO, a recent study has unveiled the effect of encapsulating cells in polymeric matrix comprising Fe_3O_4, Cu and $CuFe_2O_4$ nanoparticles on methanol production (Patel et al. 2023a). $CuFe_2O_4$ nanoparticle-based encapsulation is reported to enhance the residual efficiency of methanol production by 62.5-fold, thus opening up a new arena for research pertaining to the application of nanotechnology in methanotrophic methanol production. From the context of economic feasibility, immobilization also serves as a useful method with respect to the ease of separation of cells from the cultivation medium, as well as improve their reusability and thus residual methanol production stability across consecutive batches of biomass recycling.

2.5.2. Co-culture of cells

Co-cultivation of methanotrophic cells is a useful strategy to improve the efficiency of production through ameliorated uptake of gaseous substrates, thus leading to enhanced

methanol titer (Patel et al. 2018b). Furthermore, cells in a co-culture are characterised by a cumulative increased capacity to retain greater residual sMMO activity relative to their respective pure cultures (Patel et al. 2023b). Co-cultures are reported to be associated with an increased ratio of cellular NADH/NAD^+, and thus greater reduction current relative to individual cultures (Patel et al. 2023b). A handful of studies have reported methanol production from methanotrophic consortiums cultured from landfill soil samples, waste activated sludge, and anaerobic digestion digestate (Han et al. 2013; Su et al. 2017; AlSayed et al. 2018; Kim et al. 2018). However, the ratio of biomass density of individual cultures in a co-culture holds a significant effect on methanol yield. Co-cultures containing individual strains at defined ratios are superior to undefined methanotrophic mixed cultures or consortiums both in terms of operational stability and process efficiency (Patel et al. 2020b). Improved methanol production at the optimum ratio of biomass densities of constituent strains is attributed to the syntrophic behaviour or synchronised association among the strains at that given ratio (Patel et al. 2020b, 2022). Increments in methanol production have been reported through co-cultivation of *Methylosinus sporium* and *Methylocella tundrae* (2:1), *Methylocystis bryophila* and *Methyloferula stellata* (3:2), *Methylomonas methanica* and *Methylocella tundrae* (2:1), and *Methylosinus sporium* and *Methylocystis bryophila* (1:1) (Patel et al. 2018b, 2020b, 2022, 2023b). The combinatorial effect of immobilization and co-culture strategies on methanol production has been demonstrated in *co-immobilized* cells. For instance, Patel et al. (2018b) reported methanol titers of 3.86 and 3.57 mM, respectively, from the pure cultures of *M. methanica* and *M. tundrae*, which was enhanced to 4.87 mM through co-cultivation at 2:1 ratio. Subsequent co-immobilization on silica gel further augmented the titer to 5.06 mM.

2.5.3. Mass transfer vectors

Limited mass transfer and solubility of gaseous substrates in liquid medium presents an overwhelming challenge in methanotrophic methanol production (Han et al. 2009). To that end,

mass transfer vectors are introduced into medium to increase the solubilization of gaseous substrates, and thereby improving their bioavailability to the cells (Rocha-Rios et al. 2010). Mass transfer vectors are organic solvents, immiscible in water, possessing higher affinity for methane and oxygen as compared to aqueous mineral salt-based methanotrophic culture medium (Han et al. 2009; Rocha-Rios et al. 2010). Addition of vectors in culture medium disrupt the gas-holding bubbles, leading to increased interfacial area of contact between gaseous and aqueous phases (Rocha-Rios et al. 2011). Different vectors such as silicone oil and paraffin oil, have been used for improving methane fixation, methanotrophic growth and methanol production (Han et al. 2009; Rocha-Rios et al. 2010; Patel et al. 2020d). For instance, a seven-fold improvement was achieved in *M. trichosporium* cell density with the addition of 5% v/v paraffin oil (Han et al. 2009). Paraffin oil supplementation resulted in 18.7% increment in methane transfer efficiency, leading to 1.7-fold improvement in methanol titer (Patel et al. 2020d). It was reported to improve methane conversion yield (85.4%), residual sMMO activity (37.4%) and methanol production efficacy (28.3%), compared to control (with corresponding values of 67.2%, 16.9% and 13.4%, respectively) (Patel et al. 2023b). Further, silicone oil has been used as mass transfer vector in various reactor types (*e.g.*, airlift, stirred tank, capillary, and trickling bed) to demonstrate *two-phase partition bioreactors* to exploit the methane sequestering potential of methanotrophs for methane biodegradation (Rocha-Rios et al. 2009, 2010, 2011, 2013; Cantera et al. 2016). As an alternative to liquid vectors, Rocha-Rios et al. (2011) reported the application of organic solid polymers, *e.g.*, Desmopan®, Kraton® and Elvax®, owing to their cost-effectiveness and ease of removal from cultivation medium.

2.5.4. Repeated batch culture

Most of the studies have reported methanol production through a typical two-step process aided by appropriate carbon sources. The first step involves culturing of methanotrophic cells in nitrate mineral salt medium to generate biomass, while the second step

involves cultivation of the biomass in phosphate buffer to produce methanol (Patel et al. 2021a; Sahoo et al. 2022, 2023). Slow growth rate of methanotrophs presents a major stumbling block against efficient production of methanol. This calls for strategies for saving time and expenses incurred towards generation of fresh biomass before every methanol production batch. To that end, repeated batch mode of cultivation offers a sustainable way for re-utilization of the biomass for multiple cycles of methanol production. Methanotrophic biomass can reportedly be reused for about 4 to 10 cycles of methanol production (Xin et al. 2007; Patel et al. 2020b, 2022). Maximum cumulative methanol titer of 70.74 mM was reported in co-culture of *M. sporium* and *M. tundra* following ten batches of biomass recycling (Patel et al. 2022). The significance of certain strategies has been demonstrated in retaining higher methanol production efficiency across successive cycles in repeated batch operation. For instance, immobilization of cells aided in retaining 49.6% methanol production efficiency even after three cycles of biomass reuse, which on the contrary dropped to zero for free cells (Patel et al. 2018a). Likewise, supplementation of mass transfer vector helped in retaining a methanol production efficacy of 28.3%, which on the other hand declined to 13.4% in the control after six cycles of biomass reuse (Patel et al. 2023b). Enhancement in methanol production potential in repeated batch operation has also been achieved through exogenous addition of PHB into the medium for providing surplus reducing power to the cells (Xin et al. 2007). Retention of higher methanol production efficiency under the application of these strategies holds positive implications towards increasing the reusability of the biomass with respect to recycling of the biomass for greater number of cycles relative to the control. A possible obstacle curtailing higher methanol production could be end-product toxicity; 3 g L^{-1} being the minimum inhibitory concentration of methanol for certain methanotrophic species, such as *M. trichosporium* (Yu et al. 2009). To that end, repeated batch cultivation can be employed as a suitable strategy for methanol overproducing strains, so as to exploit their maximal methanol

production potential in multiple cycles, instead of one, thereby overcoming probable inhibition owing to end-product toxicity.

2.5.5. Elevated operating pressure

Elevation of operating pressure is a suitable approach towards overcoming limitations associated with solubility of gaseous substrates, thereby improving the product titer (Duan and Mao 2006). In addition to improving solubility, elevated pressure also exerts substantial effect on protein structure, enzymatic activity, metabolic product synthesis and permeability in microbial cells (Amulya et al. 2020). This is potentially accountable for inducing specific metabolic, physiological or genetic phenotypes in the microbe, consequently altering product synthesis pattern. The impact of elevated pressure up to 10 bar has been investigated in the formation of various value-added products (*e.g.,* biohydrogen, formate, lipase, acetate and ethanol) using gaseous substrates like, CO, CO_2, H_2, and O_2 (Van Hecke et al. 2019). However, to the best knowledge of the author, no study has explored the effect of elevated operating pressure on methanotrophic methanol production.

To summarize, common process engineering approaches involve: cell immobilization to improve cell stability and maintain biocatalytic activity; co-cultivation to achieve increased aggregate biocatalytic activity and substrate uptake efficiency; supplementation of mass transfer vectors to increase the solubility and bio-availability of gaseous substrates, thereby leading to improved methanol production. Additionally, certain approaches such as repeated batch cultivation, are being employed to make the process cost-effective and attain high cumulative methanol titer. Despite these efforts, the maximum methanol titer achieved using pure methane or methane-containing mixed feed (*e.g.*, biogas) is limited to 70.74 mM (2.27 g L^{-1}) (Patel et al. 2020c, 2022); while from that of pure CO_2 it is confined to a value of 0.52 mM (0.017 g L^{-1}) (Xin et al. 2007; Patel et al. 2018a).

2.6. Reactor configurations for methanol production

Limited gas-to-liquid mass transfer and solubility are major hurdles in methanotrophic gas fermentation processes relying on gaseous substrates as rate-limiting factor. From process engineering perspective, geometric design and configuration of bioreactor are critical parameters which can be permuted to overcome these limitations, thereby achieving improved biomass and product titer. For instance, airlift reactors characteristically offer efficient mixing and mass transfer; greater gas hold-up and liquid recirculation; cultivation-favourable environment for shear-sensitive cells, attributed to absence of mechanical stirring and consequent low energy requirement (Doran 1995). A methanol titer of 1.6 g L^{-1} was achieved in an external-loop airlift reactor with estimated volumetric mass transfer coefficients for methane ($k_L a_{CH_4}$) and oxygen ($k_L a_{O_2}$) of 70.8 h^{-1} and 97.2 h^{-1}, respectively (Ghaz-Jahanian et al. 2018). Furthermore, trickle bed reactors have been reported for efficient mass transfer characteristics attributed to loading with inert material-based beads/balls offering greater specific surface area (Sheets et al. 2017). Ceramic bead-loaded trickle bed reactor improved O_2 mass transfer and CH_4 oxidation by two- and four-folds, respectively, resulting in high methanol productivity (0.9 g L^{-1} d^{-1}) from *Methylocaldum* sp. (Sheets et al. 2017).

Researchers have incorporated various modifications in conventional reactors to ameliorate methanol production. Duan et al. (2011) introduced continuous aeration in a stirred tank reactor through individually rolled silicone tube coils for feeding oxygen and methane, thereby demonstrating a *bubble-free membrane aerated bioreactor*, yielding 0.95 g L^{-1} methanol. Kim et al. (2010) reported a *compulsory circulation diffusion system* comprising of a gas reservoir from where methane-air mixture was pumped into a cylindrical reactor through micropores configured at the reactor bottom. The micropores facilitated homogenous dispersion of gases in the liquid medium, thereby improving methane solubility and methanol

titer. Table 2.1 provides a comparison of studies reporting methanol production from different strains under varying process conditions and reactor configurations.

Table 2.1. Methanol production from different microbial strains under various process conditions and reactor configurations.

Strain	Substrate	Reactor configuration/mode of operation	Process engineering approach	Biomass density used	Methanol titer/yield	Reference
Methylosinus trichosporium IMV 3011	CH_4: CO_2: O_2: N_2 (20:40:20:20)	Ultrafiltration reactor; Continuous mode (100 mL)	Transmembrane pressure (0.6 MPa) maintained across semipermeable membrane to pump liquid medium	3 mg mL^{-1} DCW	8.22 µM	Xin et al. 2004
Methylosinus trichosporium IMV 3011	CO_2: air (50:40)	Conical flask (100 mL); Batch culture	-	3 mg mL^{-1} DCW	0.004 µmol/mg dry cell weight	Xin et al. 2007
Methylocystis bryophila DSM 21852	CO_2: air (15:85)	Serum bottle (120 mL); Repeated batch cultivation (5 batches)	Covalent immobilization of cells on chitosan	3 mg mL^{-1} DCW	0.52 mM (0.017 g L^{-1})	Patel et al. 2018a
Methylosinus trichosporium OB3b	CH_4: air (1:1)	Cylindrical reactor with (3 L); Batch operation with continuous sparging of methane and air	Reactor coupled with compulsory circulation diffusion system	0.6 mg mL^{-1} DCW	13.7 mM (0.44 g L^{-1})	Kim et al. 2010
Methylosinus trichosporium OB3b	CH_4: O_2 (1:1)	Anaerobic bottle (70 mL); Batch mode	High biomass density and high phosphate buffer concentration (400 mM)	17 g L^{-1} DCW	1.12 g L^{-1}	Duan et al. 2011
Methylosinus trichosporium OB3b	CH_4: air (1:1)	Membrane bioreactor (100 mL); Fed-batch operation	Reactor equipped with two macroporous membrane contactors for separately feeding CH_4 and air without generating gas bubbles	0.2 g L^{-1} DCW	75 mg (g dry cell)$^{-1}$ h^{-1}	Pen et al. 2014
Methylocaldum sp. 14B	Biogas: air (1:2.5)	Trickle-bed reactor (1.24 L)	Reactor loaded with ceramic beads ($k_L a_{O_2}$: 9.54 h^{-1})	0.96 g dry biomass per kg beads	0.9 g L^{-1} d^{-1}	Sheets et al. 2017

Activated sludge-derived methanotroph (Strain AS1)	CH_4: air (1:1)	External-loop airlift reactor (1L working volume); Batch and sequencing batch operation (5 batches)	Reactor coupled with CH_4 transfer chamber ($k_L a_{CH_4}$: 70.8 h^{-1})	1.7 g L^{-1} DCW	1600 mg L^{-1}	Ghaz-Jahanian et al. 2018
Methylocystis bryophila DSM 21852	CH_4: air (30:70)	Serum bottle (120 mL); Repeated batch cultivation (8 batches)	Covalent immobilization of cells on coconut coir and supplementation of mass transfer vector (5% v/v paraffin oil)	3 mg mL^{-1} DCW	52.9 mM (1.69 g L^{-1})	Patel et al. 2020c
Methylosinus sporium and *Methylocystis bryophila*	Combination of biogas obtained through anaerobic digestion and dark fermentation of rice straw (30% CH_4 and 15% H_2)	Serum bottle (13 mL); Repeated batch cultivation (6 batches)	Cell co-culture and supplementation of mass transfer vector (5% v/v paraffin oil)	3 mg mL^{-1} DCW	64.6 mM (2.07 g L^{-1})	Patel et al. 2023b
Methylosinus sporium and *Methylocella tundrae*	Biogas obtained through anaerobic digestion of wheat straw (30% CH_4)	Serum bottle (120 mL); Repeated batch cultivation (10 batches)	Cell co-culture and immobilization within magnetic nanoparticle-doped polymers	3 mg mL^{-1} DCW	70.74 mM (2.27 g L^{-1})	Patel et al. 2022

From the perspective of methanotrophic methanol production, reactor engineering still stands at a nascent stage. However, there are several reactor configurations reported for methane sequestration, and production of biomass and other metabolic products from methanotrophs, which may be explored for methanol production as well. As discussed already in the sub-section on "*Mass transfer vectors"*, researchers have demonstrated a range of *two-phase partition bioreactors (TPPB)* through supplementation of mass transfer vectors in conventional reactor types. For instance, addition of silicone oil improved CH_4 degradation by 700% and 131% in stirred tank- and trickle bed-based TPPB, respectively (Rocha-Rios et al. 2009, 2010). Likewise, silicone oil supplementation enhanced $k_L a$ by 38% and 100% in capillary- and internal loop airlift-based TPPB, respectively (Rocha-Rios et al. 2011, 2013). Certain reactor configurations, *e.g.*, Taylor flow reactor and bubble column reactor (with internal gas re-circulation) have been investigated for methanotrophic PHB production coupled with CH_4 abatement (Rodríguez et al. 2020; Cattaneo et al. 2022).

2.7. Methanol as a renewable alternate transportation fuel

Researchers are striving to explore non-petroleum based renewable and cleaner alternative fuels in an attempt to meet the rapidly rising global energy demand and increasingly strict regulations on emissions, which cannot be satisfied by the existing non-renewable fossil fuel reserves. Lately, alcohols (*e.g.*, methanol, ethanol and butanol) are being used as diesel fuel additives attributed to their renewable characteristics, lower carbon and higher oxygen content (Chen et al. 2021). Moreover, methanol as a diesel additive is considered to be superior over ethanol and butanol in certain aspects such as: (a) lower viscosity which facilitates easier injection, spraying and atomization, (b) higher O_2 content (50%) which improves combustion characteristics, and (c) improved combustion leading to increased thermal efficiency, and reduced emissions of soot, hydrocarbon and carbon monoxide (Zhang et al. 2022). Further, methanol is regarded as a suitable fuel for engines with high compression ratios attributed to

its octane number and heat of evaporation which are relatively higher than that of other alcohols and diesel (Zhen and Wang 2015). While high octane number supports substantial increment in the compression ratio, high heat of evaporation facilitates cooling down of the incoming air-fuel mixture charge, consequently leading to improved volumetric efficiency and enhanced power output. Higher octane number of methanol has been reported to improve the anti-knocking property of diesel-methanol blends, thereby lowering the ringing intensity, which can otherwise result in increased combustion noise and potential damage to engine parts (Maurya and Saxena 2018; Ning et al. 2020). Moreover, the auto-ignition temperature of methanol is significantly higher that of diesel and other alcohols, thus assuring safety during storage and transport (Zhen and Wang 2015). A comparison of the characteristics of diesel and alcohols has been provided in Table 2.2.

Table 2.2. Characteristics of diesel and alcohols (Ning et al. 2020; Chen et al. 2021; Zhang et al. 2022).

Characteristics	**Diesel**	**Methanol**	**Ethanol**	**n-Butanol**
Chemical formula	-	CH_3OH	C_2H_5OH	C_4H_9OH
Carbon content (%, w/w)	85	37.5	52	64.87
Oxygen content (%, w/w)	0	50	35	21.62
Kinematic viscosity ($mm^2\ s^{-1}$) at 40 °C	2.72	0.58	1.08	2.22
Density ($kg\ m^{-3}$) at 20 °C	847	795	790	810
Latent heat of evaporation ($kJ\ kg^{-1}$)	260	1162.2	913	585.6
Stoichiometric air to fuel ratio	14.3	6.5	9	11.21
Octane number	17	111	103	96
Low heat value ($MJ\ kg^{-1}$)	42.5	20.1	26.9	30.63
Auto-ignition temperature (°C)	250	463	420	343

Relatively high latent heat of evaporation and low heat value of methanol was reported to reduce the emissions of carbon monoxide, hydrocarbon and soot by 30.08, 51.56 and 76.86%, respectively, in a four-stroke diesel engine fuelled with a blend of 20% methanol in diesel (Zhang et al. 2022). Another study reported that with the increase in alcohol blending proportion from 0 to 40% in diesel, the emission of carbon monoxide decreased by 80% in case of diesel-methanol blends, as compared to 38% reduction with diesel-ethanol blends (Jamrozik 2017). This is attributed to the higher content of oxygen and lower content of carbon in the molecules of methanol relative to ethanol.

In addition to improvement in the emission characteristics of engine, blending of methanol with diesel has been reported to upgrade the engine performance characteristics as well. For instance, 20% blend of methanol in diesel led to significant improvement in brake thermal efficiency and brake specific fuel consumption, as compared to pure diesel, and blends of ethanol and n-heptane in diesel at the same concentration under varying engine speed and load (Vargün et al. 2022). Similarly, decrease in brake specific fuel consumption and increase in brake thermal efficiency were observed with the increase in engine load (from 2 to 6 Nm) and proportion of methanol blending in diesel from 0 to 14% (Hassan et al. 2021).

Although many studies have reported the effect of diesel-methanol blends on the emission and performance characteristics of internal combustion engine, however, these are limited to commercially available chemically synthesized methanol.

2.8. Bottlenecks

A detailed review of the current state-of-the-art of methanotrophic methanol production reveals that:

- Efficient methanotrophic methanol production is constrained by low titers of methanotrophic biomass and methanol.

- Inferior mass transfer and low solubility of methane and CO_2 in liquid medium are the primary challenges limiting the titers of biomass and methanol.
- Low methanol titer is imposing difficulty in the recovery of methanol from fermentation medium, thereby obstructing its potential application as an alternate transportation fuel.
- Alternative fuel technology is relying on chemical methods for methanol synthesis which are energy-intensive, as well as economically and environmentally non-sustainable.

2.9. References

1. Ali S, Sørensen K, Nielsen MP (2020) Modeling a novel combined solid oxide electrolysis cell (SOEC) - Biomass gasification renewable methanol production system. Renew Energy 154:1025–1034. https://doi.org/10.1016/J.RENENE.2019.12.108
2. AlSayed A, Fergala A, Khattab S, et al (2018) Optimization of methane bio-hydroxylation using waste activated sludge mixed culture of type I methanotrophs as biocatalyst. Appl Energy 211:755–763. https://doi.org/10.1016/J.APENERGY.2017.11.090
3. Amulya K, Kopperi H, Venkata Mohan S (2020) Tunable production of succinic acid at elevated pressures of CO2 in a high pressure gas fermentation reactor. Bioresour Technol 309:123327. https://doi.org/10.1016/J.BIORTECH.2020.123327
4. Bai Z, Liu Q, Gong L, Lei J (2019) Investigation of a solar-biomass gasification system with the production of methanol and electricity: Thermodynamic, economic and off-design operation. Appl Energy 243:91–101. https://doi.org/10.1016/J.APENERGY.2019.03.132

5. Baxter NJ, Hirt RP, Bodrossy L, et al (2002) The ribulose-1,5-bisphosphate carboxylase/oxygenase gene cluster of Methylococcus capsulatus (Bath). Arch Microbiol 177:279–289. https://doi.org/10.1007/S00203-001-0387-X
6. Bennett RK, Dzvova N, Dillon M, et al (2021) Expression of soluble methane monooxygenase in Escherichia coli enables methane conversion. bioRxiv 2021.08.05.455234. https://doi.org/10.1101/2021.08.05.455234
7. Bozbag SE, Sot P, Nachtegaal M, et al (2018) Direct Stepwise Oxidation of Methane to Methanol over Cu-SiO2. ACS Catal 8:5721–5731. https://doi.org/10.1021/ACSCATAL.8B01021
8. Cantera S, Estrada JM, Lebrero R, et al (2016) Comparative performance evaluation of conventional and two-phase hydrophobic stirred tank reactors for methane abatement: Mass transfer and biological considerations. Biotechnol Bioeng 113:1203–1212. https://doi.org/10.1002/BIT.25897
9. Cattaneo CR, Rodríguez Y, Rene ER, et al (2022) Biogas bioconversion into poly(3-hydroxybutyrate) by a mixed microbial culture in a novel Taylor flow bioreactor. Waste Management 150:364–372. https://doi.org/10.1016/J.WASMAN.2022.07.017
10. Chang K, Wang T, Chen JG (2017) Hydrogenation of CO2 to methanol over CuCeTiOx catalysts. Appl Catal B 206:704–711. https://doi.org/10.1016/J.APCATB.2017.01.076
11. Chen Z, He J, Chen H, et al (2021) Comparative study on the combustion and emissions of dual-fuel common rail engines fueled with diesel/methanol, diesel/ethanol, and diesel/n-butanol. Fuel 304:121360. https://doi.org/10.1016/J.FUEL.2021.121360
12. Chidambarampadmavathy K, Obulisamy P. K, Heimann K (2015) Role of copper and iron in methane oxidation and bacterial biopolymer accumulation. Eng Life Sci 15:387–399. https://doi.org/10.1002/ELSC.201400127

13. Cho S, Lee YS, Chai H, et al (2022) Enhanced production of ectoine from methane using metabolically engineered Methylomicrobium alcaliphilum 20Z. Biotechnology for Biofuels and Bioproducts 15:1–13. https://doi.org/10.1186/S13068-022-02104-2
14. Crombie A, Murrell JC (2011) Development of a System for Genetic Manipulation of the Facultative Methanotroph Methylocella silvestris BL2. Methods Enzymol 495:119–133. https://doi.org/10.1016/B978-0-12-386905-0.00008-5
15. Dalena F, Senatore A, Marino A, et al (2018) Methanol Production and Applications: An Overview. Methanol: Science and Engineering 3–28. https://doi.org/10.1016/B978-0-444-63903-5.00001-7
16. Dedysh SN, Horz HP, Dunfield PF, Liesack W (2001) A novel pmoA lineage represented by the acidophilic methanotrophic bacterium Methylocapsa acidophila B2. Arch Microbiol 177:117–121. https://doi.org/10.1007/S00203-001-0362-6
17. Dedysh SN, Khmelenina VN, Suzina NE, et al (2002) Methylocapsa acidiphila gen. nov., sp. nov., a novel methane-oxidizing and dinitrogen-fixing acidophilic bacterium from Sphagnum bog. Int J Syst Evol Microbiol 52:251–261. https://doi.org/10.1099/00207713-52-1-251
18. Doran PM (1995) Bioprocess Engineering Principles, second ed. Elsevier
19. Duan C, Luo M, Xing X (2011) High-rate conversion of methane to methanol by Methylosinus trichosporium OB3b. Bioresour Technol 102:7349–7353. https://doi.org/10.1016/J.BIORTECH.2011.04.096
20. Duan Z, Mao S (2006) A thermodynamic model for calculating methane solubility, density and gas phase composition of methane-bearing aqueous fluids from 273 to 523 K and from 1 to 2000 bar. Geochim Cosmochim Acta 70:3369–3386. https://doi.org/10.1016/J.GCA.2006.03.018

21. Fei Q, Guarnieri MT, Tao L, et al (2014) Bioconversion of natural gas to liquid fuel: Opportunities and challenges. Biotechnol Adv 32:596–614. https://doi.org/10.1016/J.BIOTECHADV.2014.03.011
22. Frei MS, Mondelli C, García-Muelas R, et al (2019) Atomic-scale engineering of indium oxide promotion by palladium for methanol production via CO2 hydrogenation. Nature Communications 2019 10:1 10:1–11. https://doi.org/10.1038/s41467-019-11349-9
23. Ge X, Yang L, Sheets JP, et al (2014) Biological conversion of methane to liquid fuels: Status and opportunities. Biotechnol Adv 32:1460–1475. https://doi.org/10.1016/J.BIOTECHADV.2014.09.004
24. Ghaz-Jahanian MA, Khoshfetrat AB, Hosseinian Rostami M, Haghighi M (2018) An innovative bioprocess for methane conversion to methanol using an efficient methane transfer chamber coupled with an airlift bioreactor. Chemical Engineering Research and Design 134:80–89. https://doi.org/10.1016/J.CHERD.2018.03.039
25. Gregory GJ, Bennett RK, Papoutsakis ET (2022) Recent advances toward the bioconversion of methane and methanol in synthetic methylotrophs. Metab Eng 71:99–116. https://doi.org/10.1016/J.YMBEN.2021.09.005
26. Han B, Su T, Wu H, et al (2009) Paraffin oil as a “methane vector” for rapid and high cell density cultivation of methylosinus trichosporium OB3b. Appl Microbiol Biotechnol 83:669–677. https://doi.org/10.1007/S00253-009-1866-2
27. Han B, Yang Y, Xu Y, et al (2016) A review of the direct oxidation of methane to methanol. Cuihua Xuebao/Chinese Journal of Catalysis 37:1206–1215. https://doi.org/10.1016/S1872-2067(15)61097-X
28. Han JS, Ahn CM, Mahanty B, Kim CG (2013) Partial oxidative conversion of methane to methanol through selective inhibition of methanol dehydrogenase in methanotrophic

consortium from landfill cover soil. Appl Biochem Biotechnol 171:1487–1499. https://doi.org/10.1007/S12010-013-0410-0

29. Hanson RS, Hanson TE (1996) Methanotrophic bacteria. Microbiol Rev 60:439–471. https://doi.org/10.1128/MR.60.2.439-471.1996
30. Hassan QH, Shaker Abdul Ridha G, Hafedh KAH, Alalwan HA (2021) The impact of Methanol-Diesel compound on the performance of a Four-Stroke CI engine. Mater Today Proc 42:1993–1999. https://doi.org/10.1016/J.MATPR.2020.12.247
31. Henard CA, Akberdin IR, Kalyuzhnaya MG, Guarnieri MT (2019) Muconic acid production from methane using rationally-engineered methanotrophic biocatalysts. Green Chemistry 21:6731–6737. https://doi.org/10.1039/C9GC03722E
32. Jamrozik A (2017) The effect of the alcohol content in the fuel mixture on the performance and emissions of a direct injection diesel engine fueled with diesel-methanol and diesel-ethanol blends. Energy Convers Manag 148:461–476. https://doi.org/10.1016/J.ENCONMAN.2017.06.030
33. Jeong J, Kim TH, Jang N, et al (2023) A highly efficient and versatile genetic engineering toolkit for a methanotroph-based biorefinery. Chemical Engineering Journal 453:139911. https://doi.org/10.1016/J.CEJ.2022.139911
34. Kalyuzhnaya MG (2016) Methane Biocatalysis: Selecting the Right Microbe. Biotechnology for Biofuel Production and Optimization 353–383. https://doi.org/10.1016/B978-0-444-63475-7.00013-3
35. Kalyuzhnaya MG, Puri AW, Lidstrom ME (2015) Metabolic engineering in methanotrophic bacteria. Metab Eng 29:142–152. https://doi.org/10.1016/J.YMBEN.2015.03.010

36. Keller M, Sharma A (2022) Reverse Boudouard reforming produces CO directly suitable for the production of methanol from CO2 and CH4. Chemical Engineering Journal 431:134127. https://doi.org/10.1016/J.CEJ.2021.134127

37. Kim HG, Han GH, Kim SW (2010) Optimization of lab scale methanol production by methylosinus trichosporium OB3b. Biotechnology and Bioprocess Engineering 15:476–480. https://doi.org/10.1007/S12257-010-0039-6

38. Kim HJ, Huh J, Kwon YW, et al (2019) Biological conversion of methane to methanol through genetic reassembly of native catalytic domains. Nature Catalysis 2019 2:4 2:342–353. https://doi.org/10.1038/s41929-019-0255-1

39. Kim IT, Yoo YS, Yoon YH, et al (2018) Bio-Methanol Production Using Treated Domestic Wastewater with Mixed Methanotroph Species and Anaerobic Digester Biogas. Water 2018, Vol 10, Page 1414 10:1414. https://doi.org/10.3390/W10101414

40. Kim Y, Kim TY, Lee H, Yi J (2017) Distinct activation of Cu-MOR for direct oxidation of methane to methanol. Chemical Communications 53:4116–4119. https://doi.org/10.1039/C7CC00467B

41. Koo CW, Rosenzweig AC (2021) Biochemistry of aerobic biological methane oxidation. Chem Soc Rev 50:3424–3436. https://doi.org/10.1039/D0CS01291B

42. Kumar P, Kumar A, Sreedhar B, et al (2014) Cobalt phthalocyanine immobilized on graphene oxide: An efficient visible-active catalyst for the photoreduction of carbon dioxide. Chemistry - A European Journal 20:6154–6161. https://doi.org/10.1002/CHEM.201304189

43. Le HTQ, Nguyen AD, Park YR, Lee EY (2021) Sustainable biosynthesis of chemicals from methane and glycerol via reconstruction of multi-carbon utilizing pathway in obligate methanotrophic bacteria. Microb Biotechnol 14:2552–2565. https://doi.org/10.1111/1751-7915.13809

44. Li Y, Hu Y, Chu J, et al (2023) Investigation of renewable methanol production from CO2 hydrogeneration based on spectral splitting and heat integration. Fuel 352:129041. https://doi.org/10.1016/J.FUEL.2023.129041

45. Mai DHA, Nguyen TT, Lee EY (2021) The ethylmalonyl-CoA pathway for methane-based biorefineries: a case study of using Methylosinus trichosporium OB3b, an alpha-proteobacterial methanotroph, for producing 2-hydroxyisobutyric acid and 1,3-butanediol from methane. Green Chemistry 23:7712–7723. https://doi.org/10.1039/D1GC02866A

46. Maurya RK, Saxena MR (2018) Characterization of ringing intensity in a hydrogen-fueled HCCI engine. Int J Hydrogen Energy 43:9423–9437. https://doi.org/10.1016/J.IJHYDENE.2018.03.194

47. Nguyen AD, Hwang IY, Lee OK, et al (2018) Systematic metabolic engineering of Methylomicrobium alcaliphilum 20Z for 2,3-butanediol production from methane. Metab Eng 47:323–333. https://doi.org/10.1016/J.YMBEN.2018.04.010

48. Nguyen LT, Lee EY (2019) Biological conversion of methane to putrescine using genome-scale model-guided metabolic engineering of a methanotrophic bacterium Methylomicrobium alcaliphilum 20Z. Biotechnol Biofuels 12:1–12. https://doi.org/10.1186/S13068-019-1490-Z

49. Nguyen TT, Lee OK, Naizabekov S, Lee EY (2020) Bioconversion of methane to cadaverine and lysine using an engineered type II methanotroph, Methylosinus trichosporium OB3b. Green Chemistry 22:7803–7811. https://doi.org/10.1039/D0GC02232B

50. Ning L, Duan Q, Chen Z, et al (2020) A comparative study on the combustion and emissions of a non-road common rail diesel engine fueled with primary alcohol fuels

(methanol, ethanol, and n-butanol)/diesel dual fuel. Fuel 266:117034. https://doi.org/10.1016/J.FUEL.2020.117034

51. Park S yeong, Kim C gyun (2019) Application and development of methanotrophs in environmental engineering. J Mater Cycles Waste Manag 21:415–422. https://doi.org/10.1007/S10163-018-00826-W
52. Patel SKS, Gupta RK, Kalia VC, Lee JK (2022) Synthetic design of methanotroph co-cultures and their immobilization within polymers containing magnetic nanoparticles to enhance methanol production from wheat straw-based biogas. Bioresour Technol 364:128032. https://doi.org/10.1016/J.BIORTECH.2022.128032
53. Patel SKS, Gupta RK, Kalia VC, Lee JK (2021a) Integrating anaerobic digestion of potato peels to methanol production by methanotrophs immobilized on banana leaves. Bioresour Technol 323:124550. https://doi.org/10.1016/J.BIORTECH.2020.124550
54. Patel SKS, Gupta RK, Kim I-W, Lee J-K (2023a) Encapsulation of Methanotrophs within a Polymeric Matrix Containing Copper- and Iron-Based Nanoparticles to Enhance Methanol Production from a Simulated Biogas. Polymers (Basel) 15:3667. https://doi.org/10.3390/polym15183667
55. Patel SKS, Gupta RK, Kondaveeti S, et al (2020a) Conversion of biogas to methanol by methanotrophs immobilized on chemically modified chitosan. Bioresour Technol 315:. https://doi.org/10.1016/j.biortech.2020.123791
56. Patel SKS, Gupta RK, Kumar V, et al (2020b) Biomethanol Production from Methane by Immobilized Co-cultures of Methanotrophs. Indian J Microbiol 60:318–324. https://doi.org/10.1007/S12088-020-00883-6
57. Patel SKS, Jeon MS, Gupta RK, et al (2019) Hierarchical Macroporous Particles for Efficient Whole-Cell Immobilization: Application in Bioconversion of Greenhouse

Gases to Methanol. ACS Appl Mater Interfaces 11:18968–18977. https://doi.org/10.1021/ACSAMI.9B03420

58. Patel SKS, Kalia VC, Joo JB, et al (2020c) Biotransformation of methane into methanol by methanotrophs immobilized on coconut coir. Bioresour Technol 297:122433. https://doi.org/10.1016/J.BIORTECH.2019.122433
59. Patel SKS, Kalia VC, Lee JK (2023b) Integration of biogas derived from dark fermentation and anaerobic digestion of biowaste to enhance methanol production by methanotrophs. Bioresour Technol 369:128427. https://doi.org/10.1016/J.BIORTECH.2022.128427
60. Patel SKS, Kondaveeti S, Otari S V., et al (2018a) Repeated batch methanol production from a simulated biogas mixture using immobilized Methylocystis bryophila. Energy 145:477–485. https://doi.org/10.1016/J.ENERGY.2017.12.142
61. Patel SKS, Kumar V, Mardina P, et al (2018b) Methanol production from simulated biogas mixtures by co-immobilized Methylomonas methanica and Methylocella tundrae. Bioresour Technol 263:25–32. https://doi.org/10.1016/J.BIORTECH.2018.04.096
62. Patel SKS, Mardina P, Kim D, et al (2016a) Improvement in methanol production by regulating the composition of synthetic gas mixture and raw biogas. Bioresour Technol 218:202–208. https://doi.org/10.1016/J.BIORTECH.2016.06.065
63. Patel SKS, Mardina P, Kim SY, et al (2016b) Biological Methanol Production by a Type II Methanotroph Methylocystis bryophila. J Microbiol Biotechnol 26:717–724. https://doi.org/10.4014/JMB.1601.01013
64. Patel SKS, Selvaraj C, Mardina P, et al (2016c) Enhancement of methanol production from synthetic gas mixture by Methylosinus sporium through covalent immobilization. Appl Energy 171:383–391. https://doi.org/10.1016/J.APENERGY.2016.03.022

65. Patel SKS, Shanmugam R, Kalia VC, Lee JK (2020d) Methanol production by polymer-encapsulated methanotrophs from simulated biogas in the presence of methane vector. Bioresour Technol 304:123022. https://doi.org/10.1016/J.BIORTECH.2020.123022

66. Patel SKS, Shanmugam R, Lee JK, et al (2021b) Biomolecules Production from Greenhouse Gases by Methanotrophs. Indian Journal of Microbiology 2021 61:4 61:449–457. https://doi.org/10.1007/S12088-021-00986-8

67. Patel SKS, Singh RK, Kumar A, et al (2017) Biological methanol production by immobilized Methylocella tundrae using simulated biohythane as a feed. Bioresour Technol 241:922–927. https://doi.org/10.1016/J.BIORTECH.2017.05.160

68. Pen N, Soussan L, Belleville MP, et al (2014) An innovative membrane bioreactor for methane biohydroxylation. Bioresour Technol 174:42–52. https://doi.org/10.1016/J.BIORTECH.2014.10.001

69. Razumovsky SD, Efremenko EN, Makhlis TA, et al (2008) Effect of immobilization on the main dynamic characteristics of the enzymatic oxidation of methane to methanol by bacteria Methylosinus sporium B-2121. Russian Chemical Bulletin 57:1633–1636. https://doi.org/10.1007/S11172-008-0211-8

70. Rocha-Rios J, Bordel S, Hernández S, Revah S (2009) Methane degradation in two-phase partition bioreactors. Chemical Engineering Journal 152:289–292. https://doi.org/10.1016/J.CEJ.2009.04.028

71. Rocha-Rios J, Kraakman NJR, Kleerebezem R, et al (2013) A capillary bioreactor to increase methane transfer and oxidation through Taylor flow formation and transfer vector addition. Chemical Engineering Journal 217:91–98. https://doi.org/10.1016/J.CEJ.2012.11.065

72. Rocha-Rios J, Muñoz R, Revah S (2010) Effect of silicone oil fraction and stirring rate on methane degradation in a stirred tank reactor. Journal of Chemical Technology & Biotechnology 85:314–319. https://doi.org/10.1002/JCTB.2339

73. Rocha-Rios J, Quijano G, Thalasso F, et al (2011) Methane biodegradation in a two-phase partition internal loop airlift reactor with gas recirculation. Journal of Chemical Technology & Biotechnology 86:353–360. https://doi.org/10.1002/JCTB.2523

74. Rodríguez Y, Firmino PIM, Pérez V, et al (2020) Biogas valorization via continuous polyhydroxybutyrate production by Methylocystis hirsuta in a bubble column bioreactor. Waste Management 113:395–403. https://doi.org/10.1016/j.wasman.2020.06.009

75. Sahoo KK, Datta S, Goswami G, Das D (2022) Two-stage integrated process for bio-methanol production coupled with methane and carbon dioxide sequestration: Kinetic modelling and experimental validation. J Environ Manage 301:113927. https://doi.org/10.1016/J.JENVMAN.2021.113927

76. Sahoo KK, Goswami G, Das D (2021) Biotransformation of Methane and Carbon Dioxide Into High-Value Products by Methanotrophs: Current State of Art and Future Prospects. Front Microbiol 12:. https://doi.org/10.3389/FMICB.2021.636486

77. Sahoo KK, Sinha A, Das D (2023) Process engineering strategy for improved methanol production in Methylosinus trichosporium through enhanced mass transfer and solubility of methane and carbon dioxide. Bioresour Technol 371:128603. https://doi.org/10.1016/J.BIORTECH.2023.128603

78. Sheets JP, Lawson K, Ge X, et al (2017) Development and evaluation of a trickle bed bioreactor for enhanced mass transfer and methanol production from biogas. Biochem Eng J 122:103–114. https://doi.org/10.1016/J.BEJ.2017.03.006

79. Su Z, Ge X, Zhang W, et al (2017) Methanol Production from Biogas with a Thermotolerant Methanotrophic Consortium Isolated from an Anaerobic Digestion

System. Energy and Fuels 31:2970–2975. https://doi.org/10.1021/ACS.ENERGYFUELS.6B03471

80. Taylor A, Molzahn P, Bushnell T, et al (2018) Immobilization of Methylosinus trichosporium OB3b for methanol production. J Ind Microbiol Biotechnol 45:201–211. https://doi.org/10.1007/S10295-018-2010-Z
81. Torre A, Metivier A, Chu F, et al (2015) Genome-scale metabolic reconstructions and theoretical investigation of methane conversion in Methylomicrobium buryatense strain 5G(B1). Microb Cell Fact 14:1–15. https://doi.org/10.1186/S12934-015-0377-3
82. Van Hecke W, Bockrath R, De Wever H (2019) Effects of moderately elevated pressure on gas fermentation processes. Bioresour Technol 293:122129. https://doi.org/10.1016/J.BIORTECH.2019.122129
83. Vargün M, Yılmaz lker T, Sayın C (2022) Investigation of performance, combustion and emission characteristics in a diesel engine fueled with methanol/ethanol/nHeptane/diesel blends. Energy 257:124740. https://doi.org/10.1016/J.ENERGY.2022.124740
84. Verhelst S, Turner JW, Sileghem L, Vancoillie J (2019) Methanol as a fuel for internal combustion engines. Prog Energy Combust Sci 70:43–88. https://doi.org/10.1016/j.pecs.2018.10.001
85. Wang L, Yi Y, Wu C, et al (2017) One-Step Reforming of CO2 and CH4 into High-Value Liquid Chemicals and Fuels at Room Temperature by Plasma-Driven Catalysis. Angewandte Chemie - International Edition 56:13679–13683. https://doi.org/10.1002/ANIE.201707131
86. Xin JY, Cui JR, Niu JZ, et al (2004) Production of methanol from methane by methanotrophic bacteria. Biocatalysis and Biotransformation 22:225-229. https://doi.org/10.1080/10242420412331283305

87. Xin JY, Zhang YX, Zhang S, et al (2007) Methanol production from CO2 by resting cells of the methanotrophic bacterium Methylosinus trichosporium IMV 3011. J Basic Microbiol 47:426–435. https://doi.org/10.1002/JOBM.200710313

88. Yan X, Chu F, Puri AW, et al (2016) Electroporation-based genetic manipulation in type I methanotrophs. Appl Environ Microbiol 82:2062–2069. https://doi.org/10.1128/AEM.03724-15

89. Yu Y, Ramsay JA, Ramsay BA (2009) Production of soluble methane monooxygenase during growth of Methylosinus trichosporium on methanol. J Biotechnol 139:78–83. https://doi.org/10.1016/J.JBIOTEC.2008.09.005

90. Zhang Z, Tian J, Li J, et al (2022) Investigation on combustion, performance and emission characteristics of a diesel engine fueled with diesel/alcohol/n-butanol blended fuels. Fuel 320:123975. https://doi.org/10.1016/J.FUEL.2022.123975

91. Zhen X, Wang Y (2015) An overview of methanol as an internal combustion engine fuel. Renewable and Sustainable Energy Reviews 52:477–493. https://doi.org/10.1016/J.RSER.2015.07.083

Web references

1. Global Methane Tracker (2023). International Energy Agency. https://www.iea.org/news/methane-emissions-remained-stubbornly-high-in-2022-even-as-soaring-energy-prices-made-actions-to-reduce-them-cheaper-than-ever. (Accessed 30 September 2023).

2. International Energy Agency (2023). https://www.iea.org/news/global-co2-emissions-rose-less-than-initially-feared-in-2022-as-clean-energy-growth-offset-much-of-the-impact-of-greater-coal-and-oil-use. (Accessed 30 September 2023).

3. IPCC (2018). Summary for Policymakers. In: *Global Warming of 1.5°C. An IPCC Special Report on the impacts of global warming of 1.5°C above pre-industrial levels and related global greenhouse gas emission pathways, in the context of strengthening the global response to the threat of climate change, sustainable development, and efforts to eradicate poverty.* https://www.ipcc.ch/sr15/chapter/spm/. (Accessed 01 November 2023).
4. The Paris Agreement (2016). United Nations Climate Change. https://unfccc.int/process-and-meetings/the-paris-agreement. (Accessed 01 November 2023).
5. Trends in Atmospheric Carbon Dioxide (2023). NOAA-ESRL. https://gml.noaa.gov/ccgg/trends/data.html. (Accessed 30 September 2023).
6. Trends in Atmospheric Methane (2023). NOAA-ESRL. https://gml.noaa.gov/ccgg/trends_ch4/. (Accessed 30 September 2023).
7. Understanding Global Warming Potentials (2023). United States Environmental Protection Agency. https://www.epa.gov/ghgemissions/understanding-global-warming-potentials. (Accessed 01 November 2023).
8. United Nations Climate Action (2022). https://www.un.org/en/climatechange/net-zero-coalition. (Accessed 01 November 2023).

CHAPTER 3

Characterization of *M. trichosporium* NCIMB 11131 for growth and methanol production using methane and CO_2, respectively

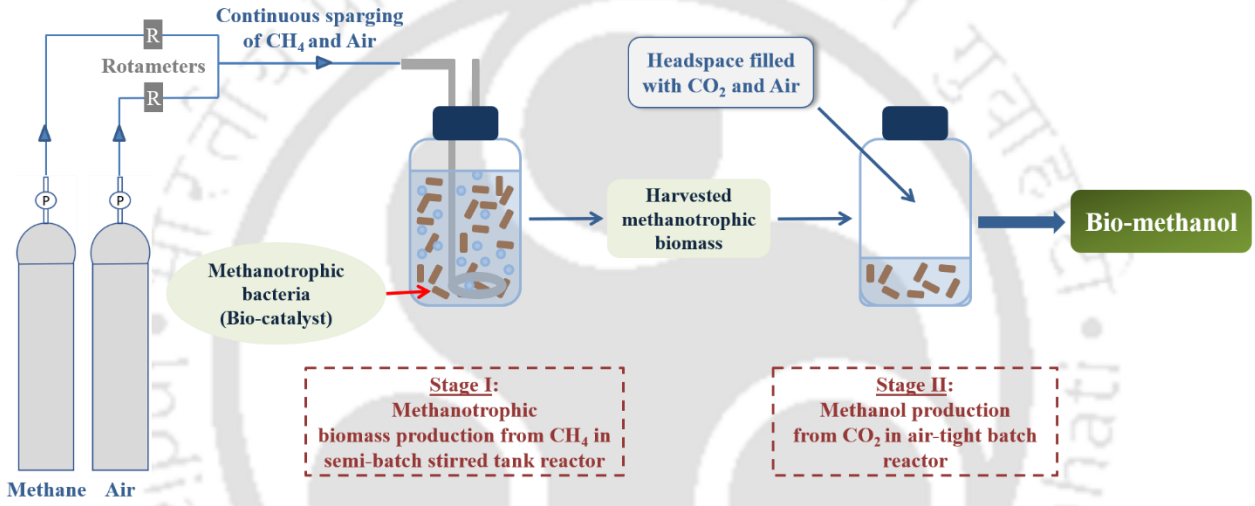

Fig. 3.1. Graphical abstract

3.1. Background and motivation

Emission of greenhouse gases, *viz.*, methane and carbon dioxide, has been increasing globally at an alarming rate hitting the global average atmospheric concentrations of 1911.82 ppb and 418.53 ppm, respectively, in 2022 (NOAA-ESRL, 2023). There are ongoing efforts to transform these greenhouse gases into various value-added chemicals and liquid fuels, such as methanol (Wang et al., 2017). Methanol is a widely used industrial solvent, a precursor for synthesis of other chemicals (*e.g.*, formaldehyde, acetic acid, dimethyl ether and methyl tert-butyl ether), and a potential fuel for transportation (Dalena et al., 2018; Verhelst et al., 2019). However, the conventionally used chemical routes for methanol production are constrained by

the requirement of: (i) expensive catalysts, (ii) extreme process conditions, *e.g.*, high temperature (~850 °C) and pressure (~100 bar), and (iii) release of toxic by-products, such as carbon monoxide (Ali et al., 2020; Keller and Sharma, 2022; Kumar et al., 2014; Li et al., 2023).

Alternatively, methanotrophic microorganisms can be used as potential biocatalyst to mitigate these noxious C1-carbon compounds under mild operating conditions, without the requirement of expensive chemical catalysts and release of toxic by-products, and thereby attaining better economic and environmental viability. Methanotrophs are Gram-negative proteobacteria that utilize methane as their sole source of carbon and energy for growth. Methane, bio sequestered by methanotrophs, is catalytically oxidized into methanol by methane monooxygenase (MMO), an endogenous irreversible enzyme. The produced methanol gets subsequently converted into formaldehyde, formate, and CO_2 via sequential oxidations catalysed by three reversible enzymes: methanol dehydrogenase (MDH), formaldehyde dehydrogenase and formate dehydrogenase, respectively (Sahoo et al., 2021; Xin et al., 2007). There have been initiatives on methanol production via MMO catalysed biological oxidation of methane (Mardina et al., 2016; Patel et al., 2020b). However, MDH and other enzymes cause subsequent sequential oxidation of the produced methanol into intermediate metabolites and CO_2, thus limiting extracellular methanol accumulation (Sheets et al., 2016). To that end, various MDH inhibitors (*e.g.*, NaCl, NH_4Cl, phosphate, EDTA and $MgCl_2$) are supplemented in the fermentation media to prevent methanol oxidation (Patel et al., 2016c; Sheets et al., 2016). However, the MDH inhibitor-induced inhibition of methanol oxidation result in depletion of NADH, an essential co-factor required for the activity of MMO (Sahoo et al., 2021). Therefore, formate is exogenously added as a source of NADH to maintain the activity of MMO in presence of MDH inhibitors and achieve improved methanol titer (Patel et al.,

2020c; Sheets et al., 2016). But the use of MDH inhibitors and formate increase the overall cost of production.

Even with all these initiatives, a lower methanol titer in the range of 0.16 - 0.4 g L^{-1} (Hwang et al., 2015; Mardina et al., 2016; Patel et al., 2016c) has been achieved under native conditions in batch mode. Moreover, methanol production through biological oxidation of methane is constrained by high cost of pure CH_4 as feed, low methanol titer associated with low solubility of CH_4 in liquid medium, low CH_4 utilization efficiency and consequent slow growth rate of methanotrophs, and so on. Researchers have tried to overcome these limitations through the use of biogas as low-cost feedstock (Patel et al., 2020a; Sheets et al., 2016), immobilization of cells/biocatalyst (Patel et al., 2020a, 2020b), repeated-batch cultures for reusability of cells (Patel et al., 2020a, 2020c), co-culture of cells for improved biocatalytic activity (Patel et al., 2020b) and, addition of methane vector to improve solubility (Patel et al., 2020c). An alternative to the current approaches could be the utilization of CO_2, the end-product in the methanotrophic metabolism, as feedstock for methanol production. CO_2, when fed to the cells in excess concentration, shifts the equilibrium in the backward direction (Xin et al., 2007). Since the activity of MMO is irreversible, the process results in the accumulation of methanol as an extracellular end-product (Xin et al., 2007).

The present chapter reports a sequential two-stage integrated process for bio-methanol production using *Methylosinus trichosporium* NCIMB 11131, coupled with the sequestration of methane and carbon dioxide. While the first stage of the process involves generation of methanotrophic biomass via sequestration of methane as the sole carbon source, the second stage deals with the application of this biomass as biocatalyst for the reduction of CO_2 into methanol. High biomass titer and improved methane sequestration were achieved in the first stage via optimization of process parameters, *e.g.*, methane concentration in the inlet gas stream and flow rate of the gas mixture in a semi-batch stirred tank reactor, and composition of other

limiting nutrients in the growth medium. Further, to achieve an improved methanol titer in the second stage, selection of appropriate process design for methanol production from CO_2, and optimization of CO_2 concentration in the headspace and liquid to headspace volume ratio were carried out in an air-tight batch reactor.

3.2. Materials and methods

3.2.1. Organism and inoculum preparation

Methylosinus trichosporium NCIMB 11131 was procured from National Collection of Industrial Food and Marine Bacteria and was cultured on nitrate mineral salt (NMS) medium containing (g L^{-1}): KNO_3 (1.0), $MgSO_4.6H_2O$ (1.0), $CaCl_2$ (0.2), Fe-EDTA (0.0038), $Na_2MoO_4.2H_2O$ (0.00026), $Na_2HPO_4.12H_2O$ (0.716), and KH_2PO_4 (0.26). Trace metal solution (1 mL) containing (g L^{-1}): $CuSO_4.5H_2O$ (0.2), $FeSO_4.7H_2O$ (0.5), $ZnSO_4.7H_2O$ (0.4), H_3BO_3 (0.015), $CoCl_2.6H_2O$ (0.05), EDTA di-sodium salt (0.25), $MnCl_2.4H_2O$ (0.02), and $NiCl_2.6H_2O$ (0.01) was added to the media. The pH of the medium was adjusted to 6.8 using 1 M NaOH and 1 M H_2SO_4. All the chemicals were of analytical grade and procured from Himedia. All the reagents were prepared in Milli-Q water (18 MΩ). Inoculum preparation was carried out by culturing the cells in 500 mL customized air-tight bottles containing 100 mL of NMS medium at 30 °C in a shaker incubator (ORBITEK, Scigenics Biotech) at 150 rpm with intermittent sparging of methane and air. The mid-log phase culture (10% v/v) with an optical density of 5 was used as inoculum for all experiments.

3.2.2. Generation of methanotrophic biomass coupled with CH_4 sequestration

3.2.2.1. Characterisation of the organism in air-tight batch reactor

In the first step, characterization of the organism in terms of growth and CH_4 utilization was carried out in customized air-tight batch reactors (Borosil reagent bottles fitted with Duran bromo-butyl rubber stoppers) of 250 mL capacity with a working volume of 32 mL of NMS medium, under different concentrations of CH_4 (5%, 10%, 15%, 20%, 40%, 60%, and 80%

v/v) in the headspace mixed with air. The organism was grown at 30 °C in a shaker incubator (ORBITEK, Scigenics Biotech) at 150 rpm for 96 h. Sampling was carried out at an interval of 24 h to obtain the dynamic profiles for growth and CH_4 utilization from headspace.

3.2.2.2. Characterisation of the organism in semi-batch stirred tank reactor

In the next step, the characterization of the organism was carried out in a customized semi-batch stirred-tank reactor (Fig. 3.2a) of 1 L capacity containing 800 mL NMS medium under varying concentrations of CH_4 mixed with air in the inlet gas stream (1%, 2.5%, and 5% v/v) and different inlet gas flow-rates (0.25, 0.5, and 0.75 vvm). The reactor was equipped with a ring sparger with uniform pore sizes for continuous sparging of a gas mixture of methane and air. To maintain the cultivation temperature at 30 °C and facilitate efficient mass transfer of the continuously inflowing gases, the reactor was placed in a water bath on a hot-plate magnetic stirrer (IKA C-MAG HS7) with constant stirring (motor speed: 2.0). The concentration of CH_4 and the flow rate of the inlet gas stream were maintained using rotameters. Sampling was carried out at an interval of 8 h to obtain the dynamic profiles for growth. Methane fixation rate was calculated as per Eq. (3.1)

$$\text{Methane fixation rate } (\text{g L}^{-1}\text{d}^{-1}) = P_x \times E_c \times \left(\frac{16}{12}\right) \quad (3.1)$$

Where, P_x is the biomass productivity (g L^{-1} d^{-1}), E_c is the elemental carbon content in the biomass. 16 and 12 are molecular weight of methane and carbon, respectively.

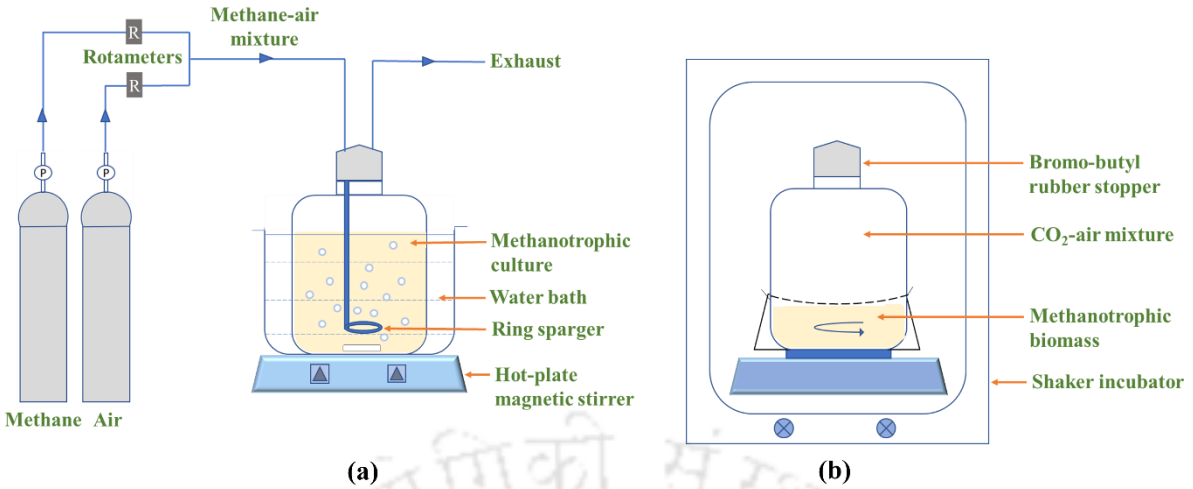

Fig. 3.2. Schematic diagram of (a) semi-batch stirred tank reactor and (b) air-tight batch reactor used for methanotrophic biomass generation and methanol production, respectively.

3.2.2.3. Characterisation of the organism under varying concentrations of limiting components in growth medium

The growth of the organism was evaluated under different concentrations of trace metals (0.5X, 0.75X, 1X, 1.25X and 1.5X unit), by varying the strength of the trace metals stock solution in NMS media. The experiment was carried out in customized semi-batch stirred-tank reactors (as described in section 3.2.2.2) under similar culture conditions. Sampling was done once in every 8 hours to estimate growth. At the end of the batch, culture was centrifuged to collect the cell-free supernatant for analysing the utilisation of nitrate and phosphate.

3.2.3. Methanol production

3.2.3.1. Methanotrophic biomass as biocatalyst for methanol production under different process designs

The methanotrophic biomass, generated from the first stage, was evaluated for its potential to be used as a biocatalyst for methanol production from CO_2 under three different process designs: (i) the biomass was harvested from the first stage of growth and subsequently

resuspended in freshly prepared NMS medium for methanol production in the second stage; (ii) a two-phase fermentation in NMS medium where, in the first phase, the organism was grown with CH_4 as the only carbon source, followed by methanol production in the second phase utilizing CO_2 as the sole carbon source; & (iii) the biomass was harvested from the first stage of growth and subsequently resuspended in 20 mM phosphate buffer medium containing 5 mM $MgCl_2$ (pH 6.8) for methanol production in the second stage. In all the three processes, methanol production experiments (second stage in case of processes i and iii or second phase in case of process ii) were carried out in customized air-tight batch reactors (Borosil reagent bottles fitted with Duran bromo-butyl rubber stoppers) (Fig. 3.2b) supplied with a mixture of CO_2 and air (1:1 v/v) in the headspace. The cultures were incubated at 30 °C and 150 rpm. Sampling was carried out at regular time intervals to obtain dynamic profiles for methanol production and growth.

3.2.3.2. Effect of headspace CO_2 concentration and liquid to headspace volume ratio on methanol production

The effect of CO_2 composition and headspace volume on methanol production was studied in air-tight batch reactors (Fig. 3.2b). The characterization was carried out in 20 mM phosphate buffer (pH 6.8) containing 5 mM $MgCl_2$, using harvested biomass as biocatalyst (3.39 g L^{-1}). The culture was assessed for methanol production at varying CO_2 concentrations (10%, 30%, 40%, 50%, 60%, and 70% v/v) in the headspace with liquid to headspace volume ratio of 10:90. In the next step, the methanol production was evaluated under different liquid to headspace volume ratios (50:50, 40:60, 30:70, 20:80 and 10:90) maintaining optimal headspace CO_2 concentration at 50%. The cultures were incubated at 30 °C and 150 rpm. Sampling was carried out at regular time intervals to obtain dynamic profiles for methanol production and growth.

3.2.4. Analytical methods

To monitor cell growth, absorbance of the culture was measured at 600 nm (A_{600}) using UV-Vis spectrophotometer (Cary Series 100, Agilent Technologies). The absorbance values were converted into dry cell weight (DCW) using the correlation, one optical density = 0.42 g dry cells L^{-1} (R^2 = 0.99). Cell-free supernatant, obtained from centrifugation (HERAEUS, MULTIFUGE X3R Centrifuge, Thermo Scientific) of the sample at 10,000 rpm for 15 min, was analysed for methanol formation. Methanol concentration in the sample was estimated by using high performance liquid chromatography (HPLC) (Ultimate 3000, Dionex, Thermofisher Scientific, Germany) in refractive index detector (RID) using Rezex ROA column (300 × 7.8 mm, Phenomenex) and 0.005 N H_2SO_4 as mobile phase at a flow rate of 0.5 mL min^{-1}, as described previously (Mukherjee et al., 2019) for analysis of alcoholic solvents. Refractive index detector and column oven were kept at 37 °C and room temperature, respectively. Analysis of CH_4 concentration in the headspace of air-tight batch reactor was carried out using gas chromatography (GC) (TRACE 1110, Thermo Scientific) equipped with Packed column (Restek PC2 6952, 15' x 1/8", mesh 80/100) and thermal conductivity detector (TCD). Argon was used as the carrier gas at a flow rate of 12 mL min^{-1}. The oven, injector, and detector temperatures were maintained at 40 °C, 150 °C, and 150 °C, respectively. Elemental composition (C, H, and N) of the biomass was carried out using CHNS analyser (EuroEA Elemental Analyser).

3.3. Results and discussion

In the sequential two-stage integrated process for bio-methanol production, while the first stage involved generation of methanotrophic biomass via sequestration of methane as the sole carbon source; CO_2 was reduced to methanol in the second stage through the application of the methanotrophic biomass as biocatalyst.

3.3.1. First stage of methanotrophic biomass production with concomitant CH_4 sequestration

3.3.1.1. Growth of *M. trichosporium* in air-tight batch reactor

The extent of growth is the critical component that determines the overall performance of the organism in terms of CH_4 sequestration and methanotrophic biomass generation. Therefore, it was essential to characterize the growth kinetics of *M. trichosporium* under various process parameters and modes of operation of the reactor. To that end, the organism was characterized for growth under different headspace gas compositions by varying the methane concentration from 5% to 80% v/v in an air-tight reactor operated under batch mode. Biomass titer was found to increase linearly with the increase in methane concentration from 5% and reached a maximum value of 1.06 g L^{-1} at a methane concentration of 15% (Fig. 3.3a). The maximum biomass productivity and methane fixation rate at 15% v/v CH_4 concentration were calculated to be 0.29 g L^{-1} d^{-1} and 0.154 g L^{-1} d^{-1}, respectively. Further increase in methane concentration beyond 15% resulted in significant reduction in growth of the organism. Low biomass titer at 5% (0.4 g L^{-1}) and 10% (0.67 g L^{-1}) methane concentrations may be attributed to the substrate limitation, as is evident from the complete utilization of methane from headspace within 48 h of cultivation (Fig. 3.3b). However, a reduction in biomass titer at higher methane concentrations of 20%–80% may be attributed to the combinatorial effect of inadequate availability of methane in the liquid phase due to poor mass transfer and decreased concentration of oxygen in the reactor causing interference in the aerobic metabolism of the organism.

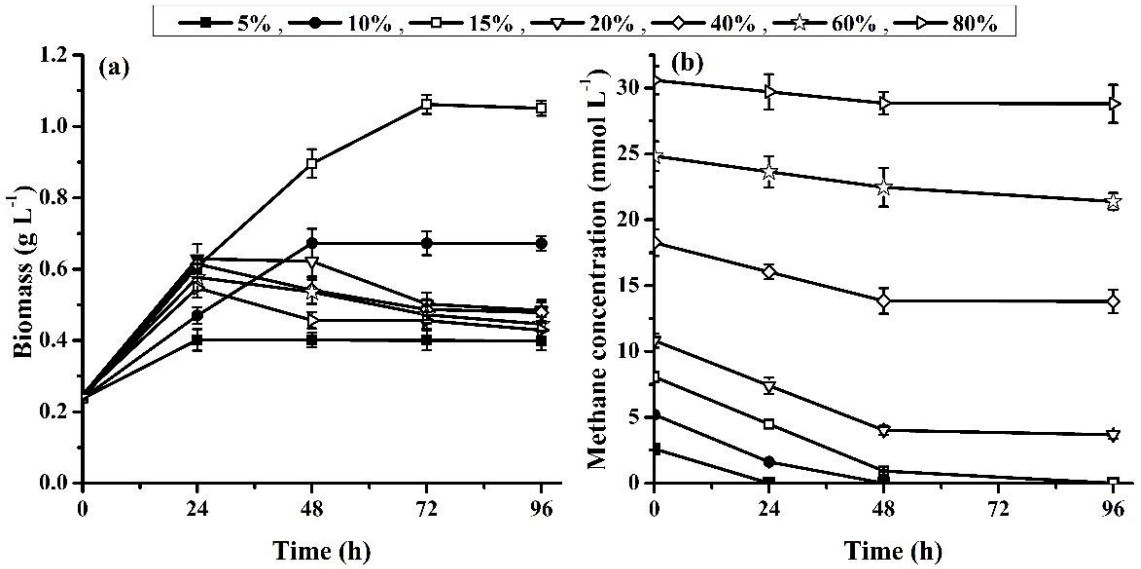

Fig. 3.3. Dynamic profile of (a) biomass and (b) methane concentration in the headspace. The organism was grown under different headspace gas compositions by varying the methane concentration from 5% to 80% v/v in an air-tight batch reactor.

3.3.1.2. Growth of *M. trichosporium* in semi-batch stirred tank reactor

To overcome the key challenges of poor mass transfer of methane and substrate limitation, the growth of the organism was evaluated under continuous sparging of methane and air mixture in a semi-batch stirred tank reactor. At methane concentrations of 1%, 2.5%, and 5% v/v in the inlet gas stream with a flow rate of 0.5 vvm, the biomass titer was found to be comparable at 3.31 g L^{-1}, 3.39 g L^{-1}, and 3.8 g L^{-1}, respectively (Fig. 3.4a). Further, the biomass productivity in the semi-batch mode was estimated to be in the range of 0.49 g L^{-1} d^{-1} – 0.63 g L^{-1} d^{-1} (Fig. 3.4b). The methane fixation rate was estimated to be comparable for growth at 2.5% (0.324 g L^{-1} d^{-1}) and 5% (0.344 g L^{-1} d^{-1}) methane concentration, respectively, albeit a marginally lower value was estimated for 1% methane concentration (0.27 g L^{-1} d^{-1}) (Fig. 3.4b). Even though, the results indicate similar growth performance and methane fixation rate at 2.5% and 5% methane concentration in the inlet gas stream, the latter resulted in higher

amount of unutilized methane being released into the atmosphere. Hence, subsequent experiments under different inlet gas flow rates were carried out with a methane concentration of 2.5%. While, at inlet gas flow rate of 0.25 vvm, biomass titer (2.97 g L^{-1}) and productivity (0.517 g L^{-1} d^{-1}) were compromised marginally, these parameters remained comparable for both 0.5 vvm and 0.75 vvm (Fig. 3.4c, d). A similar profile was observed for methane fixation rate with values of 0.281 g L^{-1} d^{-1}, 0.324 g L^{-1} d^{-1}, and 0.315 g L^{-1} d^{-1} at inlet gas flow rates of 0.25, 0.5, and 0.75 vvm, respectively (Fig. 3.4d). Therefore, in the present study, inlet methane concentration of 2.5% with a gas flow rate of 0.5 vvm was chosen for the generation of methanotrophic biomass in semi-batch stirred tank reactor resulting in biomass titer of 3.39 g L^{-1}, productivity 0.596 g L^{-1} d^{-1} and methane fixation rate of 0.324 g L^{-1} d^{-1}. The semi-batch stirred tank reactor with continuous gas sparging resulted in significant improvement in biomass titer (~3.2-fold), biomass productivity (~2-fold) and methane fixation rate (~2.1-fold), compared to the batch reactor. The semi-batch stirred tank reactor used in the present study enabled continuous supply of gas mixture using a sparger, located above the magnetic stirrer bar, resulting in uniform distribution of the gas bubbles. Constant mixing was achieved using magnetic stirrer, facilitating bottom-driven mass transfer. These attributes of the reactor prevented cell-settling and dead-zone formation thereby offering improved growth kinetics. The mass transfer of methane is the limiting step in the optimal performance of methanotrophic systems due to the low solubility of methane in aqueous solutions. Pauss et al. (1990) reported a three-fold increment in volumetric mass transfer coefficient ($k_L a$) value for CH_4 in a completely stirred tank reactor (0.09 h^{-1}) as compared to sludge bed reactor operated without mechanical stirring (0.03 h^{-1}).

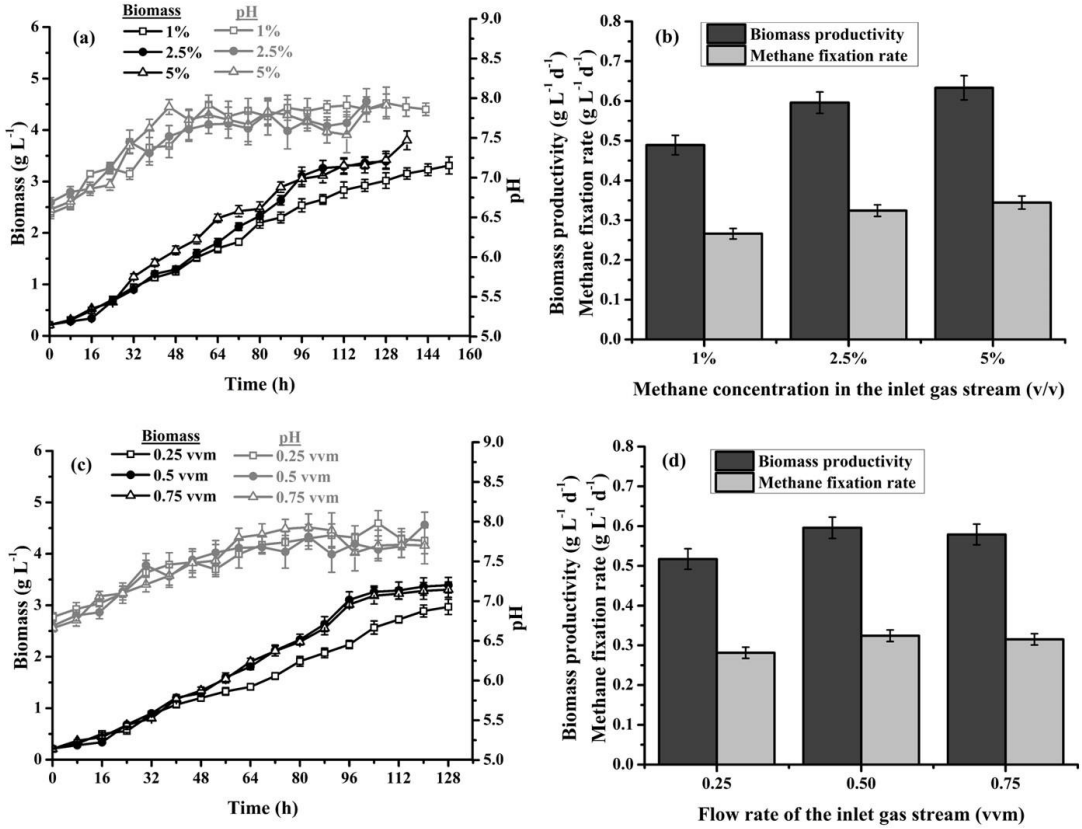

Fig. 3.4. Biomass titer (a & c) and pH (a & c), biomass productivity (b & d) and methane fixation rate (b & d) of *Methylosinus trichosporium* NCIMB 11131. The organism was grown under different methane concentrations in the inlet gas stream and flow rates of the inlet gas stream in a semi-batch stirred tank reactor.

Gilman et al. (2015) reported maximum biomass titer of 0.46 g L^{-1} and average productivity of 0.23 g L^{-1} d^{-1} for continuous cultivation of *Methylomicrobium buryatense* with methane concentration of 2.5% mixed with air and fed at a flow rate of 100 mL min^{-1}. Cultivation of *M. trichosporium* OB3b in 5 L bioreactor with continuous flow of methane (140 mL min^{-1}) and air (1000 mL min^{-1}) for 240 h resulted in biomass titer of 2 g L^{-1} (Han et al., 2009). Therefore, in the present study, biomass titer and productivity achieved for *Methylosinus trichosporium* NCIMB 11131 in semi-batch stirred tank reactor was found to be superior than the studies reported in the literature. The organism also exhibited improved performance in terms methane sequestration ability in comparison to the other methanotrophic fermentation

processes. For instance, under chosen process parameters, both specific methane fixation rate of 45.44 x 10^{-4} g CH_4. g biomass^{-1} h^{-1} and volumetric methane fixation rate of 0.324 g L^{-1} d^{-1} (0.844 mmol h^{-1}) were found to be higher than methanotrophic consortium (7.7 x 10^{-4} g CH_4. g biomass^{-1} h^{-1}) grown in batch reactor containing 8% CH_4 (Cantera et al., 2016) and *Methylocaldum* sp. (0.54 mmol h^{-1}) in a trickle bed reactor (Sheets et al., 2017), respectively. However, higher volumetric methane fixation rate of ~0.984 g L^{-1} d^{-1} was reported for *Methylocystis hirsuta* grown in bubble column bioreactor coupled with internal gas re-circulation (Rodríguez et al., 2020).

Fig. 3.4a and c also present the profiles of pH during the growth of the organism. The pH was observed to vary within a range of 6.8–7.96. A pH range of 7–10 has been reported to be an optimum range for the growth of methanotrophs, via methane oxidation, without any adverse effect on their biocatalytic activity (Reddy et al., 2020).

3.3.1.3. Growth of *M. trichosporium* under varying concentrations of limiting nutrients in NMS medium

In the first step, growth of the organism was evaluated under different concentrations of trace metals (0.5X-1.5X unit) in semi-batch stirred tank reactor (Fig. 3.5). Maximum biomass titer of 4.5 g L^{-1} was achieved with 0.75X unit concentration of trace metals. The corresponding biomass productivity and methane fixation rate were estimated to be 0.855 g L^{-1} d^{-1} and 0.466 g L^{-1} d^{-1}, respectively. At the end of every batch, the culture was centrifuged to collect cell-free supernatant for analyzing the utilization of nitrate and phosphate. With 0.75X unit concentration of trace metals, analyses of nitrate and phosphate revealed that the amounts of nitrate and phosphate consumed were 97.63% and 42.77% of their initial concentrations (*viz.*, 610.16 and 565.93 mg L^{-1}) in the growth media, respectively, suggesting that these nutrients were not limiting in the growth media. However, the amount of unutilized phosphate was found to be present in excess concentration. Therefore, the excess residual phosphate

(57.23%) was cut down, thus bringing down the working concentration to 242.06 mg L^{-1}. Maximum biomass titer, biomass productivity and methane fixation rate of 4.45 g L^{-1}, 0.872 g L^{-1} d^{-1} and 0.476 g L^{-1} d^{-1}, respectively, were achieved with 242.06 mg L^{-1} phosphate and 0.75X unit concentration of trace metals. Thus, the organism exhibited comparable performance in terms of biomass titer, biomass productivity and methane fixation rate at 565.93 mg L^{-1} (original/control concentration) as well as 242.06 mg L^{-1} (reduced concentration) of phosphate (Table 3.1). Hence, this work suggested that the excess amount of phosphate present in NMS media can be removed to reduce the overall cost of the growth media, without compromising the growth performance and methane sequestration characteristics of the strain.

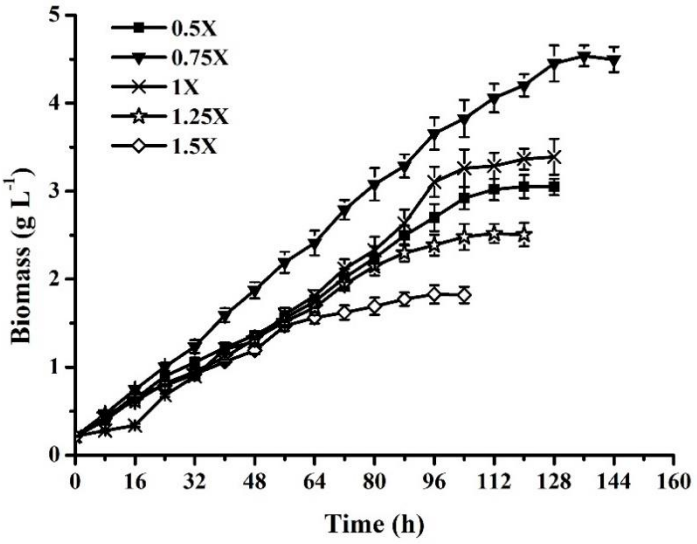

Fig. 3.5. Effect of the concentration of trace metals on growth.

Table 3.1. Comparison of growth and methane sequestration under control and reduced concentrations of phosphate in NMS media.

Phosphate concentration (mg L^{-1})	**565.93**	**242.06**
Biomass titer (g L^{-1})	4.5±0.14	4.45±0.12
Biomass productivity (g L^{-1} d^{-1})	0.855±0.03	0.872±0.04
Methane fixation rate (g L^{-1} d^{-1})	0.466±0.01	0.476±0.02

Nitrate and phosphate play critical roles in the synthesis of bacterial cell biomass, owing to their direct involvement as the constituent of nucleotides (which provide cellular energy, *e.g.*, ATP), phospholipids in plasma membranes and organelle membranes, as well as high-

molecular-weight intracellular biomolecules (*e.g.*, DNA, RNA, and proteins) (Kritmetapak and Kumar, 2021; Grzyb et al., 2021). Since, cell growth is directly related to availability of nitrate and phosphate, biomass formation was not assessed at lower concentrations of these nutrients in the media. Hence, 610.16 mg L^{-1} and 242.06 mg L^{-1} were considered as the optimum concentrations of nitrate and phosphate (at 0.75X unit concentration of trace metals), respectively, for maximum production of biomass (Table 3.2). The optimized media resulted in increments of 31.3% in biomass titer, 46.3% in biomass productivity, and 46.9% in methane fixation rate, relative to unoptimized media. As has been already discussed in Chapter 2, the concentrations of trace metals like copper and iron play a critical role in regulating the activity of MMO, which catalyses methane metabolism, consequently influencing biomass production. Other studies have also reported the pivotal effect of the concentrations of copper and iron ions on methane sequestration (Boiesen et al., 1993) and growth of methanotrophs (Patel et al., 2016b; Takeguchi and Okura, 2000).

Table 3.2. Optimization of the concentration of key nutrients in growth media.

Component	Unoptimized media	Optimized media
Trace metal concentration (X units)	1.0	0.75
Phosphate (mg L^{-1})	565.93	242.06
Nitrate (mg L^{-1})	610.16	610.16
Biomass titer (g L^{-1})	3.39±0.15	4.45±0.12
Biomass productivity (g L^{-1} d^{-1})	0.596±0.03	0.872±0.04
Methane fixation rate (g L^{-1} d^{-1})	0.324±0.02	0.476±0.02

3.3.2. Second stage for conversion of CO_2 into methanol using methanotrophic biomass

3.3.2.1. Evaluation of *M. trichosporium* as a potential biocatalyst for methanol biosynthesis under different process designs

The highest methanol titer of 0.56 g L^{-1} was recorded when the biomass was harvested from the first stage of growth and subsequently resuspended in phosphate buffer medium (Fig. 3.6a). However, methanol titer was found to reduce significantly (0.15 - 0.18 g L^{-1}) when either

freshly prepared NMS medium or same NMS medium (used for the growth) was employed for methanol synthesis. Phosphate buffer also resulted in improved methanol productivity (0.026 g L^{-1} h^{-1}) as compared to the other two process designs (0.01 – 0.013 g L^{-1} h^{-1}) (Fig. 3.6a). One of the key problems with methanol production from methane is the subsequent conversion of methanol into formaldehyde, catalysed by the enzyme methanol dehydrogenase (Sahoo et al., 2021). Several researchers have reported the role of phosphate as an inhibitor for the enzyme methanol dehydrogenase, either by adding a specific concentration of phosphate to the NMS media (Han et al., 2013; Sheets et al., 2016) or by directly using phosphate buffer as a medium (Mardina et al., 2016; Patel et al., 2016c, 2020c) for methanol production via methane oxidation. Although in our study, methanol is being produced through the CO_2 reduction pathway, there may be a possibility of the back-conversion of methanol into intermediate metabolites and CO_2, owing to the reversible nature of the enzymes: methanol dehydrogenase, formaldehyde dehydrogenase and formate dehydrogenase. This is where the role of phosphate buffer as a cultivation medium for methanol production from CO_2 comes into play, resulting in higher methanol titer and productivity relative to the NMS media. It is important to note that in none of the media, further growth of the organism was observed during methanol synthesis stage or phase. In general, methanotrophic cells stay in the resting phase while being used as biocatalyst for methanol production from CO_2 (Xin et al., 2007) and hence do not require other media components to sustain their growth. Intracellularly stored NADH supply the reducing energy to accomplish the reduction of CO_2 to methanol. These reducing equivalents are produced by the cell during the sequential oxidation of methane to CO_2 (first stage). In second stage, these reducing equivalents (in presence of excess CO_2) drive the equilibrium in backward direction causing the conversion of CO_2 into methanol (Xin et al., 2007). Therefore, phosphate buffer serves as the low-cost medium for methanol biosynthesis without any additional nutrient requirement.

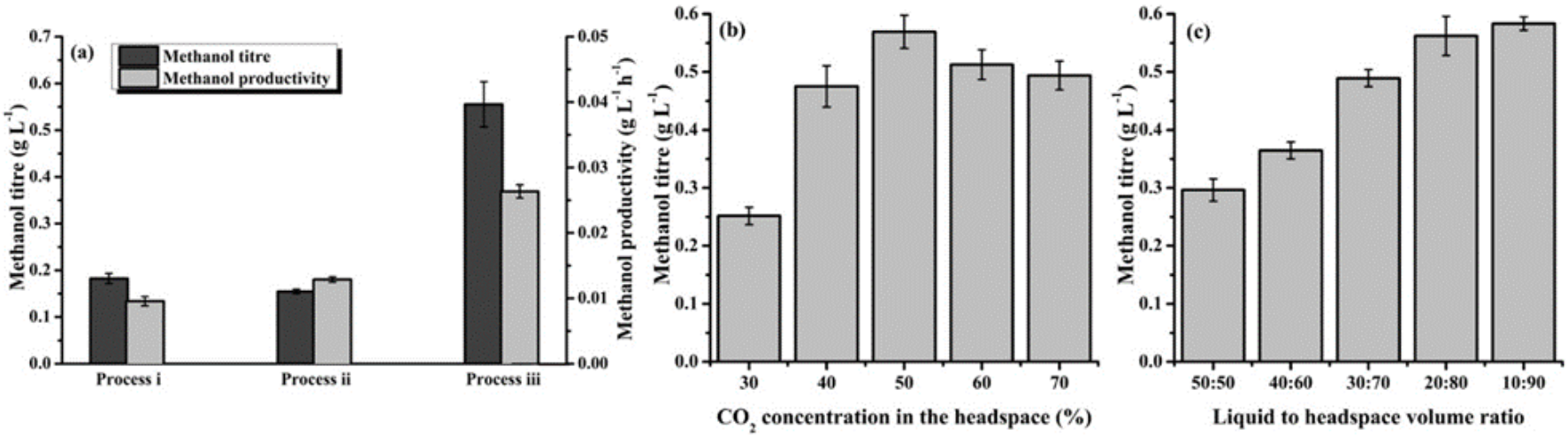

Fig. 3.6. (a) Methanol titer and productivity under three different process designs: (i) the biomass was harvested from the first stage of growth and subsequently resuspended in freshly prepared NMS medium for methanol production in the second stage using CO_2; (ii) a two-phase fermentation in NMS medium where, in the first phase, the organism was grown with CH_4 as the only carbon source, followed by methanol production in the second phase utilizing CO_2 as the sole carbon source; & (iii) the biomass was harvested from the first stage of growth and subsequently resuspended in phosphate buffer medium for methanol production in the second stage using CO_2. (b) Methanol titer under varying concentration of CO_2 in the headspace and (c) methanol titer under different liquid to headspace volume ratios using Process iii. The organism was grown in air-tight batch reactor.

3.3.2.2. Methanol production under varying CO_2 concentrations and liquid to headspace volume ratios

In the first step, methanol production was attempted in a semi-batch stirred tank reactor by continuous sparging of CO_2 (2.5% v/v) mixed with air at a flow rate of 0.5 vvm under atmospheric pressure. However, no methanol was detected in the extracellular medium. It has been reported that, at high partial pressure, the solubility of gases increases resulting in better interaction of the gaseous substrate with the key enzymes and in turn, positively regulates growth or product formation metabolism (Hurst and Lewis, 2010). Hence, in the present study, failure to induce methanol production in semi-batch stirred tank reactor may be attributed to the lower partial pressure of CO_2 in the gas mixture, which is considered to be the critical parameter for methanol production. Therefore, the second stage of methanol production was carried out in air-tight batch reactor with CO_2 mixed with air supplied in the headspace.

The extent of methanol formation was carried out under varying CO_2 concentrations in the headspace ranging from 10% - 70% v/v. No methanol was produced at the lowest CO_2 concentration of 10%. The methanol titer was found to increase concomitantly with the increase in CO_2 concentration from 30% and reached a maximum value of 0.57 g L^{-1} (17.79 mM) at a CO_2 concentration of 50% (Fig. 3.6b). The CO_2 fixation percentage at 50% CO_2 concentration was estimated to be 8.95% of the initial amount of CO_2 present in the headspace. However, further increase in CO_2 concentration beyond 50% resulted in a marginal decrease in methanol titer. These results point towards the role of CO_2 partial pressure in the headspace as a critical parameter for methanol induction. However, down-regulation of methanol biosynthesis at higher CO_2 partial pressure may be attributed to the possible inhibitory effect on enzymatic activity, electron transport chain, and carbon metabolism (Ceron-Chafla et al., 2020). There are a handful of studies towards the biological production of methanol via CO_2 reduction pathway. *Methylosinus sporium* was reported to produce methanol with a very low titer of 0.33 mM

when grown in the presence of 30% CO_2 (Patel et al., 2016a). Xin et al. (2007) reported production of 0.004 μmol methanol per mg dry cell weight from *Methylosinus trichosporium* cells, using 55.5% CO_2 in the headspace. With the increase in liquid to headspace volume ratio from 50:50, methanol titer increased linearly, and a maximum titer of 0.58 g L^{-1} (18.10 mM) was obtained at a ratio of 10:90 (Fig. 3.6c). The corresponding CO_2 fixation percentage was estimated to be 9.06%. The results suggest that headspace volume is another process parameter influencing methanol production since it is directly linked to the availability of CO_2, as the substrate for reduction reaction, at a fixed partial pressure. Thus, the occurrence of the highest methanol titer at liquid to headspace volume ratio of 10:90 could be attributed to the absence of substrate limitation (Pen et al., 2014). Characterization of *M. sporium* towards methanol biosynthesis through methane oxidation under different headspace volumes resulted in highest titer of 5.40 mM at headspace volume of 83.33% (Patel et al., 2016c). Pen et al. (2014) reported an improved methanol titer of 290 mg L^{-1} from methane biohydroxylation using *M. trichosporium* in batch reactor with 90% headspace volume as compared to cultivation with 37.5% headspace volume (35 mg L^{-1}). The biomass density remained almost constant during methanol production stage under varying CO_2 concentrations in the headspace and different liquid to headspace volume ratios (Fig. 3.7a, b).

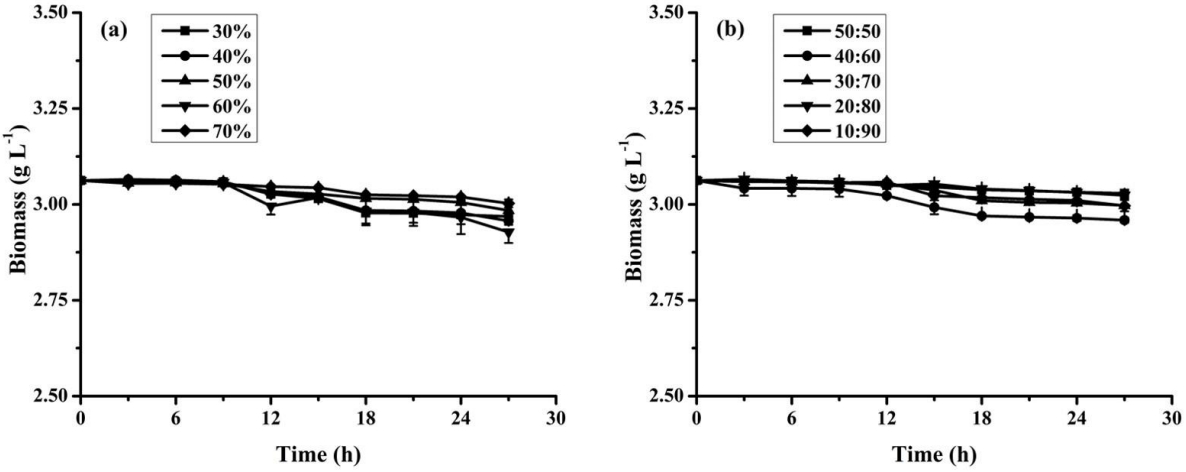

Fig. 3.7. (a) Biomass titer under varying concentration of CO_2 in the headspace and (b) biomass titer under different liquid to headspace volume ratios in air-tight batch reactor.

As discussed earlier, researchers have reported several strategies to overcome the limitations associated with methanol production from biological oxidation of CH_4, including, use of biogas as feedstock, cell immobilisation, repeated-batch cultivation, co-culture of cells, supplementation of methane vector, *etc*. (Patel et al., 2020a, 2020b, 2020c; Sheets et al., 2016). Despite of these approaches, the reported methanol titre is limited to the range of 5.37-13.42 mM (or, 0.17-0.43 g L^{-1}). Further, methanol production from biological reduction of CO_2, is also limited to a low methanol titer of up to 0.33 mM (Patel et al., 2016a; Xin et al., 2007). Therefore, it can be concluded that the maximum methanol titer achieved in the present study under optimum conditions is significantly higher than the similar studies reported in literature.

3.4. Conclusions

Two-stage integrated bioprocess was demonstrated for bio-methanol synthesis using *M. trichosporium* coupled with sequestration of methane and carbon dioxide. Improved biomass titer, methane fixation rate and methanol titer were achieved via optimization of process parameters. Semi-batch stirred tank reactor used in the first stage addresses the key challenge of mass transfer limitation of methane from gas to liquid phase. Methanol titer in the second

stage was found to be critically dependent on the partial pressure of carbon dioxide in the headspace of batch reactor.

3.5. References

1. Ali, S., Sørensen, K., Nielsen, M.P., 2020. Modeling a novel combined solid oxide electrolysis cell (SOEC) - Biomass gasification renewable methanol production system. Renew Energy 154, 1025–1034. https://doi.org/10.1016/J.RENENE.2019.12.108
2. Boiesen, A., Arvin, E., Broholm, K., 1993. Effect of mineral nutrients on the kinetics of methane utilization by methanotrophs. Biodegradation 4, 163–170. https://doi.org/10.1007/BF00695118
3. Cantera, S., Lebrero, R., García-Encina, P.A., Muñoz, R., 2016. Evaluation of the influence of methane and copper concentration and methane mass transport on the community structure and biodegradation kinetics of methanotrophic cultures. J Environ Manage 171, 11–20. https://doi.org/10.1016/j.jenvman.2016.02.002
4. Ceron-Chafla, P., Kleerebezem, R., Rabaey, K., Van Lier, J.B., Lindeboom, R.E.F., 2020. Direct and Indirect Effects of Increased CO2Partial Pressure on the Bioenergetics of Syntrophic Propionate and Butyrate Conversion. Environ Sci Technol 54, 12583–12592. https://doi.org/10.1021/ACS.EST.0C02022
5. Dalena, F., Senatore, A., Marino, A., Gordano, A., Basile, M., Basile, A., 2018. Methanol Production and Applications: An Overview. Methanol: Science and Engineering 3–28. https://doi.org/10.1016/B978-0-444-63903-5.00001-7
6. Gilman, A., Laurens, L.M., Puri, A.W., Chu, F., Pienkos, P.T., Lidstrom, M.E., 2015. Bioreactor performance parameters for an industrially-promising methanotroph Methylomicrobium buryatense 5GB1. Microb Cell Fact 14. https://doi.org/10.1186/S12934-015-0372-8

7. Grzyb, A., Wolna-Maruwka, A., Niewiadomska, A., 2021. The significance of microbial transformation of nitrogen compounds in the light of integrated crop management. Agronomy 11(7), p.1415. https://doi.org/10.3390/agronomy11071415

8. Han, B., Su, T., Wu, H., Gou, Z., Xing, X.H., Jiang, H., Chen, Y., Li, X., Murrell, J.C., 2009. Paraffin oil as a "methane vector" for rapid and high cell density cultivation of methylosinus trichosporium OB3b. Appl Microbiol Biotechnol 83, 669–677. https://doi.org/10.1007/s00253-009-1866-2

9. Han, J.S., Ahn, C.M., Mahanty, B., Kim, C.G., 2013. Partial oxidative conversion of methane to methanol through selective inhibition of methanol dehydrogenase in methanotrophic consortium from landfill cover soil. Appl Biochem Biotechnol 171, 1487–1499. https://doi.org/10.1007/S12010-013-0410-0

10. Hurst, K.M., Lewis, R.S., 2010. Carbon monoxide partial pressure effects on the metabolic process of syngas fermentation. Biochem Eng J 48, 159–165. https://doi.org/10.1016/j.bej.2009.09.004

11. Hwang, I.Y., Hoon Hur, D., Hoon Lee, J., Park, C.H., Chang, I.S., Lee, J.W., Yeol Lee, E., 2015. Batch conversion of methane to methanol using methylosinus trichosporium OB3B as biocatalyst. J Microbiol Biotechnol 25, 375–380. https://doi.org/10.4014/JMB.1412.12007

12. Keller, M., Sharma, A., 2022. Reverse Boudouard reforming produces CO directly suitable for the production of methanol from CO2 and CH4. Chemical Engineering Journal 431, 134127. https://doi.org/10.1016/J.CEJ.2021.134127

13. Kritmetapak, K., Kumar, R., 2021. Phosphate as a signaling molecule. Calcified tissue international 108(1), pp.16-31. https://doi.org/10.1007/s00223-019-00636-8

14. Kumar, P., Kumar, A., Sreedhar, B., Sain, B., Ray, S.S., Jain, S.L., 2014. Cobalt phthalocyanine immobilized on graphene oxide: An efficient visible-active catalyst for

the photoreduction of carbon dioxide. Chemistry - A European Journal 20, 6154–6161. https://doi.org/10.1002/CHEM.201304189

15. Li, Y., Hu, Y., Chu, J., Yao, Y., Lv, H., Xu, C., 2023. Investigation of renewable methanol production from CO2 hydrogeneration based on spectral splitting and heat integration. Fuel 352, 129041. https://doi.org/10.1016/J.FUEL.2023.129041
16. Mardina, P., Li, J., Patel, S.K.S., Kim, I.W., Lee, J.K., Selvaraj, C., 2016. Potential of Immobilized Whole-Cell Methylocella tundrae as a Biocatalyst for Methanol Production from Methane. J. Microbiol. Biotechnol. 26, 1234–1241. https://doi.org/10.4014/JMB.1602.02074
17. Mukherjee, M., Sarkar, P., Goswami, G., Das, D., 2019. Regulation of butanol biosynthesis in Clostridium acetobutylicum ATCC 824 under the influence of zinc supplementation and magnesium starvation. Enzyme Microb Technol 129. https://doi.org/10.1016/j.enzmictec.2019.05.009
18. Patel, S.K.S., Gupta, R.K., Kondaveeti, S., Otari, S. V., Kumar, A., Kalia, V.C., Lee, J.K., 2020a. Conversion of biogas to methanol by methanotrophs immobilized on chemically modified chitosan. Bioresour Technol 315. https://doi.org/10.1016/j.biortech.2020.123791
19. Patel, S.K.S., Gupta, R.K., Kumar, V., Kondaveeti, S., Kumar, A., Das, D., Kalia, V.C., Lee, J.K., 2020b. Biomethanol Production from Methane by Immobilized Co-cultures of Methanotrophs. Indian J Microbiol 60, 318–324. https://doi.org/10.1007/S12088-020-00883-6
20. Patel, S.K.S., Mardina, P., Kim, D., Kim, S.Y., Kalia, V.C., Kim, I.W., Lee, J.K., 2016a. Improvement in methanol production by regulating the composition of synthetic gas mixture and raw biogas. Bioresour Technol 218, 202–208. https://doi.org/10.1016/J.BIORTECH.2016.06.065

21. Patel, S.K.S., Mardina, P., Kim, S.Y., Lee, J.K., Kim, I.W., 2016b. Biological Methanol Production by a Type II Methanotroph Methylocystis bryophila. J. Microbiol. Biotechnol. 26, 717–724. https://doi.org/10.4014/JMB.1601.01013

22. Patel, S.K.S., Selvaraj, C., Mardina, P., Jeong, J.H., Kalia, V.C., Kang, Y.C., Lee, J.K., 2016c. Enhancement of methanol production from synthetic gas mixture by Methylosinus sporium through covalent immobilization. Appl Energy 171, 383–391. https://doi.org/10.1016/J.APENERGY.2016.03.022

23. Patel, S.K.S., Shanmugam, R., Kalia, V.C., Lee, J.K., 2020c. Methanol production by polymer-encapsulated methanotrophs from simulated biogas in the presence of methane vector. Bioresour Technol 304, 123022. https://doi.org/10.1016/J.BIORTECH.2020.123022

24. Pauss, A., Andre, G., Perrier, M., Guiot, S.R., 1990. Liquid-to-Gas mass transfer in anaerobic processes: Inevitable transfer limitations of methane and hydrogen in the biomethanation process. Appl Environ Microbiol 56, 1636–1644. https://doi.org/10.1128/AEM.56.6.1636-1644.1990

25. Pen, N., Soussan, L., Belleville, M.P., Sanchez, J., Charmette, C., Paolucci-Jeanjean, D., 2014. An innovative membrane bioreactor for methane biohydroxylation. Bioresour Technol 174, 42–52. https://doi.org/10.1016/J.BIORTECH.2014.10.001

26. Reddy, K.R., Rai, R.K., Green, S.J., Chetri, J.K., 2020. Effect of pH on Methane Oxidation and Community Composition in Landfill Cover Soil. Journal of Environmental Engineering 146. https://doi.org/10.1061/(ASCE)EE.1943-7870.0001712

27. Rodríguez, Y., Firmino, P.I.M., Pérez, V., Lebrero, R., Muñoz, R., 2020. Biogas valorization via continuous polyhydroxybutyrate production by Methylocystis hirsuta in

a bubble column bioreactor. Waste Management 113, 395–403. https://doi.org/10.1016/j.wasman.2020.06.009

28. Sahoo, K.K., Goswami, G., Das, D., 2021. Biotransformation of Methane and Carbon Dioxide Into High-Value Products by Methanotrophs: Current State of Art and Future Prospects. Front Microbiol 12. https://doi.org/10.3389/FMICB.2021.636486
29. Sheets, J.P., Ge, X., Li, Y.F., Yu, Z., Li, Y., 2016. Biological conversion of biogas to methanol using methanotrophs isolated from solid-state anaerobic digestate. Bioresour Technol 201, 50–57. https://doi.org/10.1016/j.biortech.2015.11.035
30. Sheets, J.P., Lawson, K., Ge, X., Wang, L., Yu, Z., Li, Y., 2017. Development and evaluation of a trickle bed bioreactor for enhanced mass transfer and methanol production from biogas. Biochem Eng J 122, 103–114. https://doi.org/10.1016/J.BEJ.2017.03.006
31. Takeguchi, M., Okura, I., 2000. Role of iron and copper in particulate methane monooxygenase of Methylosinus trichosporium oB3b. Catalysis Surveys from Japan 4, 51–63. https://doi.org/10.1023/A:1019036105038
32. Verhelst, S., Turner, J.W., Sileghem, L., Vancoillie, J., 2019. Methanol as a fuel for internal combustion engines. Prog Energy Combust Sci 70, 43–88. https://doi.org/10.1016/j.pecs.2018.10.001
33. Wang, L., Yi, Y., Wu, C., Guo, H., Tu, X., 2017. One-Step Reforming of CO2 and CH4 into High-Value Liquid Chemicals and Fuels at Room Temperature by Plasma-Driven Catalysis. Angewandte Chemie - International Edition 56, 13679–13683. https://doi.org/10.1002/ANIE.201707131
34. Xin, J.Y., Zhang, Y.X., Zhang, S., Xia, C.G., Li, S. Ben, 2007. Methanol production from CO2 by resting cells of the methanotrophic bacterium Methylosinus trichosporium IMV 3011. J Basic Microbiol 47, 426–435. https://doi.org/10.1002/JOBM.200710313

Web references

1. Trends in Atmospheric Carbon Dioxide, 2023. NOAA-ESRL. https://gml.noaa.gov/ccgg/trends/data.html. (Accessed 30 September 2023).
2. Trends in Atmospheric Methane, 2023. NOAA-ESRL. https://gml.noaa.gov/ccgg/trends_ch4/. (Accessed 30 September 2023).

CHAPTER 4

Process engineering strategy for improved methanotrophic biomass production through enhanced mass transfer and solubility of methane

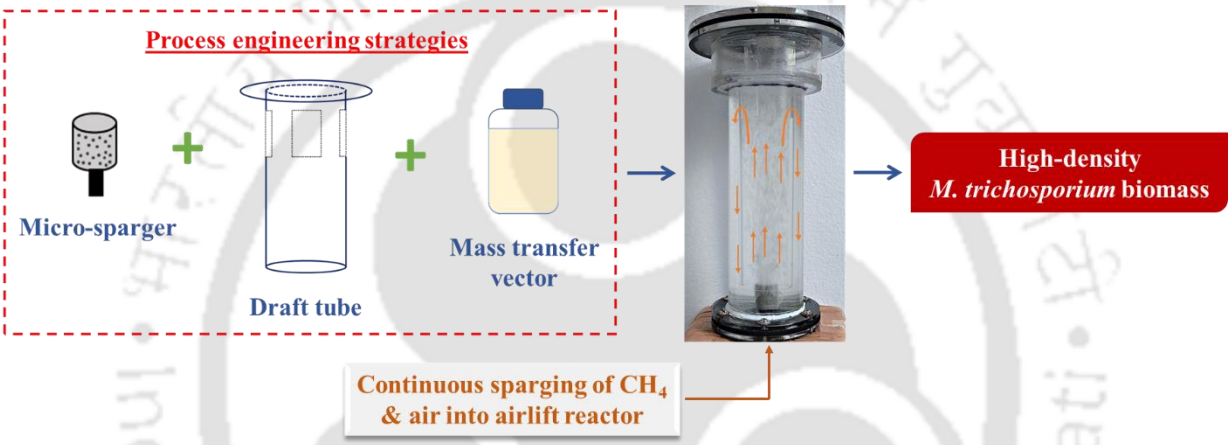

Fig. 4.1. Graphical abstract

4.1. Background and motivation

Chemical methods to catalytically convert greenhouse gases into value-added chemicals and fuels are typically constrained by the requirement for expensive catalysts, extreme operating conditions, such as high pressure and temperature, and release of noxious by-products, as have been already discussed in Chapters 2 and 3. To that end, researchers are exploring the application of gas fermentation technology involving microorganism-driven biological routes to convert greenhouse gases, *e.g.*, carbon dioxide, methane and carbon monoxide, into various high-value products such as ethanol (Tang et al., 2021), succinic acid (Amulya et al., 2020), lipids and single-cell proteins (Rasouli et al., 2018), poly-β-hydroxybutyrate (Zhang et al., 2017) and bio-hydrogen (Zhao et al., 2011). From a contextual

perspective, methanotrophs are being explored as novel platform to produce methanol (a potential fuel). Chapter 3 reported a two-stage integrated process for methanol production. The process involved utilization of methane in the first stage to produce methanotrophic biomass, while carbon dioxide was utilized in the second stage to produce methanol using the biomass as biocatalyst. However, one of the key challenges in the biological process for methanol synthesis from methane and CO_2 is the low titer of the biomass and methanol, which is primarily attributed to inferior mass transfer rates and limited solubility of the gaseous substrates in the liquid medium (Sahoo et al., 2022, 2021).

Process engineering strategies from the perspective of suitable reactor configuration and design, and supplementation of exogenous mass transfer vectors, are potential approaches towards combating the hurdles associated with limited mass transfer and solubility. Airlift reactors are considered to be advantageous over other reactor configurations attributed to better mixing and mass transfer, greater liquid recirculation and gas hold-up, absence of mechanical agitation and lower power requirement (Doran, 1995). Researchers have reported the application of airlift bioreactors for the cultivation of methanotrophic biomass towards the enhancement of methane biodegradation and methanol production through direct oxidation of methane (Ghaz-Jahanian et al., 2018; Rocha-Rios et al., 2011). Reactor design aspects, especially from the point of view of design of sparger and configuration of draft tube in an airlift reactor hold a significant importance in defining the reactor performance characteristics when the reactions occurring inside the system are limited by mass transfer phenomena. Spargers predominantly play key role in generation and dispersion of gases in the form of bubbles. In contrast to conventional spargers which generate coarse bubbles, micro-spargers lead to generation of fine microbubbles, characterized by higher specific interfacial area (larger ratio of surface area to volume), and thus offer improvement in volumetric mass transfer coefficient (Hanotu et al., 2017). Another key distinguishing feature of an airlift reactor is the

draft tube. Draft tubes have been reported to improve circulation and axial mixing inside the reactor. Moreover, the draft tube induces a unidirectional pattern of liquid circulation leading to unidirectional movement of bubbles, and consequent reduction in bubble coalescence (Duan and Shi, 2014).

The limited solubility of gaseous substrates in liquid medium is yet another hurdle associated with gas fermentation. At a temperature of 373.15 K and pressure of 10 MPa, the highest solubility of methane in water is 6×10^{-3} mole percent (Pruteanu et al., 2017). Mass transfer vectors, a class of organic solvents are reported to enhance the solubility of gaseous substances in the liquid medium. For instance, paraffin oil and silicone oil are reported to enhance the bioavailability of methane and oxygen to the cells (Han et al., 2009; Rocha-Rios et al., 2009). This could be attributed to the fact that relative to aqueous mineral salt media, mass transfer vectors possess greater affinity for oxygen and methane. This increased dissolution of gases upon vector supplementation in the media has been reported to have positive influence not only on the production of biomass (Han et al., 2009), but also on methanol (Patel et al., 2020). For instance, Patel et al. (2020) reported 1.7-fold increment in methanol production by adding methane vectors to methanotrophic culture as compared to control. Similarly, Patel et al. (2023) reported a residual methanol production efficacy of 28.3% in presence of paraffin oil as methane vector, as compared to 13.4% in control, after 6 cycles of biomass reuse. Moreover, the supplementation of methane vectors has shown to enhance the biocatalytic activity of MMO. For instance, Patel et al. (2023) reported residual MMO activity of 37.4% in presence of paraffin oil relative to 16.9% in case of control after 6 cycles of biomass reuse. However, lower mass transfer and limited solubility of methane still presents a major bottleneck, exerting a limiting impact on the titer and productivity of biomass in the first stage of the two-stage integrated process, which consequently limits methanol production.

The present chapter addresses the key challenge of limited mass transfer and solubility of methane, in the first stage, towards improving its bioavailability to methanotrophic bacteria for growth and biomass generation. A combinatorial approach of design of micro-sparger, engagement of draft tube and use of mass transfer vector was employed to achieve improved mass transfer and solubility of methane and in turn, increased titer of *Methylosinus trichosporium* biomass as biocatalyst. The employment of these process engineering strategies resulted in increments of 72.6%, 67.32% and 67.02%, in biomass titer, biomass productivity and methane fixation rate, respectively, as compared to the semi-batch stirred tank reactor reported in Chapter 3.

4.2. Materials and methods

4.2.1. Organism and culture conditions

Methylosinus trichosporium NCIMB 11131 was obtained from National Collection of Industrial Food and Marine Bacteria and was grown on nitrate mineral salt (NMS) medium containing (g L^{-1}): KNO_3 (1.0), $Na_2HPO_4.12H_2O$ (0.306), KH_2PO_4 (0.111), $MgSO_4.6H_2O$ (1.0), $CaCl_2$ (0.2), Fe-EDTA (0.0038) and $Na_2MoO_4.2H_2O$ (0.00026). Trace metal solution (1 mL) comprising of (g L^{-1}): $CuSO_4.5H_2O$ (0.15), $FeSO_4.7H_2O$ (0.375), $ZnSO_4.7H_2O$ (0.3), H_3BO_3 (0.01125), $CoCl_2.6H_2O$ (0.0375), EDTA di-sodium salt (0.1875), $MnCl_2.4H_2O$ (0.015) and $NiCl_2.6H_2O$ (0.0075) was added to the media. Medium pH was calibrated to 6.8 by adding 1 M H_2SO_4 and 1 M NaOH. Milli-Q water (18 MΩ) was used to prepare all the reagents. All the chemicals were of analytical grade and bought from Himedia and other commercial suppliers. Inoculum preparation was carried out as described previously in Chapter 3 by cultivating the cells in 100 mL of NMS medium in customized air-tight bottles. Cultures were incubated in a shaker incubator (ORBITEK, Scigenics Biotech) at 30 °C and 150 rpm with intermittent sparging of air and methane. The cells from mid-log phase culture with an optical density (A_{600}) of 5.0 were used as inoculum (10% v/v concentration) for all experiments.

4.2.2. Growth of methanotrophs using methane as sole carbon source in customized airlift bioreactor

Generation of methanotrophic biomass was carried out in the first stage of two-stage integrated process using methane as sole carbon source. The strain *M. trichosporium* was evaluated for its growth using micro-sparger with varying pore size, use of draft tube and presence of mass transfer vectors. All the experiments were carried out in customized airlift bioreactor using optimized NMS media at room temperature and the culture was sparged continuously with methane-air mixture. The concentration of methane in the inlet gas stream and the gas flow rate were maintained at 2.5% v/v and 0.5 vvm, respectively, based on the results obtained in Chapter 3. Samples were collected at an interval of 8 h to obtain dynamic profiles of growth. $k_L a$ for oxygen and methane were estimated as described later in the Section 4.2.2.3. Methane fixation rate was calculated using Eq. (4.1)

$$\text{Methane fixation rate } (\text{g L}^{-1}\text{d}^{-1}) = \text{P}_\text{x} \times \text{E}_\text{c} \times \left(\frac{16}{12}\right) \qquad (4.1)$$

where, P_x is the biomass productivity (g L^{-1} d^{-1}), E_c is the content of elemental carbon in the biomass. 16 and 12 are molecular weight of methane and carbon, respectively.

4.2.2.1. Design of airlift reactor

A laboratory-scale (Total volume: 700 mL, working volume: 500 mL) internal loop airlift reactor was constructed from clear polycarbonate sheet with a total height of 23.5 cm, and the inner diameter of the column being 7 cm (Fig. 4.2). A draft tube with a total height of 22.5 cm and inner diameter of 4 cm was mounted coaxially attached to the headplate. Three rectangular openings (5 cm × 1.5 cm) were provided in the upper portion of the draft tube, and a clearance of 1 cm between the lower rim of the draft tube and the bottom of the reactor column for allowing the circulation of the liquid through the riser and the downcomer sections. The reactor column contained a gas separator section at the top with a height of 2.5 cm and an

inner diameter of 10 cm to facilitate liquid recirculation and bubble disengagement. Gaseous substrates (mixture of air and methane) were introduced into the reactor column through a removable sintered metal gas sparger attached to the centre of the reactor bottom below the draft tube. The cross-sectional channel inside the draft tube, and the annulus between the draft tube and the reactor column, were used as the riser and the downcomer, respectively. Ports were provided on the headplate for exhaust and placement of DO probe.

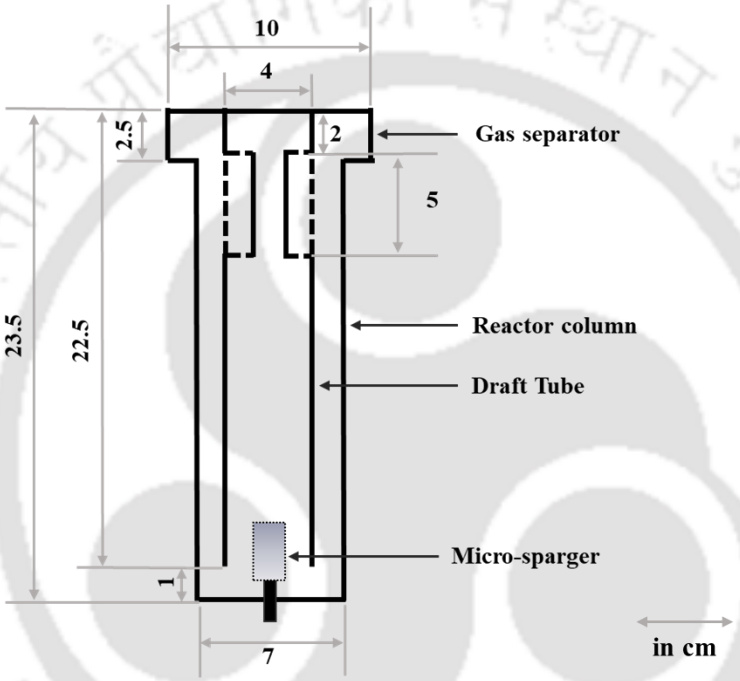

Fig. 4.2. Schematic diagram of customised internal loop airlift reactor. All the dimensions are in centimetres.

4.2.2.2. Effect of sparger pore size, draft tube, and mass transfer vector on growth of the strain

Sintered metal micro-spargers with a height of 2.67 cm and diameter of 1.5 cm were customized for the airlift reactor for the given pore sizes: 5, 10, 40, 70 and 100 µm. The growth characterisation of the strain was carried out in the customized airlift reactor equipped with micro-spargers of varying pore sizes (5-100 µm). In the next step, the growth characterization was performed in the absence of draft tube, where draft tube mounting was not provided in the

headplate. The effect of mass transfer vector was assessed by supplementing varying concentrations (5-10% v/v) of two different organic solvents, *viz.*, paraffin oil and silicone oil, in the cultivation medium.

4.2.2.3. Estimation of $k_L a$ for oxygen and methane

Volumetric mass transfer coefficient for oxygen ($k_L a_{O_2}$) was estimated using the gas out–gas in unsteady-state mass balance method for oxygen, as described earlier by Ghaz-Jahanian et al. (2018). Change in the concentration of oxygen in the culture media was measured using dissolved oxygen (DO) probe (METTLER TOLEDO, Switzerland). Initially, deoxygenation of NMS media was carried out by purging nitrogen into the reactor until the DO concentration dropped to zero. Subsequently, the media was reoxygenated by purging air into the reactor at a uniform flow rate of 0.5 vvm. The variation in DO concentration (C_t) during reoxygenation was recorded as a function of time, and continued until the DO concentration reached a steady-state value ($\overline{C}$). The rate of change in DO concentration is equal to the rate of oxygen transfer from gas to liquid. Therefore,

$$\frac{dC_t}{dt} = k_L a_{O_2} (\overline{C} - C_t) \qquad (4.2)$$

where, C_t is the DO concentration at time t, and ($\overline{C}$) is the steady-state DO concentration.

Integrating Eq. (4.2) between t_1 and t_2 results in:

$$k_L a_{O_2} = \frac{ln\frac{(\overline{C}-C_{t_1})}{(\overline{C}-C_{t_2})}}{(t_2-t_1)} \qquad (4.3)$$

where, C_{t_1} and C_{t_2} are the DO concentrations are time points t_1 and t_2, and $k_L a_{O_2}$ is the slope obtained by plotting $\ln\frac{(\overline{C}-C_{t_1})}{(\overline{C}-C_{t_2})}$ against time. The volumetric mass transfer coefficient for

methane ($k_L a_{CH_4}$) was calculated using the value of $k_L a_{O_2}$ as per the equation reported by Ghaz-Jahanian et al. (2018) for upcoming bubbles in airlift bioreactor:

$$k_L a \propto \left(\frac{1}{V_m}\right)^{0.3} \qquad (4.4)$$

where, V_m is the molecular volume, which is 25.6 and 37.9 cm^3 $gmol^{-1}$ for oxygen and methane, respectively. Thus, based on the molecular volumes of oxygen and methane, $k_L a_{CH_4}$ was calculated from $k_L a_{O_2}$ using Eq. (4.5).

$$k_L a_{CH_4} = 0.889\ k_L a_{O_2} \qquad (4.5)$$

4.2.3. Analytical methods

Cell growth was estimated by measuring the absorbance at 600 nm (A_{600}) using UV–Vis spectrophotometer (Cary Series 100, Agilent Technologies). The absorbance values were converted into dry cell weight (DCW) using the correlation, one optical density = 0.42 g dry cells L^{-1} (R^2 = 0.99). Elemental composition (C, H, and N) of the biomass was obtained using CHNS analyser (EuroEA Elemental Analyser).

4.3. Results and discussion

The first stage of methanotrophic biomass production was carried out in customized airlift bioreactor. Certain approaches from the perspective of reactor design, such as, use of micro-sparger and placement of draft tube, along with another process engineering strategy, *i.e.*, exogenous addition of mass transfer vector, were applied to the airlift reactor. Subsequently, characterisation was carried out to evaluate the consequent impact on $k_L a$, biomass titer, biomass productivity and methane fixation rate.

4.3.1. Evaluation of the effect of varying pore sizes of micro-sparger

Design of the sparger plays a critical role in delineating the performance characteristics of airlift reactors, where there are no other moving parts to ensure adequate mass transfer of

gaseous substrates in liquid media. In this regard, the pore size of the sparger holds significant importance, as the size of the pores on sparger regulate the size of the bubbles generating thereof, which in turn impact the volumetric mass transfer coefficient based on the characteristic interfacial area of the generated bubbles. To that end, characterisation of the organism was carried out using micro-spargers of various pore sizes ranging from 5 to 100 µm. Biomass titer was found to increase linearly from 4.54 to 6.4 g L^{-1} with the decrease in pore size of the micro-sparger from 100 to 5 µm (Fig. 4.3a). Similarly, the highest $k_L a$ for oxygen and methane of 78.12 and 69.45 h^{-1}, respectively, were obtained using the micro-sparger of 5 µm pore size (Fig. 4.3b), which was a 27-fold improvement over the values of $k_L a$ obtained using 100 µm micro-sparger. Furthermore, the maximum biomass productivity and methane fixation rate with 5-µm micro-sparger were estimated to be 1.272 and 0.694 g L^{-1} d^{-1}, respectively (Fig. 4.3c). Spargers with larger pore sizes are known to generate larger or coarse bubbles associated with lower volumetric mass transfer coefficient (Hanotu et al., 2017; Lukić et al., 2017). On the other hand, with the reduction in the pore size, micro-spargers (with pore sizes in the range of micrometres) generate even finer microbubbles, characterized by higher specific interfacial area (larger ratio of surface area to volume), leading to improvement in $k_L a$, lower probability of bubble coalescence, and greater residence time inside the reactor. Moreover, in contrast to coarse bubbles, microbubbles are known to impart greater degree of aggregate convective force, consequently leading to a thoroughly mixed homogenous liquid phase (Hanotu et al., 2017). AL-Mashhadani et al. (2015) reported that the reduction in the size of microbubbles promoted downward penetration of gas bubbles through an increased vertical depth into the downcomer section, owing to an intensification in the downward drag force relative to the buoyant force, thus inducing greater liquid recirculation and mixing efficiency. Therefore, the improvement in biomass titer, biomass productivity and methane fixation rate with the decrease in the pore size of the micro-sparger could be attributed to the increase in

mass transfer and mixing with 5-µm micro-sparger, and the consequent upsurge in the availability of methane to the cells.

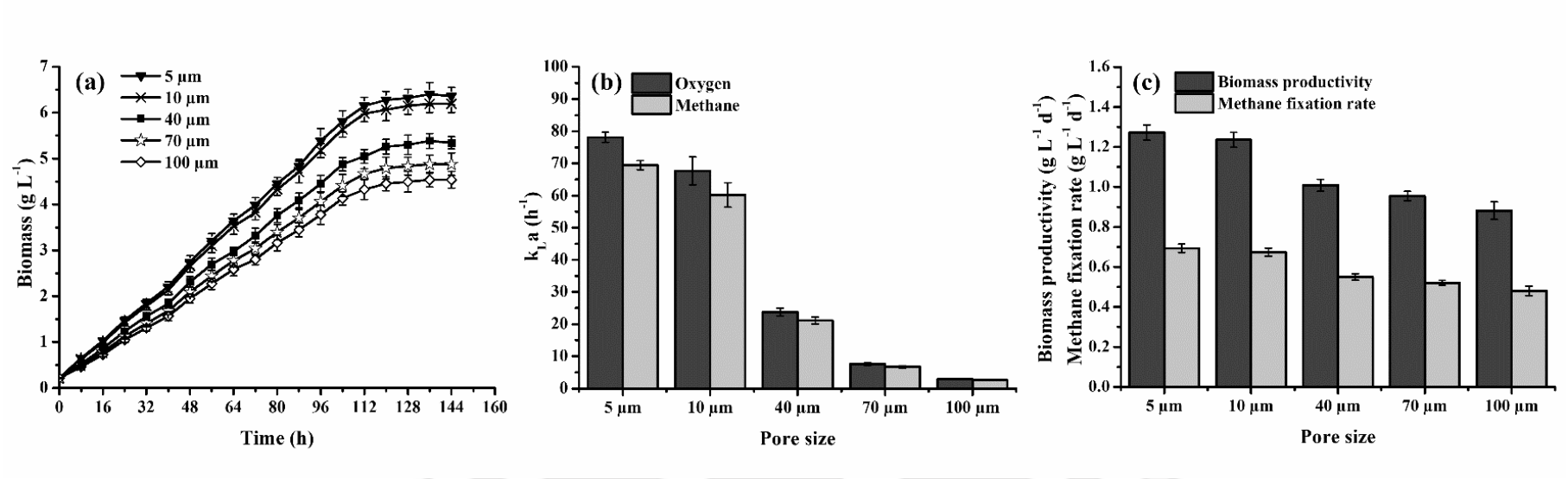

Fig. 4.3. (a) Biomass titer, (b) volumetric mass transfer coefficient for oxygen ($k_L a_{O_2}$) and volumetric mass transfer coefficient for methane ($k_L a_{CH_4}$) and (c) biomass productivity and methane fixation rate obtained in airlift reactor with varying pore sizes of micro-sparger.

Researchers have outlined the effect of sparger structure and pore size on volumetric mass transfer coefficient in different types of airlift reactors. Luo et al. (2011) reported that in an internal loop airlift reactor while a 2-orifice nozzle (pore diameter: 2.6 mm) resulted in a $k_L a$ of 0.0018 s^{-1} (6.48 h^{-1}), a 4-orifice nozzle (pore diameter: 1.84 mm) resulted in a much higher $k_L a$ of 0.0023 s^{-1} (8.28 h^{-1}), suggesting that spargers with lesser pore sizes generate bubbles with lower mean diameter, and thus are associated with greater specific interfacial area and liquid circulation velocity, consequently leading to a relatively higher $k_L a$. A similar study in an external loop airlift reactor reported 550% improvement in $k_L a$ with a sinter plate sparger with mean pore diameter of 115 µm, as compared to a single orifice sparger with a pore size of 4 mm (Lukić et al., 2017). Sintered-type spargers reportedly produce very stable and smaller bubbles and generate a bubbly flow regime along with prolonged bubble residence time, resulting in an improved $k_L a$ (Lukić et al., 2017). The findings of the present study align well in accordance with these literature reports, thus signifying the importance of smaller pore sizes in spargers towards enhancing the mass transfer in airlift reactors.

4.3.2. Evaluation of the effect of engagement of draft tube

In order to evaluate the effect of engagement of draft tube in airlift reactor, the growth of the organism was assessed with and without the placement of draft tube in the reactor equipped with 5-µm micro-sparger. The biomass titer was found to decrease by 8.59% in the absence of the draft tube, *i.e.*, from 6.4 g L^{-1} to 5.85 g L^{-1} (Fig. 4.4a). Additionally, the values of $k_L a_{O_2}$ and $k_L a_{CH_4}$ were observed to decrease by 27.42% each (Fig. 4.4b). Likewise, biomass productivity and methane fixation rate showed decrements of 13.3% and 13.4%, respectively, in the absence of the draft tube (Fig. 4.4c). These experimental observations emphasized the indispensable requirement for placement of draft tube in the airlift reactor towards achieving improved mass transfer coefficient, and consequent augmentations in biomass titer, biomass productivity and methane fixation rate.

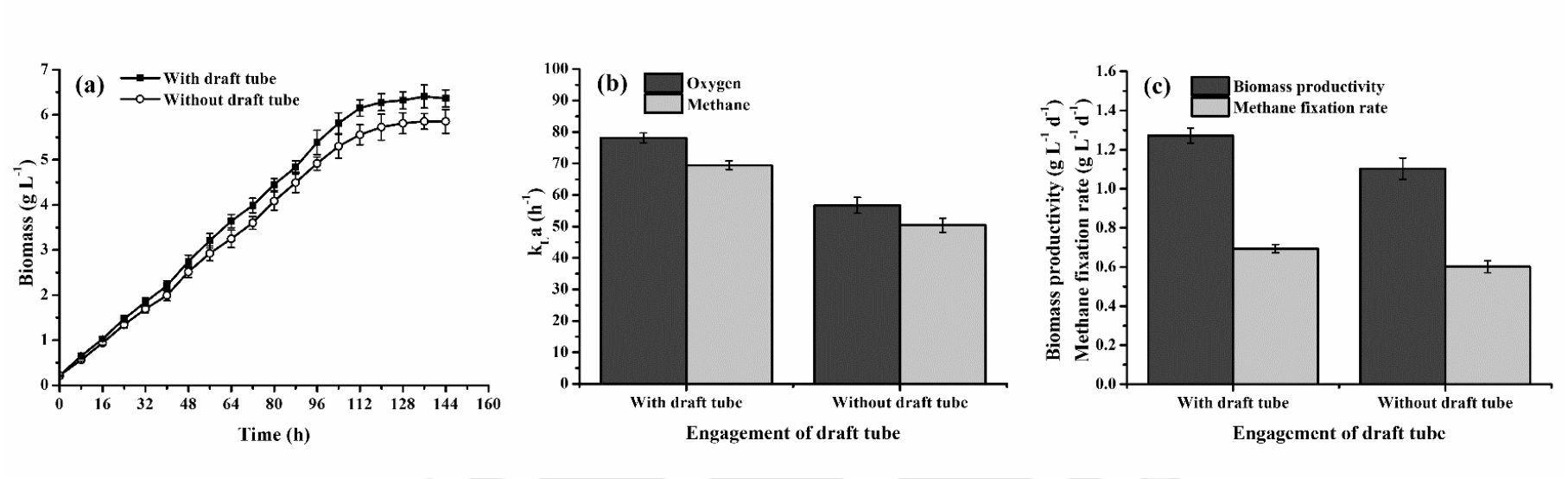

Fig. 4.4. Effect of draft tube on (a) biomass titer, (b) volumetric mass transfer coefficient for oxygen ($k_L a_{O_2}$) and volumetric mass transfer coefficient for methane ($k_L a_{CH_4}$) and (c) biomass productivity and methane fixation rate in airlift reactor equipped with micro-sparger of 5 µm pore size.

The presence of draft tube in an airlift reactor divides the vessel longitudinally into riser and downcomer sections. Bubbles rise inside the riser section causing vertical flow of the liquid in upward direction. This upward force exerted in the riser section is counter-balanced by vertical downflow of the liquid inside the downcomer section (Duan and Shi, 2014). The up-flow and downflow of the liquid result in efficient circulation and mixing of the liquid. Improved liquid circulation imparts a uniform velocity to the bubbles causing them to traverse in uniform direction. This kind of flow pattern has been reported to consequently minimize the probability of bubble coalescence and improve the $k_L a$. Researchers have highlighted the significance of draft tube in controlling the mass transfer and the hydrodynamic behaviour of airlift reactor. For instance, Hekmat et al. (2010) outlined that draft tube facilitated the circulation of liquid through a complete cycle inside the reactor, and decreased the quantity of liquid hold-up in the gaseous phase of the reactor, and thus cutting down the requirement for gas-liquid separation steps for the products exiting the reactor outlet. Li et al. (2020) reported that the geometric configuration of draft tube has notable influence on gas hold-up, gas residence time and mass transfer, which in turn regulate the power efficiency of airlift reactors. Researchers have even reported 40-100% improvement in $k_L a$ with the installation of draft tube in conventional mechanically agitated stirred tank reactor (Lueske et al., 2015). These literature reports in line with the present experimental results fairly justify the role of draft tube in airlift reactors for attaining improved performance.

4.3.3. Evaluation of the effect of supplementation of mass transfer vector

To overcome the limited solubility of methane and oxygen in NMS media, and increase their bioavailability to the cells, the media was supplemented with mass transfer vectors. *M. trichosporium* growth was evaluated under 0-10% v/v of paraffin oil and silicone oil. While, the absence of mass transfer vector (control) resulted in 6.4 g L^{-1} of biomass titer, the addition of 5% v/v paraffin oil yielded an improved titer of 7.2 g L^{-1} after 136 h of cultivation. With

further increase in the concentration of paraffin oil to 10% v/v, the biomass titer reduced marginally to 7 g L^{-1} (Fig. 4.5a). Similar observations have also been reported by Han et al. (2009), where at the end of 170 h of cultivation of *M. trichosporium*, the biomass titer obtained in the control was 2 g L^{-1}, which increased to 6 g L^{-1} with the addition of 5% v/v paraffin oil, and dropped to 1.8 g L^{-1} with further increase in the concentration to 10% v/v. These observations point towards the improved performance of *M. trichosporium* in the present study in airlift reactor under similar concentrations of paraffin oil. Furthermore, the biomass titer improved with the increase in the concentration of silicone oil from 5% v/v, and reached a maximum titer of 7.68 g L^{-1} at 10% v/v (Fig. 4.5a). Thus, under the supplementation of 10% v/v silicone oil, the biomass titer achieved for *M. trichosporium* in airlift reactor was significantly higher than that obtained for methanotrophic consortium ($\sim 0.004 \times 10^{-9}$ g L^{-1}) in two-phase partition trickling bed reactor (Rocha-Rios et al., 2009).

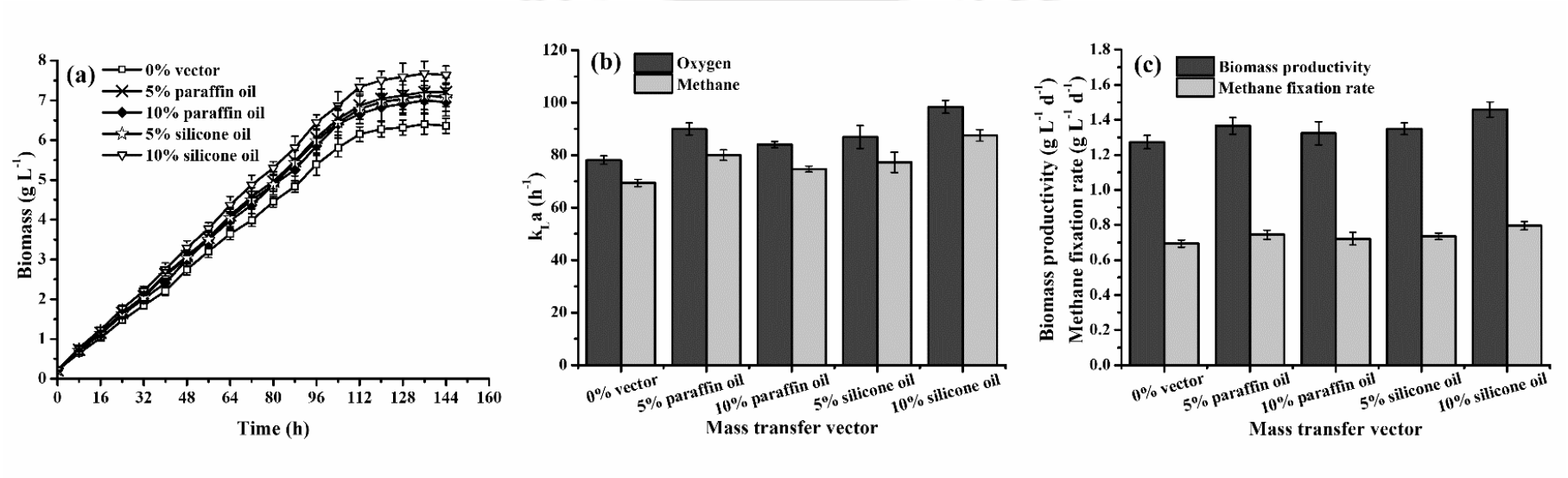

Fig. 4.5. (a) Biomass titer, (b) volumetric mass transfer coefficient for oxygen ($k_L a_{O_2}$) and volumetric mass transfer coefficient for methane ($k_L a_{CH_4}$) and (c) biomass productivity and methane fixation rate obtained in airlift reactor with varying concentrations of different mass transfer vectors.

Furthermore, the performance characteristics of the airlift reactor also improved under the chosen concentration of the mass transfer vector. For instance, with the addition of 10% v/v silicone oil, the highest values of $k_L a$ obtained for oxygen and methane in airlift reactor were 98.46 and 87.53 h^{-1}, respectively (Fig. 4.5b), which were remarkably higher than that obtained for stirred tank reactor (~0.011 s^{-1} or 39.6 h^{-1}) operated at 500 rpm with the same concentration of silicone oil (Rocha-Rios et al., 2010). Similarly, the maximum biomass productivity and methane fixation rate with 10% v/v silicone oil were estimated to be 1.459 and 0.795 g L^{-1} d^{-1}, respectively (Fig. 4.5c). As compared to aqueous mineral salt media, mass transfer vectors have been reported to possess greater affinity for oxygen and methane (Rocha-Rios et al., 2009). The addition of 10% v/v silicone oil to the fermentation media resulted in 26.04% increment each in $k_L a_{O_2}$ and $k_L a_{CH_4}$, relative to the control (without any vector supplementation). This improvement in gas-to-liquid mass transfer rate could be accountable for increase in the dissolution of gases in the fermentation media, and enhancement in the delivery of oxygen and methane to the cells thereof (Patel et al., 2020). The improved bioavailability of these gases consequently led to increments of 20% in biomass titer, 14.7% in biomass productivity and 14.55% in methane fixation rate as compared to the control. Methane available to the cells is oxidized into methanol and subsequently into formaldehyde, formic acid, and CO_2. Biomass formation occurs as a result of the assimilation of a part of the intermediately produced formate or formaldehyde as carbon source via RuMP or serine pathway (Sahoo et al., 2021). Therefore, in addition to mass transfer, biomass production is also influenced by the activities of the respective enzymes (MMO, MDH and formaldehyde dehydrogenase) responsible for the production and assimilation of formaldehyde/formate.

This is the first study presenting a combinatorial approach of design of micro-sparger, engagement of draft tube and supplementation of mass transfer vector in an airlift reactor towards achieving improved biomass production and methane sequestration in methanotrophic

cultivation system. Altogether, under the application of these specified process engineering strategies in airlift reactor, the present study showed an improvement of 72.6% in biomass titer, 67.32% in biomass productivity, and 67.02% in methane fixation rate (Fig. 4.6), as compared to the previous work carried out in semi-batch stirred tank reactor in Chapter 3. In general, airlift reactors are preferable over stirred tank reactors owing to the absence of mechanical moving parts, and thereby providing a low shear stress environment for cultivation of cells, accompanied by the advantage of relatively minimal energy requirement (Lechowska et al., 2019; Teli and Mathpati, 2021). Moreover, airlift reactors have been reported to exhibit better performance as compared to stirred tank reactors particularly in case of high cell density cultures which are susceptible to poor mixing and mass transfer limitations (AL-Mashhadani et al., 2015). For instance, under selected process parameters in internal loop airlift reactor (present study), the highest $k_L a_{CH_4}$(87.53 h^{-1}) attained was 460-folds greater than that was estimated in case of semi-batch stirred tank reactor (0.19 h^{-1}) (Sahoo et al., 2022). In addition to $k_L a_{CH_4}$, the highest value of $k_L a_{O_2}$ (98.46 h^{-1}) achieved in this study was also found to be higher than trickle-bed reactor ($k_L a_{O_2}$: 9.54 h^{-1}, Sheets et al., 2017) and methane transfer chamber coupled-external loop airlift reactor ($k_L a_{O_2}$: 97.2 h^{-1}, $k_L a_{CH_4}$: 70.8 h^{-1}, Ghaz-Jahanian et al., 2018), reported for the cultivation of methanotrophs to produce methanol through biological oxidation of methane.

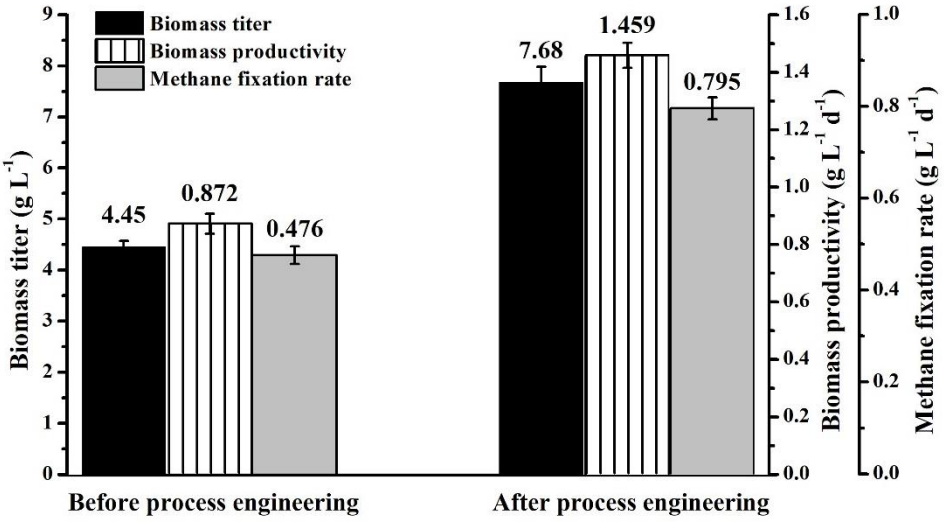

Fig. 4.6. Effect of the combinatorial process engineering strategy on biomass titer, biomass productivity and methane fixation rate.

4.4. Conclusions

A combinatorial process engineering strategy was employed to achieve improved production of *M. trichosporium* biomass. Use of micro-sparger, engagement of draft tube and supplementation of mass transfer vector in airlift reactor addressed the key challenge of mass transfer and solubility limitations of methane in the first stage. Biomass titer, biomass productivity and methane fixation rate were improved by 72.6%, 67.32% and 67.02%, respectively, compared with the two-stage process without process engineering strategy.

4.5. References

1. AL-Mashhadani, M.K.H., Wilkinson, S.J., Zimmerman, W.B., 2015. Airlift bioreactor for biological applications with microbubble mediated transport processes. Chem Eng Sci 137, 243–253. https://doi.org/10.1016/J.CES.2015.06.032

2. Amulya, K., Kopperi, H., Venkata Mohan, S., 2020. Tunable production of succinic acid at elevated pressures of CO2 in a high pressure gas fermentation reactor. Bioresour Technol 309, 123327. https://doi.org/10.1016/J.BIORTECH.2020.123327
3. Doran, P. M., 1995. Bioprocess engineering principles, second ed. Elsevier.
4. Duan, Y., Shi, F., 2014. Bioreactor design for algal growth as a sustainable energy source. Reactor and Process Design in Sustainable Energy Technology 27–60. https://doi.org/10.1016/B978-0-444-59566-9.00002-8
5. Ghaz-Jahanian, M.A., Khoshfetrat, A.B., Hosseinian Rostami, M., Haghighi, M., 2018. An innovative bioprocess for methane conversion to methanol using an efficient methane transfer chamber coupled with an airlift bioreactor. Chemical Engineering Research and Design 134, 80–89. https://doi.org/10.1016/J.CHERD.2018.03.039
6. Han, B., Su, T., Wu, H., Gou, Z., Xing, X.H., Jiang, H., Chen, Y., Li, X., Murrell, J.C., 2009. Paraffin oil as a "methane vector" for rapid and high cell density cultivation of methylosinus trichosporium OB3b. Appl Microbiol Biotechnol 83, 669–677. https://doi.org/10.1007/s00253-009-1866-2
7. Hanotu, J.O., Bandulasena, H., Zimmerman, W.B., 2017. Aerator design for microbubble generation. Chemical Engineering Research and Design 123, 367–376. https://doi.org/10.1016/J.CHERD.2017.01.034
8. Hekmat, A., Amooghin, A.E., Moraveji, M.K., 2010. CFD simulation of gas–liquid flow behaviour in an air-lift reactor: determination of the optimum distance of the draft tube. Simul Model Pract Theory 18, 927–945. https://doi.org/10.1016/J.SIMPAT.2010.02.009
9. Lechowska, J., Kordas, M., Konopacki, M., Fijałkowski, K., Drozd, R., Rakoczy, R., 2019. Hydrodynamic studies in magnetically assisted external-loop airlift reactor. Chemical Engineering Journal 362, 298–309. https://doi.org/10.1016/J.CEJ.2019.01.037

10. Li, X., Chen, Y., Zheng, Z., Gao, M., Wang, Z., Zhang, K., Liu, H., Zhan, X., 2020. Power-saving airlift bioreactor with helical sieve plates: Developmental and performance studies. Chemical Engineering Research and Design 158, 1–11. https://doi.org/10.1016/J.CHERD.2020.03.014
11. Lueske, J., Kar, K., Piras, L., Pressler, J., 2015. Power Draw and Gas-Liquid Mass Transfer Characteristics of a Stirred-Tank Reactor with Draft Tube Configuration. Chem Eng Technol 38, 1993–2001. https://doi.org/10.1002/CEAT.201500071
12. Lukić, N.L., Šijački, I.M., Kojić, P.S., Popović, S.S., Tekić, M.N., Petrović, D.L., 2017. Enhanced mass transfer in a novel external-loop airlift reactor with self-agitated impellers. Biochem Eng J 118, 53–63. https://doi.org/10.1016/J.BEJ.2016.11.014
13. Luo, L., Liu, F., Xu, Y., Yuan, J., 2011. Hydrodynamics and mass transfer characteristics in an internal loop airlift reactor with different spargers. Chemical Engineering Journal 175, 494–504. https://doi.org/10.1016/J.CEJ.2011.09.078
14. Patel, S.K.S., Kalia, V.C., Lee, J.K., 2023. Integration of biogas derived from dark fermentation and anaerobic digestion of biowaste to enhance methanol production by methanotrophs. Bioresour Technol 369, 128427. https://doi.org/10.1016/J.BIORTECH.2022.128427
15. Patel, S.K.S., Shanmugam, R., Kalia, V.C., Lee, J.K., 2020. Methanol production by polymer-encapsulated methanotrophs from simulated biogas in the presence of methane vector. Bioresour Technol 304, 123022. https://doi.org/10.1016/J.BIORTECH.2020.123022
16. Pruteanu, C.G., Ackland, G.J., Poon, W.C.K., Loveday, J.S., 2017. When immiscible becomes miscible—Methane in water at high pressures. Sci Adv 3. https://doi.org/10.1126/SCIADV.1700240

17. Rasouli, Z., Valverde-Pérez, B., D'Este, M., De Francisci, D., Angelidaki, I., 2018. Nutrient recovery from industrial wastewater as single cell protein by a co-culture of green microalgae and methanotrophs. Biochem Eng J 134, 129–135. https://doi.org/10.1016/J.BEJ.2018.03.010
18. Rocha-Rios, J., Bordel, S., Hernández, S., Revah, S., 2009. Methane degradation in two-phase partition bioreactors. Chemical Engineering Journal 152, 289–292. https://doi.org/10.1016/J.CEJ.2009.04.028
19. Rocha-Rios, J., Muñoz, R., Revah, S., 2010. Effect of silicone oil fraction and stirring rate on methane degradation in a stirred tank reactor. Journal of Chemical Technology & Biotechnology 85, 314–319. https://doi.org/10.1002/JCTB.2339
20. Rocha-Rios, J., Quijano, G., Thalasso, F., Revah, S., Muñoz, R., 2011. Methane biodegradation in a two-phase partition internal loop airlift reactor with gas recirculation. Journal of Chemical Technology & Biotechnology 86, 353–360. https://doi.org/10.1002/JCTB.2523
21. Sahoo, K.K., Datta, S., Goswami, G., Das, D., 2022. Two-stage integrated process for bio-methanol production coupled with methane and carbon dioxide sequestration: Kinetic modelling and experimental validation. J Environ Manage 301, 113927. https://doi.org/10.1016/J.JENVMAN.2021.113927
22. Sahoo, K.K., Goswami, G., Das, D., 2021. Biotransformation of Methane and Carbon Dioxide Into High-Value Products by Methanotrophs: Current State of Art and Future Prospects. Front Microbiol 12. https://doi.org/10.3389/FMICB.2021.636486
23. Sheets, J.P., Lawson, K., Ge, X., Wang, L., Yu, Z., Li, Y., 2017. Development and evaluation of a trickle bed bioreactor for enhanced mass transfer and methanol production from biogas. Biochem Eng J 122, 103–114. https://doi.org/10.1016/J.BEJ.2017.03.006

24. Tang, Y., Huang, Y., Gan, W., Xia, A., Liao, Q., Zhu, X., 2021. Ethanol production from gas fermentation: Rapid enrichment and domestication of bacterial community with continuous CO/CO2 gas. Renew Energy 175, 337–344. https://doi.org/10.1016/J.RENENE.2021.04.134
25. Teli, S.M., Mathpati, C.S., 2021. Experimental and Numerical Study of Gas-Liquid Flow in a Sectionalized External-Loop Airlift Reactor. Chin J Chem Eng 32, 39–60. https://doi.org/10.1016/J.CJCHE.2020.10.023
26. Zhang, T., Zhou, J., Wang, X., Zhang, Y., 2017. Coupled effects of methane monooxygenase and nitrogen source on growth and poly-β-hydroxybutyrate (PHB) production of Methylosinus trichosporium OB3b. Journal of Environmental Sciences 52, 49–57. https://doi.org/10.1016/J.JES.2016.03.001
27. Zhao, Y., Cimpoia, R., Liu, Z., Guiot, S.R., 2011. Kinetics of CO conversion into H 2 by Carboxydothermus hydrogenoformans. Appl Microbiol Biotechnol 91, 1677–1684. https://doi.org/10.1007/S00253-011-3509-7

Chapter 5

Process engineering strategy for enhanced methanol production from CO_2 and subsequent recovery using distillation

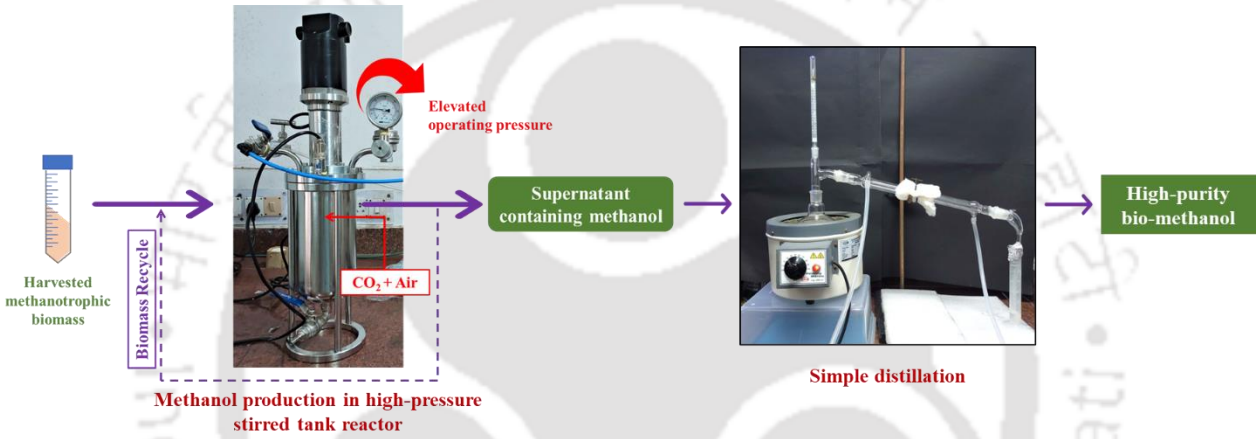

Fig. 5.1. Graphical abstract

5.1. Background and motivation

Methanol production from methanotrophs is not only advantageous over chemical routes, but also over certain microbial fermentation processes adopted for producing other bio-alcohols (*e.g.*, bio-ethanol and bio-butanol). Most of the bio-alcohols are produced using agricultural crop or lignocellulosic biomass as feedstock (*e.g.*, sugarcane, maize, and other sugar-rich plant biomass) (Dinesha et al., 2019; Renzi et al., 2016), which have raised the concern of biomass limitation and the controversial "food vs fuel" crisis. Additional operational expenses are also incurred towards extraction of fermentable sugars (*e.g.*, glucose) from the agricultural/lignocellulosic biomass (through enzymatic hydrolysis) for ultimate conversion into bio-alcohols, such as bio-ethanol and bio-butanol, using suitable microorganisms (Khan et

al., 2021; Mukherjee et al., 2020). On the other hand, production of bio-methanol using methanotrophic bacteria is accomplished through utilization of greenhouse gases (*viz.*, methane and CO_2) as carbon source, thereby circumventing the issue of biomass limitation which is a major challenge in case of lignocellulosic feedstock- or agricultural crop-dependent production of bio-alcohols. Further, since methanotrophs can directly utilize methane and CO_2 through metabolic oxidation and reduction, respectively, this makes the process cost-effective relative to other microbial processes relying on the fermentation of expensive carbon substrates (*e.g.*, fructose, glucose and xylose) to produce bio-alcohols. Chapter 3 reported a two-stage integrated process for production of methanol from methane and CO_2 using methanotrophic biomass as biocatalyst. As discussed in earlier chapters, one of the key challenges in the biological process for methanol synthesis from methane and CO_2 is the low titer of the biomass and methanol, which is primarily attributed to inferior mass transfer rates and limited solubility of the gaseous substrates in the liquid medium. To that end, Chapter 4 addressed the key challenge of limited mass transfer and solubility of methane in the first stage, by employing a combinatorial process engineering approach. However, low solubility of CO_2 in liquid medium is yet another hurdle associated with the two-stage integrated process, which limits the titer of methanol in the second stage. For instance, the maximum solubility of CO_2 in water is 0.874 mole percent at a temperature and pressure of 373.15 K and 5.03 MPa, respectively (Lucile et al., 2012).

Biological methanol production has been reported through various routes such as, reduction of CO_2 (Sahoo et al., 2022; Xin et al., 2007), and oxidation of pure methane or methane present in biogas (Patel et al., 2020a, 2020b). However, despite the route of methanotrophic methanol production, majority of these studies are executed in a characteristic two-stage process. The first stage involves methanotrophic biomass production through methane utilization in nitrate mineral salt media, whereas methanol is produced in the second

stage utilizing the harvested biomass as biocatalyst in phosphate buffer medium using appropriate carbon source (e.g., CO_2, methane, or biogas) (Patel et al., 2020b, 2020a; Sahoo et al., 2022). In general, slow growth rate of methanotrophic bacteria poses a major challenge against efficient production of methanotrophic biomass. To that end, biomass recycling strategy, is being adopted to re-utilize the biomass for multiple cycles of methanol production, thereby reducing the time and cost incurred towards growing the culture for fresh biomass generation, with concomitant attainment of an improved cumulative methanol titer (Patel et al., 2023, 2020a). Researchers have reported re-utilization of methanotrophic biomass up to 10 cycles, resulting in a maximum cumulative methanol titer of 70.74 mM (2.27 g L^{-1}) (Patel et al., 2022). However, a major hurdle imposed by the low titer of methanol is the difficulty associated with the recovery of methanol from fermentation medium, thereby obstructing its further application (*e.g.*, as a fuel).

Owing to the challenges discussed above, the present chapter describes a process engineering strategy comprising elevation of operating pressure in a customized high-pressure stirred tank reactor to enhance the solubility of CO_2, thereby increasing its conversion into methanol. Further, biomass is recycled towards achieving a high cumulative methanol titer, thus curtailing the time and resources expended towards recurrent biomass generation. This is followed by distillation to recover high-purity methanol, targeting its potential application as a fuel in the subsequent chapter.

5.2. Materials and methods

5.2.1. Microorganism, growth conditions, and methanotrophic biomass production for application as biocatalyst

Methylosinus trichosporium NCIMB 11131 was acquired from National Collection of Industrial Food and Marine Bacteria and was cultivated on nitrate mineral salt (NMS) media comprising of (g L^{-1}): KNO_3 (1.0), $CaCl_2$ (0.2), $MgSO_4 \cdot 6H_2O$ (1.0), KH_2PO_4 (0.111),

$Na_2HPO_4 \cdot 12H_2O$ (0.306), $Na_2MoO_4 \cdot 2H_2O$ (0.00026) and Fe-EDTA (0.0038). Trace metal solution (1 mL) containing (g L^{-1}): $CuSO_4 \cdot 5H_2O$ (0.15), $CoCl_2 \cdot 6H_2O$ (0.0375), EDTA di-sodium salt (0.1875), $FeSO_4 \cdot 7H_2O$ (0.375), H_3BO_3 (0.01125), $MnCl_2 \cdot 4H_2O$ (0.015), $NiCl_2 \cdot 6H_2O$ (0.0075) and $ZnSO_4 \cdot 7H_2O$ (0.3) was supplemented to the medium. Medium pH was adjusted to 6.8 by using 1 M H_2SO_4 and 1 M NaOH. All the reagents were prepared using Milli-Q water (18 MΩ). All the chemicals were of analytical standard and obtained from Himedia and other commercial traders. Inoculum was prepared as described earlier in Chapter 3 by growing the cells in customized air-tight bottles containing 100 mL NMS medium. Cultures were maintained at 30 °C and 150 rpm in a shaker incubator (ORBITEK, Scigenics Biotech) with intermittent feeding of methane and air.

In the first stage of the two-stage integrated process, high-density methanotrophic biomass was produced utilizing methane, for subsequent application as biocatalyst in the second stage involving the reduction of CO_2 to methanol. Methanotrophic biomass production was carried out in airlift reactor (500 mL working volume), equipped with 5-µm pore size micro-sparger and draft tube, as per the optimum conditions reported in Chapter 4. The reactor containing NMS media was supplemented with 10% v/v silicone oil and inoculated with 10% v/v of mid-log phase culture bearing an optical density of 5.0. The cultivation was carried out at room temperature, with continuous sparging of methane-air mixture. The gas flow rate and methane concentration in the inflowing gas mixture were maintained at 0.5 vvm and 2.5% v/v, respectively.

5.2.2. Conversion of carbon dioxide into methanol using biomass as biocatalyst: Effect of operating pressure

The methanotrophic biomass generated in the first stage of the integrated process was used as biocatalyst for conversion of carbon dioxide to methanol under varying operating pressure. A laboratory-scale stirred tank reactor with a maximum working volume of 1.2 L was

fabricated using SS-316-grade stainless steel with a total height of 22 cm and an outer diameter of 11.4 cm (Fig. 5.2). The reactor was designed to withstand pressure as high as up to 10 bar. The reactor was equipped with six-bladed Rushton disk turbine impeller for efficient mixing, temperature detector, pressure gauge, pressure release valve and ports for gas feeding and sampling. The culture was assessed for methanol production under varying headspace pressure of 1, 2, 3, 4 and 5 bar. The CO_2 concentration in the headspace and liquid to headspace volume ratio were maintained at 50% v/v and 10:90, respectively, based on the results obtained in Chapter 3. The desired pressure in the headspace was achieved by injecting a mixture of CO_2 and air in the beginning of the batch using rotameters. The reactor was operated at room temperature and 150 rpm. In this step, the harvested biomass (3.39 g L^{-1}) was resuspended in 20 mM phosphate buffer (pH 6.8) containing 5 mM $MgCl_2$, as described earlier in Chapter 3. Sampling was carried out at regular time intervals to obtain dynamic profiles for methanol production and growth.

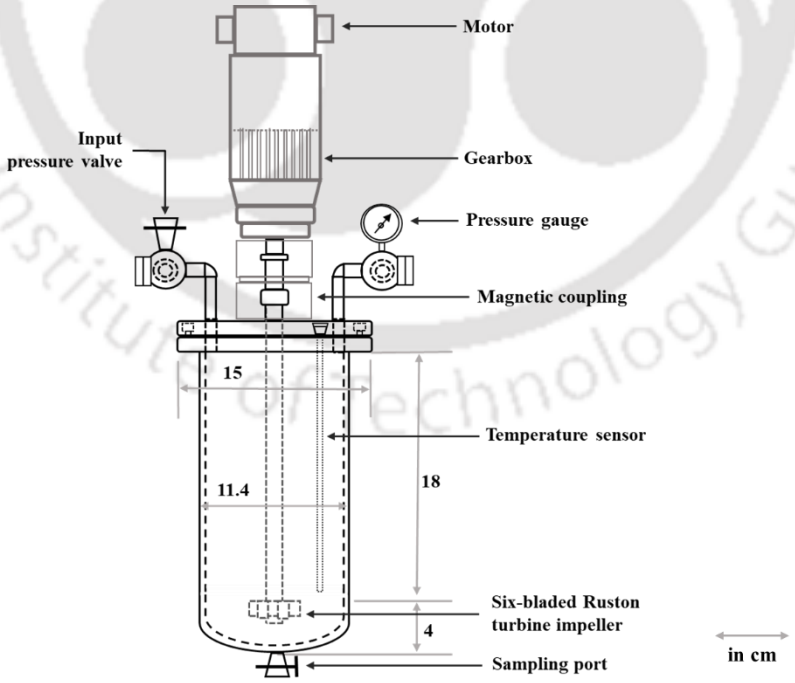

Fig. 5.2. Schematic diagram of customised high-pressure stirred tank reactor. All the dimensions are in centimetres.

5.2.3. Biomass recycling

Biomass was reutilized to evaluate methanol production by cells for multiple cycles. After each batch, biomass was harvested by centrifugation at 4000 rpm and 4 °C for 30 minutes (Patel et al., 2020a). The pellet was washed and resuspended in fresh phosphate buffer as inoculum for the subsequent cycle of methanol production. Sampling was performed at regular intervals to obtain dynamic profile for methanol production.

5.2.4. Simple distillation of culture broth

The distillation apparatus consisted of an adjustable electrical heating mantle (with a heating capacity of up to 400 °C), thermometer (0-350 °C), still head (3-way adapter), Liebig condenser (350 mm length), and receiving adaptor. The sample was taken in a 1000 mL round bottom flask. The still head was used to connect the condenser to the flask and hold the thermometer in the assembly in such a way that its bulb stayed in contact with vapours from the sample during evaporation. Other end of the condenser was connected to a receiving adapter to channel the condensed distillate into a measuring cylinder. The temperature inside condenser was maintained between 4 to 10 °C throughout the process. Distillation was carried out with 1000 mL of pooled culture supernatant from methanol production batches. The flask was gradually heated to a maximum of 65 °C. The distillate was collected in the range of 60 to 65 °C. After distillation, the flask was cooled to room temperature.

5.2.5. Analytical methods

Cell growth was estimated by measuring the absorbance at 600 nm (A_{600}) using UV–Vis spectrophotometer (Cary Series 100, Agilent Technologies). The absorbance values were converted into dry cell weight (DCW) using the correlation, one optical density = 0.42 g dry cells L^{-1} (R^2 = 0.99). Sample was centrifuged (HERAEUS, MULTIFUGE X3R Centrifuge, Thermo Scientific) at 10,000 rpm for 15 min to obtain cell-free supernatant for the estimation of methanol titer. Methanol concentration in supernatant sample and purity of distillate

(containing methanol) were estimated by high performance liquid chromatography (HPLC) (Ultimate 3000, Dionex, Thermofisher Scientific, Germany) in refractive index detector (RID) using Rezex ROA column (300 × 7.8 mm, Phenomenex) and 0.005 N H_2SO_4 as mobile phase at a flow rate of 0.5 mL min^{-1}. Refractive index detector and column oven were kept at 37 °C and room temperature, respectively.

5.3. Results and discussion

5.3.1. Evaluation of the effect of elevated operating pressure on methanol production

The effect of elevated pressure on methanol production from CO_2 was investigated under varying absolute pressure in the reactor headspace ranging from 1 to 5 bar. The methanol concentration was observed to increase concomitantly with the increase in absolute pressure from 1 bar, and attained a maximum value of 1.98 g L^{-1} (61.8 mM) at 4 bar (Fig. 5.3), which was a 235.6% increment over the titer obtained under atmospheric pressure (0.59 g L^{-1}). This remarkable improvement in methanol titer could be attributed to the increase in the availability of CO_2 in the media under elevated pressure condition. Researchers have reported that elevated pressure can exert significant impact on microbial cells at molecular level including enzymatic activity, cell permeability, protein structure and synthesis of metabolic products (Amulya et al., 2020). This in turn can potentially induce the development of specific genetic, physiological and/or metabolic phenotypes in the microorganism, with consequent effect on the pattern of product formation. Based on the amount of methanol produced, the percentage of CO_2 fixed (as extracellularly secreted methanol) at 4 bar was estimated to be 7.7%. This could be attributed to the utilization of remaining CO_2 as formate, formaldehyde, or methanol (formed via reduction), and assimilation into the biomass towards cell maintenance. Another possibility might be the limited biocatalytic potential of the cells to reduce CO_2 in reverse direction of equilibrium.

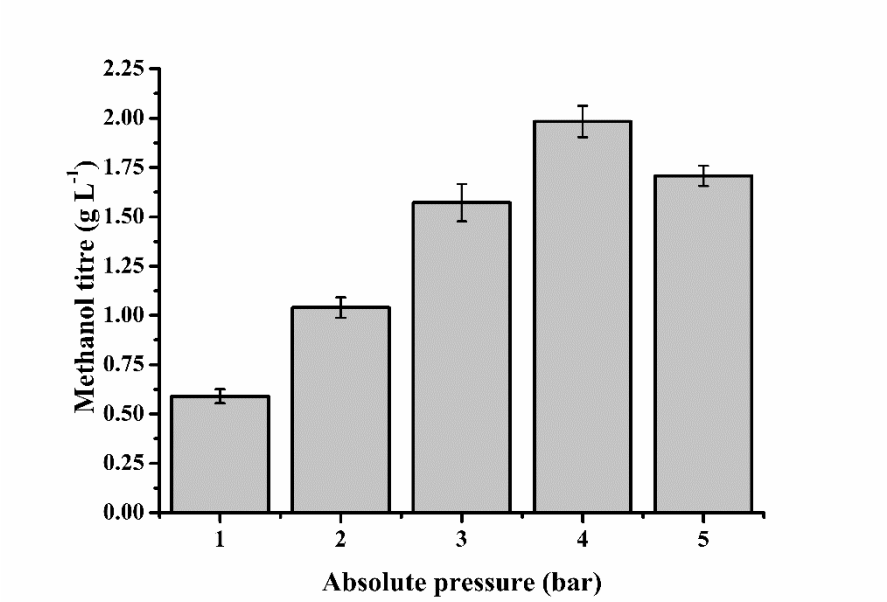

Fig. 5.3. Methanol titer under varying operating pressures in high-pressure stirred tank reactor.

Researchers have reported similar studies demonstrating the effect of elevated pressure on product metabolism in other microbial systems. Kim et al. (2017) reported a three-fold increment in H_2 production from carbon monoxide at 4 bar in *Thermococcus onnurineus* NA1. Roger et al. (2018) reported 20-fold increase in formate production from a mixture of CO_2 and H_2 at 10 bar in genetically modified *Escherichia coli* K12. Lopes et al. (2009) reported 3.7-fold enhancement in lipase productivity at 5 bar in *Yarrowia lipolytica* W29. However, this is the first study investigating the effect of elevated pressure on methanol production from CO_2 using methanotrophic biomass as biocatalyst.

Further increase in the absolute pressure above 4 bar resulted in significant reduction in methanol titer to 1.7 g L^{-1}. This observation could be attributed to the integrated effect of high pressure and high volume of CO_2 available per unit volume of the methanotrophic culture, imposing plausible inhibitory effect on electron transport chain, carbon metabolism and enzyme activity (Sahoo et al., 2022). In general, higher CO_2 pressure beyond 4-5 bar has been reported to hinder the cell viability in certain Type II methanotrophic species (Wendlandt et al., 1993). Moreover, *M. trichosporium* specifically being a Gram-negative organism is possibly

more vulnerable to phospholipid solubilisation in the cell membrane due to the lack of thick peptidoglycan layer under higher CO_2 pressure stress (Schulz et al., 2012). Methanol titer was found to increase gradually till 24th h of the batch, after which a slight decline was observed (Fig. 5.4a). This could be attributed to the exhaustion of endogenous reducing equivalents (*e.g.,* NADH and PHB), or methanol degradation owing to enzymatic or non-enzymatic interactions (Xin et al., 2007). Biomass density almost remained constant in the pressure range of 1 to 4 bar. However, it was observed to decline slightly at 5 bar with the progression of the batch, which could be another possible reason for reduced methanol titer at this pressure (Fig. 5.4b). Methanol production through CO_2 reduction is carried out in phosphate buffer medium to resist major changes in pH resulting from CO_2 solubility (Patel et al., 2016; Sahoo et al., 2022; Xin et al., 2007). In the present study, the initial and final pH (at the end of the batch) of the culture were found to decrease from 6.8 to 6.65, and 6.56 to 6.14, respectively, with the increase in pressure from 1 to 5 bar (Fig. 5.4c). The slight decrease in pH with the progression of the batch and the increase in pressure, could be attributed to the increase in solubility of CO_2. However, the use of buffer did help in resisting sharp and major decline in pH with the increasing CO_2 solubility.

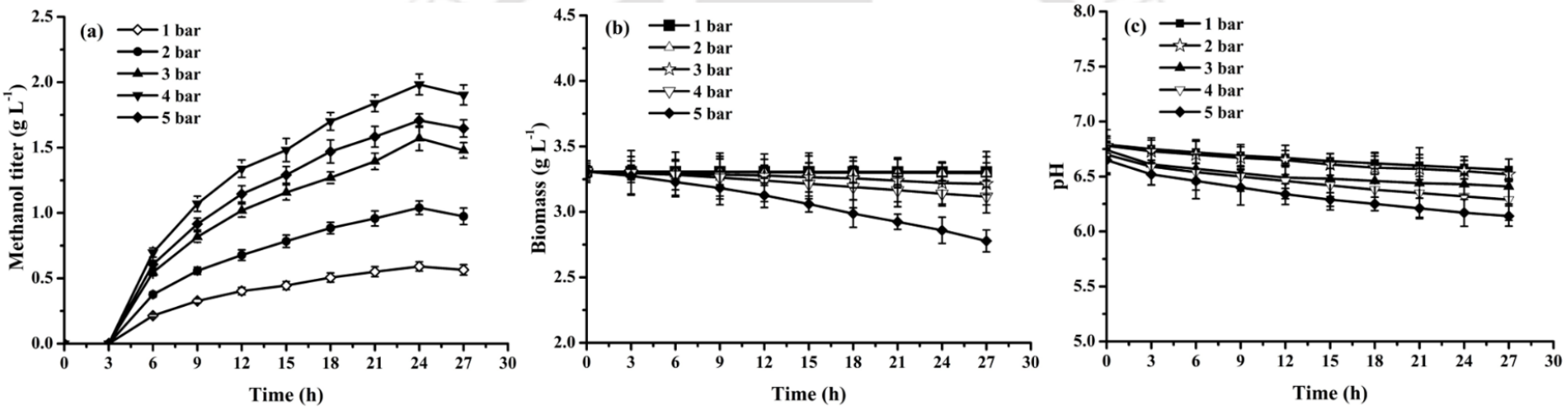

Fig. 5.4. Dynamic profile of (a) methanol, (b) biomass, and (c) pH under varying operating pressures in high-pressure stirred tank reactor.

There are very few studies reporting the production of methanol through the reduction of CO_2 in methanotrophs under atmospheric pressure (Patel et al., 2016; Xin et al., 2007). Chapter 3 reported a maximum methanol titer of 0.58 g L^{-1} (18.10 mM) using *Methylosinus trichosporium* as biocatalyst, which was till date the highest methanol titer achieved through biological CO_2 reduction pathway. In the present study, the elevation of operating pressure up to 4 bar resulted in a further 241% increment in methanol production as compared to the previous study in air-tight batch reactor. Alternatively, researchers have reported the production of methanol through biological oxidation of methane by methanotrophs. However, this specific route is constrained by further sequential oxidation of the produced methanol into subsequent intermediate metabolites, and the requirement for methanol dehydrogenase inhibitors and formate to achieve extracellular secretion of methanol into the media (Sahoo et al., 2021). Duan et al. (2011) reported a maximum methanol titer of 1.12 g L^{-1} and $Y_{p/x}$ (methanol yield coefficient relative to biomass) of 0.066, through biological oxidation of methane using a very high biomass density of *M. trichosporium* (17 g L^{-1} dry cell weight), high concentrations of methanol dehydrogenase inhibitors (400 mM phosphate and 10 mM $MgCl_2$) and paraffin oil as mass transfer vector. Another study reported the production of methanol from methane through covalent immobilisation of *Methylocystis bryophila* cells on coconut coir using paraffin oil as mass transfer vector (Patel et al., 2020a). The subsequent application of repeated batch strategy to this process resulted in a maximum cumulative methanol accumulation of 52.9 mM (1.69 g L^{-1}), with a $Y_{p/x}$ value of 0.56 at the end of eight cycles of biomass reutilisation. On the contrary, the $Y_{p/x}$ in stirred tank reactor, operated in batch mode at 4 bar, was estimated to be 0.6 in the present study, signifying the ameliorated performance of the organism under elevated operating pressure, which is a much simpler strategy relative to other contemporary approaches. Moreover, to the best knowledge of the author, this is the first study demonstrating the effect of elevated pressure on methanol production using methanotrophic bacteria as biocatalyst.

5.3.2. Recycling of biomass for methanol production

The typical two-stage bioprocess for methanol production as reported in Chapter 3, is constrained by the time and cost expended towards generating fresh methanotrophic biomass for every methanol production batch. To that end, biomass was reutilized for multiple cycles to assess the reusability of the cells for methanol production. The cumulative methanol titer was observed to increase progressively with successive cycles of biomass reutilization, and reached a maximum value of 3.6 g L^{-1} (112.4 mM) at the end of third cycle (Fig. 5.5). Further attempt to reutilize the biomass for the fourth cycle did not contribute to additional improvement in the cumulative methanol titer. The levelling-off in the value of cumulative methanol titer after three consecutive cycles of biomass reutilization has been attributed to reduction in efficiency of methanol production relative to zeroth cycle (Patel et al., 2021). Researchers have delineated decline in intracellular NADH levels and decrease in biocatalytic activity of cells, as the principal reasons behind reduction in relative efficiency of methanol production during biomass recycling (Patel et al., 2022, 2021). The gradual decline in biomass density with the progression of batch in successive recycles also explains the possible cause behind reduced efficiency of methanol production (Fig. 5.6). Based on the quantity of extracellularly accumulated methanol, the percentage of CO_2 fixation was estimated to be 14%, which was an increment of 81.8% relative to the control without biomass recycling (7.7%).

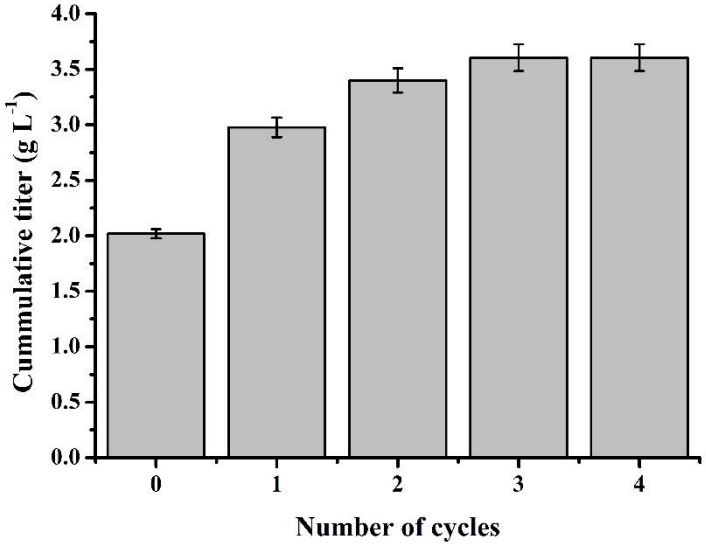

Fig. 5.5. Effect of *M. trichosporium* biomass recycling on methanol titer in high-pressure stirred tank reactor.

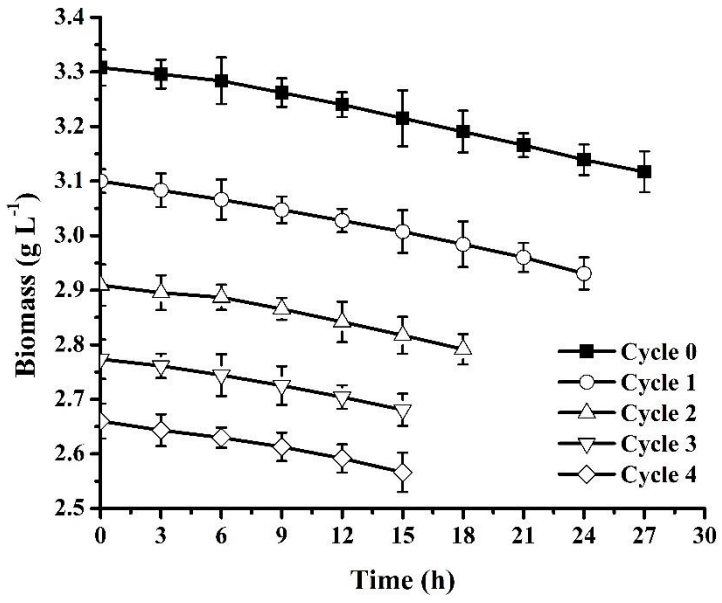

Fig. 5.6. Dynamic profile of biomass during biomass recycling in high-pressure stirred tank reactor.

Studies have reported recycling of methanotrophic biomass for up to 4-10 cycles of methanol production through oxidation of methane (pure or biogas-constituent) and reduction of CO_2 (Patel et al., 2022; Xin et al., 2007). For instance, Patel et al. (2023) reported cumulative methanol production of 64.6 mM (2.07 g L^{-1}) after six cycles of biomass reutilization in a co-culture of *M. sporium* and *M. bryophila* using biogas in presence of paraffin oil as methane vector. Another study reported methanol production in a co-culture of *M. tundrae* and *M. sporium* immobilized within magnetic nanoparticle-doped polymer using biogas (Patel et al., 2022). Following ten cycles of biomass reuse, the study resulted in a cumulative methanol titer of 70.74 mM (2.27 g L^{-1}). On the contrary, the present study reports a remarkably higher cumulative methanol titer following only three cycles of biomass reutilization through biological CO_2 reduction pathway. Limited studies have reported the effect of biomass recycling on methanol production using pure CO_2 as feed (Patel et al., 2018; Xin et al., 2007). Patel et al. (2018) reported a cumulative methanol titer of 0.52 mM (0.017 g L^{-1}) from pure CO_2 in immobilized *M. bryophila* following five batches of biomass recycling. It can be inferred that recent studies have relied on concomitant application of multiple process strategies such as, co-cultivation, cell immobilization, methane vector addition, repeated-batch culture, *etc.*, to improve methanol titer (Patel et al., 2023, 2022, 2020a). As opposed to the contemporary reports, the present study achieved significantly higher methanol titer under elevated operating pressure (4 bar) coupled with biomass recycling (3 cycles) in a stirred tank reactor, which is a much simpler approach, thus establishing the technological and economic viability of the process. Furthermore, to the best knowledge of the author, this is the first report demonstrating the effect of methanotrophic biomass recycling on methanol production under elevated operating pressure. Table 5.1 provides a comparison of studies reporting methanol production from different methanotrophic strains under varying process conditions and reactor types.

Table 5.1. Comparison of methanol production by methanotrophs under different process conditions and reactor types.

Methanotroph	Substrate	Process/Reactor specifications	Methanol yield	References
***Methylosinus trichosporium* IMV 3011**	CO_2: air (50:40)	Batch culture; 100 mL conical flask	0.004 µmol/mg dry cell weight	Xin et al., 2007
Methylosinus sporium	CO_2-air (30:70)	Batch culture; 120 mL serum bottle	0.33 mM	Patel et al., 2016
***Methylocystis bryophila* DSM 21852**	CO_2: air (15:85)	Covalent immobilization of cells on chitosan; Repeated-batch culture (5 cycles); 120 mL serum bottle	0.52 mM (0.017 g L^{-1})	Patel et al., 2018
Methylotuvimicrobium alcaliphilum	Methane: oxygen (1:1)	Fed-batch culture, 14 L fermenter	0.418 g L^{-1}	Kulkarni et al., 2021
***Methylosinus trichosporium* OB3b**	Methane: air (1:1)	Batch-mode with continuous feeding of methane-air mixture; Cylindrical reactor with circulation diffusion system (Total volume: 3 L, working volume: 1 L)	13.7 mM (0.44 g L^{-1})	Kim et al., 2010
***Methylocystis bryophila* DSM 21852**	Simulated biogas mixture of Methane: CO_2 (2:1)	Covalent immobilization of cells on chitosan; Repeated-batch culture (8 cycles); 120 mL serum bottle	25.75 mM (0.82 g L^{-1})	Patel et al., 2018
Methylocella tundrae	Biogas derived from anaerobic digestion of potato peels (30% methane)	Covalent immobilization of cells on banana leaves; Repeated-batch culture (8 cycles); 10 mL serum bottle	25.86 mM (0.83 g L^{-1})	Patel et al., 2021
***Methylocaldum sp.* 14B**	Biogas: air (1:2.5)	Trickle-bed reactor packed with ceramic balls (1.24 L)	0.9 g L^{-1} d^{-1}	Sheets et al., 2017
***Methylosinus trichosporium* OB3b**	Methane: oxygen (1:1)	Batch culture; Bubble-free membrane aerated bioreactor (Total volume: 500 mL, working volume: 300 mL)	0.95 g L^{-1}	Duan et al., 2011
Methanotrophic strains (AS1 and AS2)	Methane: air (50:50)	Batch and sequencing batch mode (5 cycles); External-loop airlift bioreactor (working volume: 1 L)	1.6 g L^{-1}	Ghaz-Jahanian et al., 2018

isolated from activated sludge				
Methylocystis bryophila	Methane: air (30:70)	Covalent immobilization of cells on coconut coir; Repeated-batch culture (8 cycles); 120 mL serum bottle	52.9 mM (1.69 g L^{-1})	Patel et al., 2020a
M. sporium* and *M. bryophila	Combination of biogas obtained through anaerobic digestion and dark fermentation of rice straw (30% CH_4 and 15% H_2)	Co-culture of cells; Repeated-batch culture (6 cycles); 13 mL serum bottle	64.6 mM (2.07 g L^{-1})	Patel et al., 2023
M. sporium* and *M. tundrae	Biogas obtained through anaerobic digestion of wheat straw (30% CH_4)	Co-culture of cells and immobilization in magnetic nanoparticle-doped polymers; Repeated-batch culture (10 cycles); 120 mL serum bottle	70.74 mM (2.27 g L^{-1})	Patel et al., 2022
***Methylosinus trichosporium* NCIMB 11131**	CO_2: air (1:1)	Repeated-batch culture (3 cycles); High-pressure stirred tank reactor (Total volume: 2 L; working volume: 1.2 L); Optimum operating pressure: 4 bar	112.4 mM (3.6 g L^{-1})	**This study**

Researchers have been working on different aspects of bioprocess to improve its economic feasibility at pilot scale. For instance, studies have reported the use of cheaper supports for cell immobilization, such as, banana leaves and coconut coir (Patel et al., 2021, 2020a). Similarly, biogas derived from anaerobic digestion of bio-wastes has been reported as an alternative feed to expensive pure gases (Patel et al., 2023). In the present study, an airlift reactor and a high-pressure stirred tank reactor have been designed. These could further be scaled-up for pilot-scale studies in potential industries such as oil-gas extraction, refineries, gas processing industries and chemical plants where large amounts of off-gases containing methane and CO_2 are available. The present study can offer a potential technology which can be an ideal solution to the industries, offering simultaneous sequestration of greenhouse gases and value-addition through methanol production. Moreover, the two reactors are designed to operate at room temperature, thus cutting-down the cost associated with maintenance of temperature, without compromising in yield and productivity.

5.3.3. Recovery of methanol from culture medium using distillation

To evaluate the application of the produced methanol as an alternative fuel, it was imperative to purify the methanol from the production medium. To that end, the culture supernatant was subjected to simple distillation to recover the methanol. The mixture appeared to boil slightly as soon as the temperature reached 60 °C. The distillate fraction containing methanol was obtained in the temperature range of 60-65 °C. Studies have reported a similar temperature range of 61-65 °C for the boiling of methanol-containing mixtures during distillation (Paulauskiene et al., 2019; Wang et al., 2020). At this stage, the purity of the distillate was estimated to be 91.17%. To further increase the concentration, distillate samples from multiple methanol production batches were pooled and subjected to a second round of distillation, yielding a purity of 94.74%. Jamrozik (2017) has demonstrated the use of 95% pure methanol (containing 5% water) as a blend with diesel for fuelling DI diesel engine.

Hence, the result obtained in the present study aligns well with the purity requirement for application of methanol as a diesel fuel blend. To the best knowledge of the author, this is the first study demonstrating the purification of methanotroph-derived bio-methanol using distillation.

5.4. Conclusions

In the second stage of the two-stage integrated process, elevation of headspace pressure in the reactor increased CO_2 solubility, leading to 235.6% increment in methanol titer, relative to atmospheric pressure. The present study aimed to cut-down the time and cost expended towards recurrent biomass production in first stage by employing biomass recycling strategy to reuse the biomass for multiple cycles of second stage and achieve a high cumulative methanol titer. Following three cycles of biomass reutilization, a maximum cumulative methanol titer of 3.6 g L^{-1} was achieved, a value significantly higher than other studies reported in literature. Methanol was recovered from cultivation medium using distillation attaining a maximum purity of 94.74%.

5.5. References

1. Amulya, K., Kopperi, H., Venkata Mohan, S., 2020. Tunable production of succinic acid at elevated pressures of CO2 in a high pressure gas fermentation reactor. Bioresour Technol 309, 123327. https://doi.org/10.1016/J.BIORTECH.2020.123327
2. Dinesha, P., Kumar, S., Rosen, M.A., 2019. Combustion, performance, and emissions of a compression ignition engine using Pongamia biodiesel and bioethanol. Environmental Science and Pollution Research 26, 8069–8079. https://doi.org/10.1007/s11356-019-04270-7
3. Duan, C., Luo, M., Xing, X., 2011. High-rate conversion of methane to methanol by Methylosinus trichosporium OB3b. Bioresour Technol 102, 7349–7353. https://doi.org/10.1016/J.BIORTECH.2011.04.096

4. Ghaz-Jahanian, M.A., Khoshfetrat, A.B., Hosseinian Rostami, M., Haghighi, M., 2018. An innovative bioprocess for methane conversion to methanol using an efficient methane transfer chamber coupled with an airlift bioreactor. Chemical Engineering Research and Design 134, 80–89. https://doi.org/10.1016/J.CHERD.2018.03.039
5. Jamrozik, A., 2017. The effect of the alcohol content in the fuel mixture on the performance and emissions of a direct injection diesel engine fueled with diesel-methanol and diesel-ethanol blends. Energy Convers Manag 148, 461–476. https://doi.org/10.1016/J.ENCONMAN.2017.06.030
6. Khan, O., Yadav, A.K., Khan, M.E., Parvez, M., 2021. Characterization of bioethanol obtained from Eichhornia Crassipes plant; its emission and performance analysis on CI engine. Energy Sources, Part A: Recovery, Utilization, and Environmental Effects 43, 1793–1803. https://doi.org/10.1080/15567036.2019.1648600
7. Kim, H.G., Han, G.H., Kim, S.W., 2010. Optimization of lab scale methanol production by Methylosinus trichosporium OB3b. Biotechnology and Bioprocess Engineering 15, 476–480. https://doi.org/10.1007/s12257-010-0039-6
8. Kim, M.S., Fitriana, H.N., Kim, T.W., Kang, S.G., Jeon, S.G., Chung, S.H., Park, G.W., Na, J.G., 2017. Enhancement of the hydrogen productivity in microbial water gas shift reaction by Thermococcus onnurineus NA1 using a pressurized bioreactor. Int J Hydrogen Energy 42, 27593–27599. https://doi.org/10.1016/J.IJHYDENE.2017.07.024
9. Kulkarni, P.P., Khonde, V.K., Deshpande, M.S., Sabale, T.R., Kumbhar, P.S., Ghosalkar, A.R., 2021. Selection of methanotrophic platform for methanol production using methane and biogas. J Biosci Bioeng 132, 460–468. https://doi.org/10.1016/J.JBIOSC.2021.07.007

10. Lopes, M., Gomes, N., Mota, M., Belo, I., 2009. Yarrowia lipolytica growth under increased air pressure: Influence on enzyme production. Appl Biochem Biotechnol 159, 46–53. https://doi.org/10.1007/s12010-008-8359-0

11. Lucile, F., Cézac, P., Contamine, F., Serin, J.P., Houssin, D., Arpentinier, P., 2012. Solubility of carbon dioxide in water and aqueous solution containing sodium hydroxide at temperatures from (293.15 to 393.15) K and pressure up to 5 MPa: Experimental measurements. J Chem Eng Data 57, 784–789. https://doi.org/10.1021/je200991x

12. Mukherjee, M., Goswami, G., Mondal, P.K., Das, D., 2020. Biobutanol as a potential alternative to petroleum fuel: Sustainable bioprocess and cost analysis. Fuel 278, 118403. https://doi.org/10.1016/J.FUEL.2020.118403

13. Patel, S.K.S., Gupta, R.K., Kalia, V.C., Lee, J.K., 2022. Synthetic design of methanotroph co-cultures and their immobilization within polymers containing magnetic nanoparticles to enhance methanol production from wheat straw-based biogas. Bioresour Technol 364, 128032. https://doi.org/10.1016/J.BIORTECH.2022.128032

14. Patel, S.K.S., Gupta, R.K., Kalia, V.C., Lee, J.K., 2021. Integrating anaerobic digestion of potato peels to methanol production by methanotrophs immobilized on banana leaves. Bioresour Technol 323, 124550. https://doi.org/10.1016/J.BIORTECH.2020.124550

15. Patel, S.K.S., Kalia, V.C., Joo, J.B., Kang, Y.C., Lee, J.K., 2020a. Biotransformation of methane into methanol by methanotrophs immobilized on coconut coir. Bioresour Technol 297, 122433. https://doi.org/10.1016/J.BIORTECH.2019.122433

16. Patel, S.K.S., Kalia, V.C., Lee, J.K., 2023. Integration of biogas derived from dark fermentation and anaerobic digestion of biowaste to enhance methanol production by methanotrophs. Bioresour Technol 369, 128427. https://doi.org/10.1016/J.BIORTECH.2022.128427

17. Patel, S.K.S., Kondaveeti, S., Otari, S. V., Pagolu, R.T., Jeong, S.H., Kim, S.C., Cho, B.K., Kang, Y.C., Lee, J.K., 2018. Repeated batch methanol production from a simulated biogas mixture using immobilized Methylocystis bryophila. Energy 145, 477–485. https://doi.org/10.1016/J.ENERGY.2017.12.142

18. Patel, S.K.S., Mardina, P., Kim, D., Kim, S.Y., Kalia, V.C., Kim, I.W., Lee, J.K., 2016. Improvement in methanol production by regulating the composition of synthetic gas mixture and raw biogas. Bioresour Technol 218, 202–208. https://doi.org/10.1016/J.BIORTECH.2016.06.065

19. Patel, S.K.S., Shanmugam, R., Kalia, V.C., Lee, J.K., 2020b. Methanol production by polymer-encapsulated methanotrophs from simulated biogas in the presence of methane vector. Bioresour Technol 304, 123022. https://doi.org/10.1016/J.BIORTECH.2020.123022

20. Paulauskiene, T., Bucas, M., Laukinaite, A., 2019. Alternative fuels for marine applications: Biomethanol-biodiesel-diesel blends. Fuel 248, 161–167. https://doi.org/10.1016/J.FUEL.2019.03.082

21. Renzi, M., Bietresato, M., Mazzetto, F., 2016. An experimental evaluation of the performance of a SI internal combustion engine for agricultural purposes fuelled with different bioethanol blends. Energy 115, 1069–1080. https://doi.org/10.1016/J.ENERGY.2016.09.050

22. Roger, M., Brown, F., Gabrielli, W., Sargent, F., 2018. Efficient Hydrogen-Dependent Carbon Dioxide Reduction by Escherichia coli. Current Biology 28, 140-145.e2. https://doi.org/10.1016/J.CUB.2017.11.050

23. Sahoo, K.K., Datta, S., Goswami, G., Das, D., 2022. Two-stage integrated process for bio-methanol production coupled with methane and carbon dioxide sequestration:

Kinetic modelling and experimental validation. J Environ Manage 301, 113927. https://doi.org/10.1016/J.JENVMAN.2021.113927

24. Sahoo, K.K., Goswami, G., Das, D., 2021. Biotransformation of Methane and Carbon Dioxide Into High-Value Products by Methanotrophs: Current State of Art and Future Prospects. Front Microbiol 12. https://doi.org/10.3389/FMICB.2021.636486
25. Schulz, A., Vogt, C., Richnow, H.H., 2012. Effects of high CO2 concentrations on ecophysiologically different microorganisms. Environmental Pollution 169, 27–34. https://doi.org/10.1016/J.ENVPOL.2012.05.010
26. Sheets, J.P., Lawson, K., Ge, X., Wang, L., Yu, Z., Li, Y., 2017. Development and evaluation of a trickle bed bioreactor for enhanced mass transfer and methanol production from biogas. Biochem Eng J 122, 103–114. https://doi.org/10.1016/J.BEJ.2017.03.006
27. Wang, Z., Paulauskiene, T., Uebe, J., Bucas, M., 2020. Characterization of Biomethanol–Biodiesel–Diesel Blends as Alternative Fuel for Marine Applications. Journal of Marine Science and Engineering 2020, Vol. 8, Page 730 8, 730. https://doi.org/10.3390/JMSE8090730
28. Wendlandt, K. -D, Jechorek, M., Brühl, E., 1993. The influence of pressure on the growth of methanotrophic bacteria. Acta Biotechnol 13, 111–115. https://doi.org/10.1002/ABIO.370130205
29. Xin, J.Y., Zhang, Y.X., Zhang, S., Xia, C.G., Li, S. Ben, 2007. Methanol production from CO2 by resting cells of the methanotrophic bacterium Methylosinus trichosporium IMV 3011. J Basic Microbiol 47, 426–435. https://doi.org/10.1002/JOBM.200710313

CHAPTER 6

Evaluation of methanol as a potential diesel fuel blend for fuelling four-stroke internal combustion engine

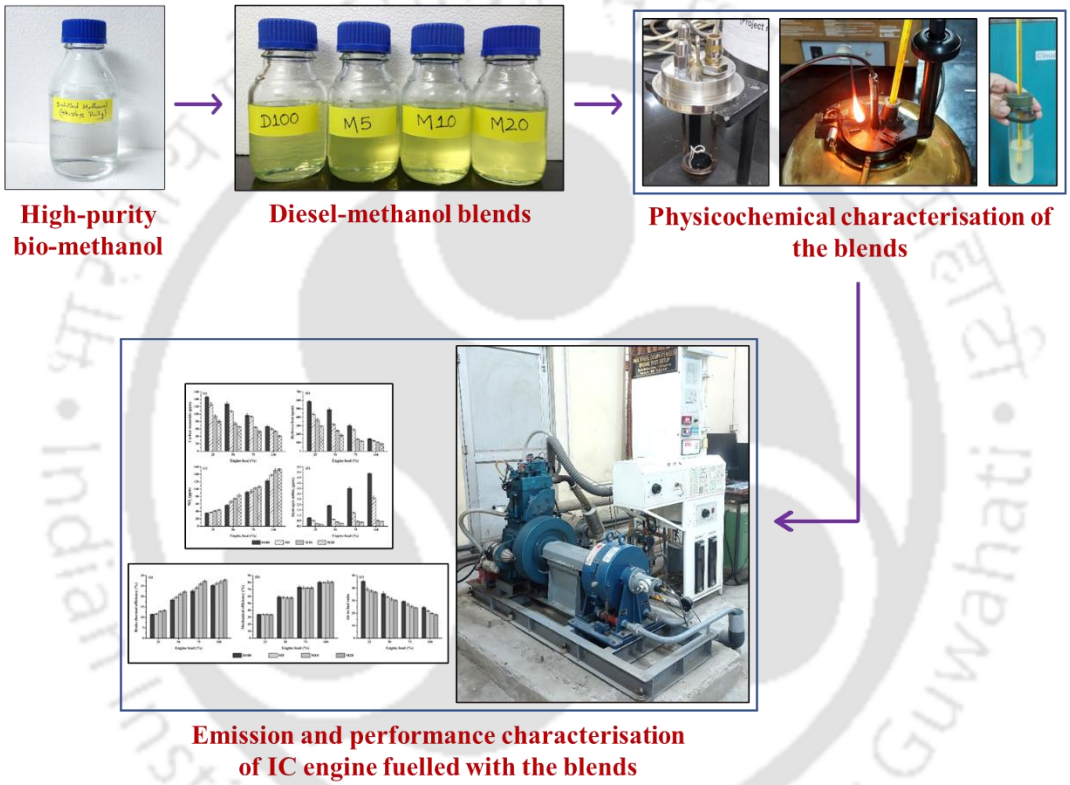

Fig. 6.1. Graphical abstract

6.1. Background and motivation

Rising energy demand, rapid depletion of non-renewable fossil fuel reserves, surging fuel prices, and environmental pollution, have driven the research focus towards exploring non-petroleum based cleaner and renewable alternatives. Alcohols are advantageous over diesel owing to their renewable characteristics, lower carbon and higher oxygen content (Chen et al., 2021a). Blending of alcohols with diesel has been reported to improve engine performance,

combustion characteristics, and reduction of environmental implications through improvement in emission characteristics (Zhang et al., 2022). Furthermore, methanol as a diesel additive is considered to be superior over ethanol and butanol in certain aspects such as: (a) lower viscosity which facilitates easier injection, spraying and atomization, (b) higher O_2 content (50%) which improves combustion characteristics, and (c) improved combustion leading to increased thermal efficiency, and reduced emissions of soot, hydrocarbon and carbon monoxide (Zhang et al., 2022). Hasan et al. (2021) reported the effect of varying methanol blend proportions (10-40%) with diesel fuel on the emission characteristics of 4-stroke DI diesel engine under varying load conditions. The emissions of smoke, CO and hydrocarbon decreased relative to pure diesel with increasing methanol percentage under each load condition. Another study reported improvement in engine performance in terms of brake specific fuel consumption and brake thermal efficiency with the use of 20% methanol blend with pure diesel (Vargün et al., 2022). Although many studies have reported the effect of diesel-methanol blends on the emission and performance characteristics of internal combustion (IC) engine, however, these are limited to commercially available methanol synthesized using conventional chemical routes, which have drawbacks of their own as described previously in Chapter 2. A few studies have demonstrated engine operation using bio-methanol synthesized through conventional biomass (wood, straw, energy crops, *etc.*) gasification, syngas reforming, preceding catalyst-driven conversion into methanol under high pressure and temperature, and thus are limited by constraints similar to that of chemical routes (Niculescu et al., 2019). The potential of bio-methanol produced through a completely biological methanotroph-based gas fermentation process, as an alternate renewable fuel, still remains unexplored.

Researchers have reported the application of other bio-alcohols as fuel in compression ignition (CI) and spark ignition (SI) engines. For instance, a study reported improvement in brake thermal efficiency, and reduction in brake specific fuel consumption and emissions of

carbon monoxide, hydrocarbon and NO_x, in a SI engine fuelled with a blend of *Mbwazirume* biomass-derived bio-ethanol (15%) and gasoline (Yusuf and Inambao, 2021). Similar outcomes in terms of engine performance and emission, have also been achieved in CI engine fuelled with a blend of diesel and bio-butanol (5-20%) produced through bacterial (*C. acetobutylicum*) fermentation of glucose derived from maize starch (Mukherjee et al., 2020). However, as described earlier in Chapter 5, most of these bio-alcohols are produced using agricultural crop or lignocellulosic biomass as feedstock (*e.g.*, sugarcane, maize and other sugar-rich plant biomass) (Dinesha et al., 2019; Renzi et al., 2016), which have raised the concern of biomass limitation and the controversial "food vs fuel" crisis. Furthermore, additional operational expenses are also incurred towards extraction of fermentable sugars (*e.g.*, glucose) from the agricultural/lignocellulosic biomass (through enzymatic hydrolysis) for ultimate conversion into bio-alcohols, such as bio-ethanol and bio-butanol, using suitable microorganisms (Khan et al., 2021; Mukherjee et al., 2020). Production of bio-methanol from methanotrophic bacteria overcomes these challenges through utilization of greenhouse gases (*viz.*, methane and CO_2) as carbon source, which not only circumvents the issue of biomass limitation, but also cuts down the cost associated with supply of expensive carbon substrates (*e.g.*, fructose, glucose and xylose). Therefore, it is quite intriguing to determine the potential of methanotroph-derived bio-methanol as an alternate transportation fuel, which has not been investigated till date.

The previous chapter reported a process engineering approach comprising elevation of operating pressure to enhance the solubility of CO_2 and increase its conversion into methanol. This was followed by recycling of methanotrophic biomass to achieve a high cumulative methanol titer of 3.6 g L^{-1}. Furthermore, employment of distillation resulted in recovery of 94.74% pure methanol. The present chapter demonstrates the application of methanotroph-derived bio-methanol as a potential diesel fuel blend, through analysis of physicochemical properties, and characterisation of emission and performance in a four-stroke internal

combustion (IC) engine, thereby establishing its suitability as a renewable alternate transportation fuel.

6.2. Materials and methods

6.2.1. Preparation of diesel-methanol blends

Methanol produced from methanotrophic CO_2 reduction was blended with commercial diesel in varying proportions (v/v) namely D100 (100% diesel+0% methanol), M5 (95% diesel+5% methanol), M10 (90% diesel+10% methanol), and M20 (80% diesel+20% methanol). The mixtures were magnetically stirred to attain homogeneity.

6.2.2. Physicochemical characterisation of blends

The blends were characterised for various physicochemical properties such as, density, kinematic and absolute viscosity, calorific value, flash point, fire point, cloud point and pour point, to evaluate their potential as alternative transportation fuel. Density of the blends was measured with 1 mL of sample using density meter (Anton Paar DMA 4500 M). Kinematic viscosity was estimated at 25 °C using U-tube viscometer with 40 mL of sample. Absolute viscosity was calculated using Eq. (6.1) (Mukherjee et al., 2020)

$$Absolute\ viscosity\ (\mu) = Kinematic\ viscosity\ (\nu) \times Density\ (\rho) \qquad (6.1)$$

Calorific value was estimated using bomb calorimeter (Toshniwal Technologies, India) with 1 mL of sample volume. Flash point and fire point were determined using Pensky Martens apparatus (Reico Equipment & Instrument, India) with 50 mL of sample.

Cloud point and pour point were measured in an apparatus, comprising of a glass tube, thermometer (-100 to 50 °C), air jacket, and chiller. The tube containing 50 mL of sample was placed inside the jacket enclosed within the chiller operating at -30 °C. Thermometer was positioned within the tube containing the sample to determine its temperature as the chiller cooled the sample gradually. Cloud point was denoted as the temperature at which the sample

started appearing foggy/cloudy. With further cooling, the sample froze and stopped flowing even when the tube was positioned horizontally. The corresponding temperature was identified as pour point.

6.2.3. Engine specifications and operation

The blends were evaluated for their effect on the emission and performance characteristics of a single cylinder, water-cooled, four-stroke internal combustion engine (TV1, Kirloskar, India) (Fig. 6.2), with detailed specifications presented in Table 6.1. A portable flue gas analyser (Testo 350, Germany) was connected to the engine for analysing the content of carbon monoxide (CO), nitrogen oxides (NO_x), hydrocarbon (HC) and sulfur oxides (SO_x) in the exhaust gas. A smoke meter was used to determine the smoke opacity. Different performance characteristics such as brake power, fuel consumption, brake specific fuel consumption, brake thermal efficiency, mechanical efficiency, air to fuel ratio, equivalence ratio and exhaust gas temperature were assessed while operating the engine with a single speed (1500 rpm) under varying load conditions (25-100%). Brake power, indicated power and fuel consumption (or fuel flow rate) were estimated using the engine performance analysis software – Engine soft. The exhaust gas temperature was determined through a thermocouple probe linked to the flue gas analyser.

Brake specific fuel consumption (BSFC, kg kW^{-1} h^{-1}) was calculated using Eq. (6.2)

$$BSFC = \frac{Fuel\ \text{consumption}}{Brake\ power} \qquad (6.2)$$

where, fuel consumption and brake power are expressed in kg h^{-1} and kW, respectively.

Brake thermal efficiency (BTE, %) was calculated using Eq. (6.3)

$$BTE = \frac{Brake\ power \times 3600}{Fuel\ \text{consumption} \times Calorific\ value} \times 100 \qquad (6.3)$$

where, calorific value is expressed in kJ kg^{-1}.

Mechanical efficiency (%) was calculated using Eq. (6.4)

$$Mechanical\ efficiency\ = \frac{Brake\ power}{Indicated\ power} \times 100 \quad (6.4)$$

where, indicated power is expressed in kW.

The experimental air to fuel ratio (AFR) was calculated using Eq. (6.5)

$$AFR\ = \frac{Air\ flow\ rate}{Fuel\ consumption} \quad (6.5)$$

where, air flow rate is expressed in kg h^{-1}.

Equivalence ratio (ϕ) was calculated using the following equations

$$\phi\ = \frac{AFR_{sbl}}{AFR} \quad (6.6)$$

$$AFR_{sbl}\ = \frac{\sum X_i \rho_i AFR_{si}}{\sum X_i \rho_i} \quad (6.7)$$

where, AFR is the actual (experimental) air to fuel ratio, AFR_s is the stoichiometric (theoretical) air to fuel ratio for different blends (bl), X is volume percentage (%), subscript i is methanol or diesel, and ρ is the density (kg m^{-3}).

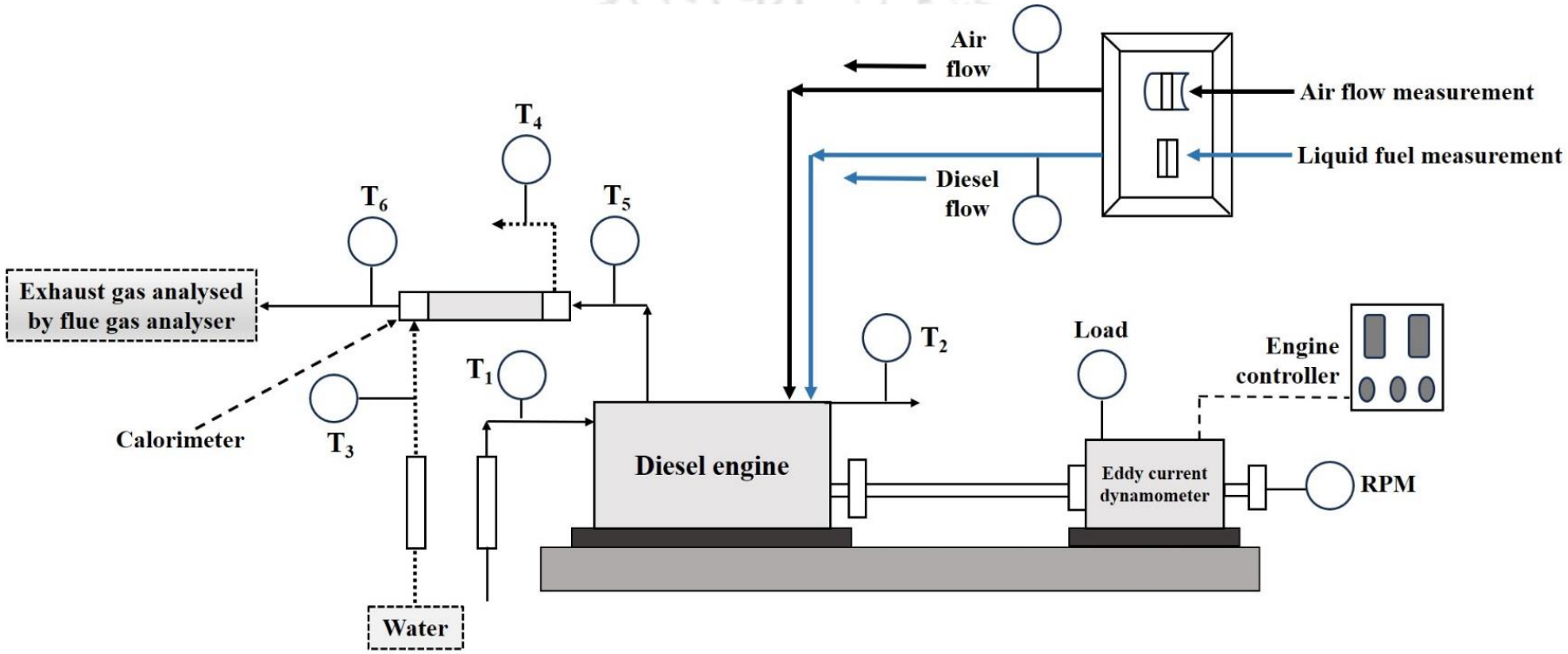

Fig. 6.2. Schematic diagram of four-stroke internal combustion engine set-up used for the characterisation of emission and performance.

Table 6.1. Specifications of the internal combustion engine.

Make and model	**Kirloskar, TV1**
Type	Single cylinder, 4-stroke, DI diesel engine
Coolant	Water
Rated power	5.2 kW (7 BHP) @ 1500 rpm
Swept volume	0.661 L
Bore × stroke	87.5×110 mm
Speed	1500 rpm (constant)
Compression ratio	17.5:1
Combustion chamber	Hemi-spherical bowl-in-piston type
Injection pressure	210 bar
Governor	Mechanical (centrifugal)
Dynamometer	Eddy current (Make: Saj; Model: AG10)
Fuel flow	Flow measuring unit (0-450 mL)
Air flow	Orifice meter and manometer
Load indicator and sensor	Model: AX-271, 0-50 kg, 230 V AC; Load cell, type strain gauge
Speed indicator and sensor	Digital; Type: non-contact
Temperature indicator and sensor	Digital, multipoint; K-type thermocouple
Rotameters	Engine cooling (40-400 LPH), calorimeter (10-100 LPH)
Software	Engine soft
Pressure transducer	
Make and type	PCB make, piezo-electric (15000 psi)
Crank angle sensor	360° encoder, Resolution: 2°
Resolution and response time	0.1 psi, 2 microseconds

6.3. Results and discussion

6.3.1. Evaluation of physicochemical characteristics of diesel-methanol blends

In order to evaluate the potential of methanol for blending with diesel as an alternate transportation fuel, the blends were characterised for various physicochemical properties such as, density, kinematic and absolute viscosity, calorific value, flash point, fire point, cloud point and pour point. The density, kinematic viscosity and absolute viscosity were observed to decrease progressively with the increase in blend proportion of methanol from 0 to 20% (Table 6.2). At 20% blending (M20), density, kinematic viscosity and absolute viscosity exhibited

decrements of 1.83, 28.8 and 30.5%, respectively, relative to D100. Lowering of density and viscosity of diesel owing to alcohol blending has been reported to improve spray characteristics of the blend resulting in homogenous air-fuel mixture, relatively complete combustion along with reduced combustion duration, and consequent reduction in particulate matter emission (Kumar et al., 2020). Researchers have reported decrease in noise level in CI engine fuelled with diesel-methanol blend attributed to reduced fuel viscosity and density (Hassan et al., 2021). Jamrozik (2017) reported densities of 836 and 831 kg m^{-3} for M10 and M20 methanol-diesel blends, respectively, which align well with the present study. Similarly, Wang et al. (2020) reported decrement in kinematic viscosity from 2.8 to 2.3 mm^2 s^{-1}, with the increase in methanol blending from 5 to 20% in a mixture of diesel containing 6.8% biodiesel. Moreover, with the addition of 5, 10 and 20% methanol, calorific values of diesel-methanol blends reduced marginally by 0.98, 1.68 and 2.34%, respectively, relative to D100 (Table 6.2). Calorific values of the blends were not much compromised, thus ensuring heat energy content nearly equivalent to D100. Similar results were reported by Hassan et al. (2021), wherein blending of 7-21% methanol in diesel led to minimal decrement of 0.18-0.29% in calorific values compared to pure diesel.

Table 6.2. Physicochemical characterisation of pure diesel and diesel-methanol blends.

Blends	**D100**	**M5**	**M10**	**M20**
Density (kg m^{-3})	845.6±0.18	837.7±0.19	835.3±0.18	830.1±0.17
Kinematic viscosity (mm^2 s^{-1})	3.02±0.03	2.68±0.02	2.46±0.01	2.15±0.01
Absolute viscosity (mPa s)	2.56±0.02	2.24±0.02	2.06±0.01	1.78±0.01
Calorific value (MJ kg^{-1})	44.76±0.01	44.32±0.01	44.01±0.01	43.71±0.01
Flash point (°C)	52±1.2	40±0.58	38	36±0.58
Fire point (°C)	58±0.58	44±1.2	41±0.58	38±0.58
Cloud point (°C)	-2.5±0.58	-5	-7±0.29	-9±0.29
Pour point (°C)	-8±0.29	-14±0.58	Less than -30	Less than -30

Flash point denotes the lowest temperature at which a flammable fuel vaporizes forming a mixture of vapour and air which can get ignited by an ignition source (*e.g.*, flame or spark) (Phoon et al., 2016). Fire point denotes the lowest temperature at which the vapour-air mixture catches fire and burns continuously even after the removal of the ignition source (Thangarasu and Anand, 2019). M5, M10 and M20 exhibited flash points and fire points in the ranges of 36 to 40 °C and 38 to 44 °C, respectively, which were substantially lower relative to pure diesel (Table 6.2). Flash point and fire point are primarily governed by the vapour pressure which determines the volatility of the fuel (Thangarasu and Anand, 2019). Hence, in the present study, the significant reduction in flash and fire points of the diesel-methanol blends could be attributed to higher vapour pressure of methanol (Phoon et al., 2016). Researchers have reported decrease in flash point from 40 to 20 °C, with the increase in methanol content from 5 to 30% in diesel-biodiesel blend (Wang et al., 2020). Lowered flash and fire points raise safety concerns associated with storage and transportation of the blends in hot climatic conditions. However, better flammability and easier ignition, improves their suitability as alternate transportation fuel in colder climate.

Moreover, cloud point and pour point are the fundamental cold flow properties of liquid fuels to evaluate their viability for application in automobile engines under low temperature conditions. The blends M5, M10 and M20 exhibited significantly reduced cloud points of -5, -7 and -9 °C, respectively, as compared to -2.5 °C for that of D100 (Table 6.2). Similarly, Wang et al. (2020) reported cloud points of -4, -12 and -13 °C for a blend of diesel and biodiesel containing 0, 5 and 10% methanol, respectively, which nearly align with the present study. On further cooling, D100 and M5 exhibited pour points at -8 and -14 °C, respectively. However, pour points could not be observed for M10 and M20 even after cooling up to -30 °C. This enormous decrement in the pour point of the blends containing 10-20% methanol could be attributed to the extremely low pour point of pure methanol, *i.e.*, -98 °C (Paulauskiene et al.,

2019). Similar observations were reported by Paulauskiene et al. (2019) wherein, pour point could not be determined in diesel-biodiesel blends containing 10-30% methanol due to persistence of fluidity in methanol-containing zones. Such exceptional cold flow characteristics of diesel-methanol blends corroborates their appropriateness as alternate transportation fuel in low temperature regions. To the best knowledge of the author, this is the first study reporting the cloud and pour points of methanol blends in pure diesel.

6.3.2. Evaluation of methanol as a potential diesel fuel blend in a four-stroke IC engine

Diesel-methanol blends were analysed for their effect on the emission and performance characteristics of a four-stroke diesel IC engine, under varying engine loads (25, 50, 75 and 100%), to evaluate their potential as alternate transportation fuel.

6.3.2.1. Emission characteristics

In order to study emission characteristics of IC engine running on diesel-methanol blends, the exhaust gas was assessed for the concentrations of carbon monoxide (CO), hydrocarbon (HC), nitrogen oxides (NO_x) and sulfur oxides (SO_x), and smoke opacity during the engine operation. Generation of CO occurs primarily due to incomplete combustion of fuel which results from oxygen-insufficiency in oxygen-deficient zones inside the combustion chamber during combustion of abundant fuel mixtures (Hasan et al., 2021). The highest CO emissions under each load condition occurred with the use of pure diesel (Fig. 6.3a). The emission of CO was observed to decrease with the increase in methanol blending from 0 to 20%. Compared to D100, use of M20 reduced CO emissions by 44.8, 48.4, 45.4 and 38.8% at the engine loads of 25, 50, 75 and 100%, respectively. This was attributed to high oxygen content in the methanol molecules, which increase with the increase in methanol blending percentage, causing complete fuel combustion (Zhang et al., 2022). Moreover, diesel-methanol blends are characterised by lower C/H ratio relative to D100, which favours the oxidation of CO into CO_2, thereby reducing CO emissions. Similar observations were reported by Jamrozik

(2017), where CO emissions reduced from 0.182 to 0.036 kg kW^{-1} h^{-1} with the increase in methanol blending from 0 to 40% with diesel. Furthermore, higher CO emissions were observed at lower engine loads (Fig. 6.3a), attributed to ineffective oxidation of CO due to the prevalence of lower temperature condition at lower load (Hasan et al., 2021).

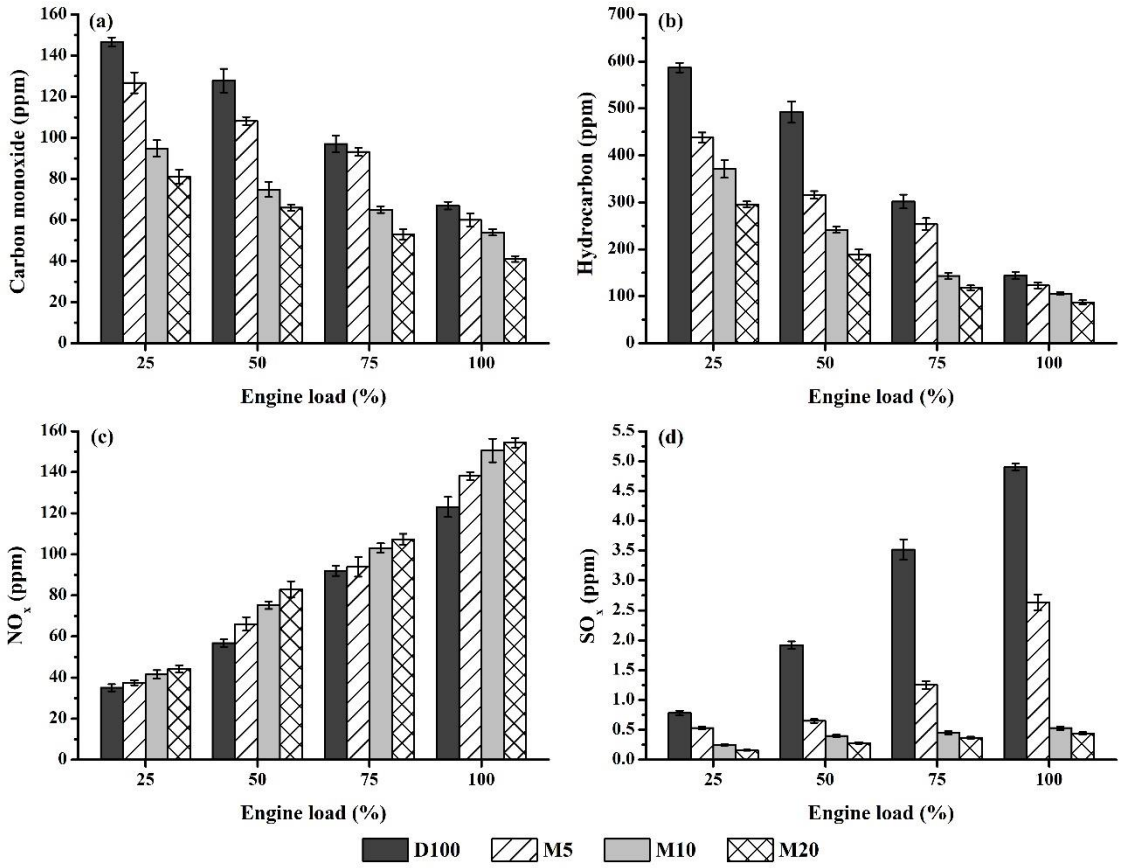

Fig. 6.3. Emissions of (a) carbon monoxide, (b) hydrocarbon, (c) NO_x and (d) SO_x from IC engine fuelled with D100, M5, M10 and M20 under varying load conditions.

Hydrocarbon emissions result from incomplete fuel combustion at low temperature which get disposed in vapour-form along with the exhaust gas (Vargün et al., 2022). HC emissions were found to decrease concomitantly with increasing methanol blending proportion (Fig. 6.3b), attributed to rise in O_2 content leading to complete combustion. Increase in methanol blending from 0 to 20%, reduced HC emissions by 49.6, 61.6, 60.9 and 39.8%, respectively, at corresponding loads of 25 to 100%. Studies have reported similar observations

attributed to reduction in fuel viscosity with increasing alcohol content, and consequent enhancement in spray and atomization properties, causing improved combustion and lowered HC emission (Zhang et al., 2022). Moreover, increasing load from 25 to 100% led to reduced HC emissions (Fig. 6.3b), owing to greater combustion temperature linked with higher engine load (Hasan et al., 2021).

NO_x emissions were observed to increase with increasing methanol content in the blends (Fig. 6.3c). Researchers have attributed this to reduced cetane number of diesel-methanol blends relative to D100, which elevates ignition delay causing upsurge in maximum cylinder pressure, and consequent increase in maximum cylinder temperature, thus leading to higher NO_x emission (Emiroğlu and Şen, 2018). O_2 content in the blends also contributes to elevation of maximum cylinder temperature. Rise in NO_x emissions with increasing engine load (Fig. 6.3c) could be attributed to increase in both fuel injection amount and cylinder temperature (Chen et al., 2021b; Emiroğlu and Şen, 2018). With the increase in methanol content from 0-20% in the blends, SO_x emissions reduced significantly by 79.6, 85.4, 89.5 and 91%, at loads of 25, 50, 75 and 100%, respectively (Fig. 6.3d). This could be attributed to dilution in sulphur content of the fuel owing to blending with sulphur-free methanol. Ampah et al. (2022) reported decrease in sulphur content of heavy fuel oil (marine diesel) from 1 to 0.45% (w/w) through blending with 30% methanol and 20% n-butanol. Another study reported substantial reduction in SO_2 emission with the blending of 10% methanol in diesel (Kumar et al., 2020), which corroborates the results in the present study. Furthermore, SO_x emission was observed to increase with increasing engine load (Fig. 6.3d), owing to increase in quantity of fuel injected into the combustion chamber (Fayad et al., 2022).

Smoke formation occurs as a result of fuel-rich regions undergoing incomplete combustion owing to deficiency of air inside the combustion chamber (Hasan et al., 2021). Fuel-rich zones form locally as a consequence of low volatility and high viscosity of fuel

leading to occurrence of large-sized droplets distributed unevenly (Dinesha et al., 2019). In the present study, smoke opacity was observed to decrease with increasing proportion of methanol blending (Fig. 6.4). For instance, 20% methanol blending reduced the smoke opacity by 27.5, 22.2, 22.7 and 21%, respectively, relative to D100 at corresponding loads of 25 to 100%. This could be attributed to increased volatility and reduced viscosity, along with higher oxygen content of the methanol-containing blends, favouring more complete combustion and reduced smoke emission.

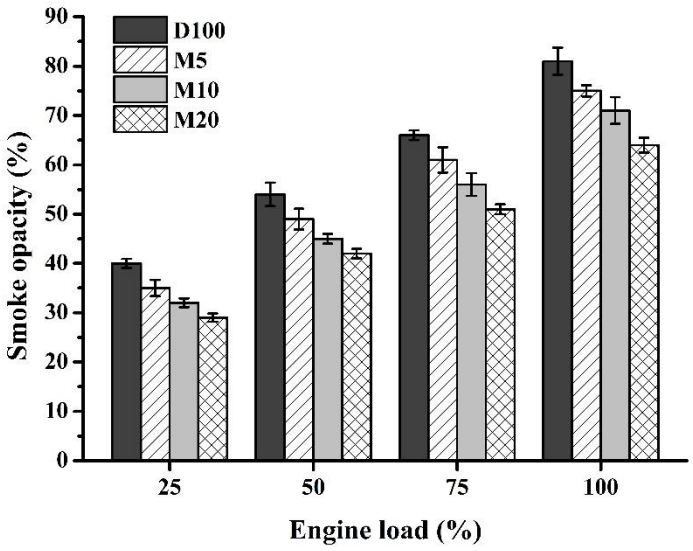

Fig. 6.4. Opacity of smoke produced from IC engine fuelled with D100, M5, M10 and M20 under varying load conditions.

6.3.2.2. Performance characteristics

Various parameters such as, brake power, fuel consumption, brake specific fuel consumption (BSFC), brake thermal efficiency (BTE), mechanical efficiency, air to fuel ratio (AFR), equivalence ratio and exhaust gas temperature were estimated to analyse the effect of diesel-methanol blends on the engine performance. Diesel-methanol blends exhibited brake power comparable with that of D100 (Fig. 6.5a). This could be attributed to the nearly equivalent calorific values of the blends and pure diesel (Table 6.2). Minimal losses (0.98-

2.34%) in the heating values resulting from blending with 5-20% methanol (Table 6.2), were deduced to be compensated by high O_2 content of alcohol resulting in improved combustion and thus equivalent brake power output (Campos-Fernández et al., 2012). Fuel consumption, and hence the directly proportional parameter, BSFC, were observed to decrease concomitantly with increase in methanol content (Fig. 6.5b, c). As methanol blending was increased from 0 to 20%, BSFC reduced by 12.0, 16.1, 16.4 and 7.92%, respectively, at corresponding loads of 25 to 100%. This could be attributed to the lower viscosity and density of diesel-methanol blends relative to pure diesel resulting in enhanced fuel atomization, which in addition to higher O_2 content, altogether lead to improved combustion (Campos-Fernández et al., 2012; Imtenan et al., 2014). The highest BSFC value (0.7 kg kW^{-1} h^{-1}) was obtained at 25% engine load with the use of D100, while lowest BSFC value (0.29 kg kW^{-1} h^{-1}) was obtained at 100% load using M20, which aligned well with literature (Hassan et al., 2021; Vargün et al., 2022). Further, the reduction in BSFC with increasing load (Fig. 6.5c) could be attributed to greater brake power output relative to fuel consumption at any given load (Vargün et al., 2022).

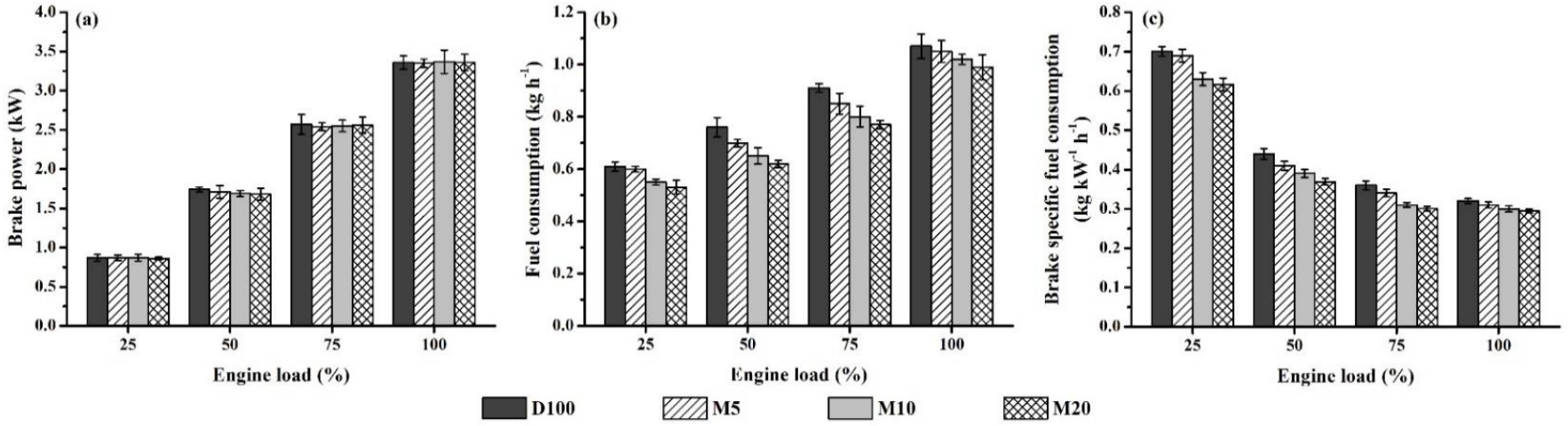

Fig. 6.5. (a) Brake power, (b) fuel consumption and (c) brake specific fuel consumption of IC engine operated with D100, M5, M10 and M20 under different load conditions.

BTE indicates the efficiency of conversion of chemical energy into mechanical energy as an outcome of fuel combustion inside the cylinder. BTE was observed to increase with increase in methanol blending percentage (Fig. 6.6a). Contextually, M20 exhibited 16.4, 21.2, 21.0 and 10.4% increments in BTE relative to D100, at 25, 50, 75 and 100% engine loads, respectively. Researchers have attributed this to the lowered cetane number of diesel-methanol blends which increases the ratio of pre-mixed and constant volume combustion and reduces heat loss (Zhang et al., 2022). Further, higher O_2 content, and improved atomization owing to lower viscosity of diesel-methanol blends, favour complete fuel combustion and hence enhance BTE (Chen et al., 2021b). Moreover, BTE was found to improve with increasing load (Fig. 6.6a), which is corroborated by similar studies (Hassan et al., 2021; Vargün et al., 2022). The present study attained a maximum of 28% BTE using M20 in IC engine operating at 100% engine load, which nearly aligns with other studies reporting about 35% BTE with M20 (Zhang et al., 2022), and 23.20% BTE at 6 Nm load with M21 (Hassan et al., 2021). Furthermore, mechanical efficiency being directly proportional to brake power, showed similar behavioural pattern as brake power with respect to changes in methanol blending percentage and engine load (Fig. 6.6b). Mechanical efficiency reportedly depends on combustion quality and energy generation from fuel (K et al., 2021). Thus, comparable mechanical efficiencies of diesel-methanol blends with that of D100, may be attributed to their nearly equivalent calorific values; or greater availability of O_2 in methanol-containing blends which improves fuel combustion thereby offsetting any deficit in calorific values. Maximum mechanical efficiency of 80.8% was attained with M10 which was comparable with other blends (79.95-80.77%) at 100% engine load. This is higher than the maximum mechanical efficiency (60-70%) reported for diesel-biodiesel blends containing 5-10% methanol (Rai et al., 2022).

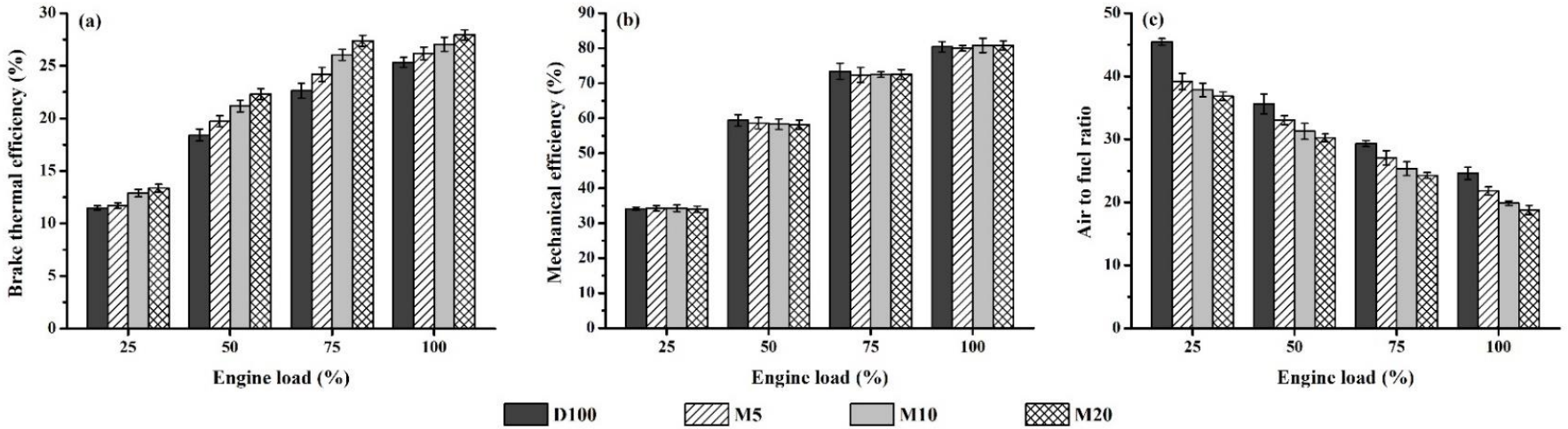

Fig. 6.6. (a) Brake thermal efficiency, (b) mechanical efficiency and (c) air to fuel ratio of IC engine fuelled with D100, M5, M10 and M20 under varying engine loads.

The stochiometric AFR for D100, M5, M10, M20 and pure methanol were theoretically estimated to be: 14.44, 13.65, 12.93, 11.69 and 6.5, respectively, as per Bayraktar (2008). Moreover, actual AFR was observed to decrease with increasing methanol blending proportion (Fig. 6.6c), attributed to lower stoichiometric AFR of methanol (Mat Yasin et al., 2014). The lower stoichiometric AFR of methanol is attributed to the higher content of molecular oxygen, which makes the methanol containing blends "leaner" mixtures (Bayraktar, 2008). Relative to D100, M20 reduced AFR by 19, 15.1, 17.2 and 23.7%, respectively, at corresponding loads of 25 to 100%. Lowered AFR of diesel-methanol blends reportedly improves combustion (Mat Yasin et al., 2014). Additionally, AFR reduced with increasing engine load, owing to increase in fuel injection quantity (Mukherjee et al., 2020). Equivalence ratio (ϕ) is defined as the ratio of stoichiometric AFR to the actual AFR (Li et al., 2021); wherein, $\phi > 1$, $\phi < 1$ and $\phi < 0.5$, denote rich, lean and ultra-lean fuel-air mixtures, respectively. Equivalence ratio was observed to reduce with the increase in methanol blending percentage (Fig. 6.7a). M20 led to leaning effect of 11.8, 6.5, 5.6 and 9.8%, respectively, at corresponding loads of 25, 50, 75 and 100%, as compared to pure diesel. The leaning effect of methanol is reported to improve the performance parameters of the engine (Bayraktar, 2008). Furthermore, exhaust gas temperature was observed to increase with increasing load and methanol content in the blend (Fig. 6.7b). A higher exhaust gas temperature indicates occurrence of faster rate of combustion inside the cylinder (Sayin et al., 2010, 2009). The impact of oxygen content and cetane number are predicted to be more predominant over latent heat of vaporisation and lower heating value of the methanol-containing blends, resulting in increased temperature (Canakci et al., 2009). This consequently leads to rise in NO_x emission with the increase in methanol blending proportion in the fuel (Fig. 6.3c).

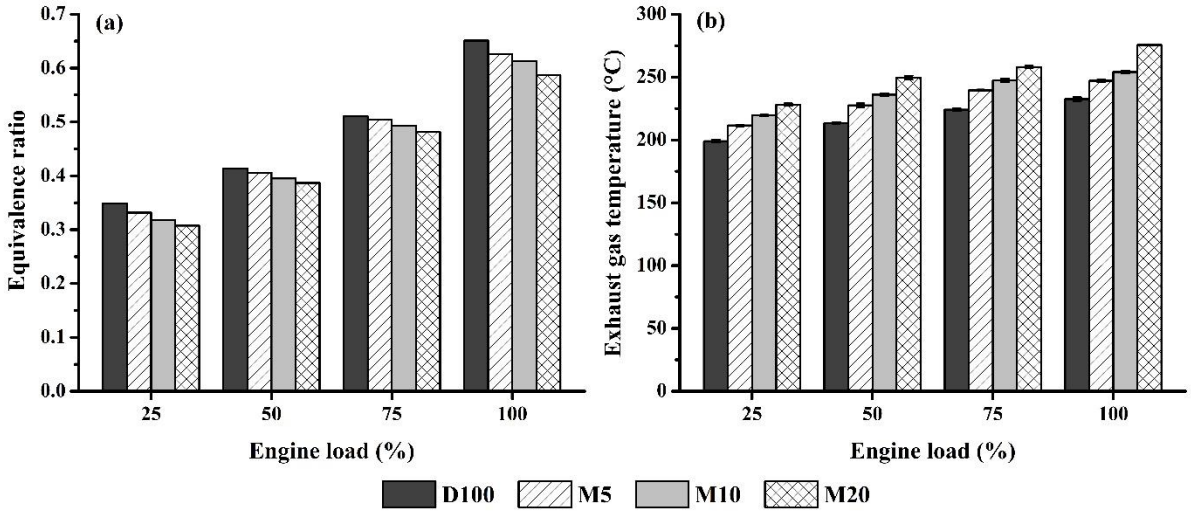

Fig. 6.7. (a) Equivalence ratio and (b) exhaust gas temperature in IC engine fuelled with D100, M5, M10 and M20 under varying engine loads.

To summarize, diesel-methanol blends exhibited physicochemical characteristics either superior or comparable to pure diesel. Methanol blending with diesel proved to improve engine characteristics in terms of CO, HC and SO_x emissions, and smoke opacity. Additionally, the blends outperformed D100 with respect to fuel consumption, BSFC, BTE, AFR and equivalence ratio, while delivering D100-equivalent output in terms of brake power and mechanical efficiency in IC engine. Hence, this study effectively demonstrates the suitability of methanotroph-derived bio-methanol as a potential diesel fuel blend for fuelling IC engine. Moreover, to the best knowledge of the author, this is the first study unveiling the potential of methanotrophic bio-methanol as a renewable alternative transportation fuel.

6.4. Conclusions

M. trichosporium-derived bio-methanol was demonstrated as a potential diesel fuel blend for fuelling IC engine. The effect of methanol blending on fuel properties and engine characteristics was most prominent with M20. Under varying engine loads, M20 reduced CO, HC and SO_x emissions by 38.8-48.4%, 39.8-61.6%, and 79.6-91.0%, respectively, and smoke opacity by 21.0-27.5%, relative to D100. Similarly, engine performance improved through

reduction in BSFC and enhancement in BTE by 7.92-16.4% and 10.4-21.2%, respectively. Furthermore, M20 reduced AFR by 15.1-23.7%, and equivalence ratio by 5.6-11.8%, making the combustion process leaner. High O_2 content of diesel-methanol blends compensated for the loss in calorific value delivering D100-equivalent brake power and mechanical efficiency.

6.5. References

1. Ampah, J.D., Liu, X., Sun, X., Pan, X., Xu, L., Jin, C., Sun, T., Geng, Z., Afrane, S., Liu, H., 2022. Study on characteristics of marine heavy fuel oil and low carbon alcohol blended fuels at different temperatures. Fuel 310, 122307. https://doi.org/10.1016/J.FUEL.2021.122307
2. Bayraktar, H., 2008. An experimental study on the performance parameters of an experimental CI engine fueled with diesel–methanol–dodecanol blends. Fuel 87, 158–164. https://doi.org/10.1016/J.FUEL.2007.04.021
3. Campos-Fernández, J., Arnal, J.M., Gómez, J., Dorado, M.P., 2012. A comparison of performance of higher alcohols/diesel fuel blends in a diesel engine. Appl Energy 95, 267–275. https://doi.org/10.1016/J.APENERGY.2012.02.051
4. Canakci, M., Sayin, C., Ozsezen, A.N., Turkcan, A., 2009. Effect of injection pressure on the combustion, performance, and emission characteristics of a diesel engine fueled with methanol-blended diesel fuel. Energy and Fuels 23, 2908–2920. https://doi.org/10.1021/ef900060s
5. Chen, S., Tian, J., Li, J., Li, W., Zhang, Z., 2021b. Investigation of the Performance and Emission Characteristics of a Diesel Engine with Different Diesel–Methanol Dual-Fuel Ratios. Processes 2021, Vol. 9, Page 1944 9, 1944. https://doi.org/10.3390/PR9111944
6. Chen, Z., He, J., Chen, H., Geng, L., Zhang, P., 2021a. Comparative study on the combustion and emissions of dual-fuel common rail engines fueled with

diesel/methanol, diesel/ethanol, and diesel/n-butanol. Fuel 304, 121360. https://doi.org/10.1016/J.FUEL.2021.121360

7. Dinesha, P., Kumar, S., Rosen, M.A., 2019. Combustion, performance, and emissions of a compression ignition engine using Pongamia biodiesel and bioethanol. Environmental Science and Pollution Research 26, 8069–8079. https://doi.org/10.1007/s11356-019-04270-7
8. Emiroğlu, A.O., Şen, M., 2018. Combustion, performance and emission characteristics of various alcohol blends in a single cylinder diesel engine. Fuel 212, 34–40. https://doi.org/10.1016/J.FUEL.2017.10.016
9. Fayad, M.A., Al-Ghezi, M.K.S., Hafad, S.A., Ibrahim, S.I., Abood, M.K., Al-Salihi, H.A., Mahdi, L.A., Chaichan, M.T., Dhahad, H.A., 2022. Emissions Characteristics and Engine Performance from the Interaction Effect of EGR and Diesel-Ethanol Blends in Diesel Engine. International Journal of Renewable Energy Development 11, 991–1001. https://doi.org/10.14710/IJRED.2022.45051
10. Hasan, A.O., Osman, A.I., Al-Muhtaseb, A.H., Al-Rawashdeh, H., Abu-jrai, A., Ahmad, R., Gomaa, M.R., Deka, T.J., Rooney, D.W., 2021. An experimental study of engine characteristics and tailpipe emissions from modern DI diesel engine fuelled with methanol/diesel blends. Fuel Processing Technology 220, 106901. https://doi.org/10.1016/J.FUPROC.2021.106901
11. Hassan, Q.H., Shaker Abdul Ridha, G., Hafedh, K.A.H., Alalwan, H.A., 2021. The impact of Methanol-Diesel compound on the performance of a Four-Stroke CI engine. Mater Today Proc 42, 1993–1999. https://doi.org/10.1016/J.MATPR.2020.12.247
12. Imtenan, S., Masjuki, H.H., Varman, M., Arbab, M.I., Sajjad, H., Rizwanul Fattah, I.M., Abedin, M.J., Abu, A.S., 2014. Emission and Performance Improvement Analysis of

Biodiesel-diesel Blends with Additives. Procedia Eng 90, 472–477. https://doi.org/10.1016/J.PROENG.2014.11.759

13. Jamrozik, A., 2017. The effect of the alcohol content in the fuel mixture on the performance and emissions of a direct injection diesel engine fueled with diesel-methanol and diesel-ethanol blends. Energy Convers Manag 148, 461–476. https://doi.org/10.1016/J.ENCONMAN.2017.06.030
14. K, S., Alagar, K., R, V.K., VJ, M.P., P, M., 2021. Performance and emission characteristics of diesel engine fueled with ternary blends of linseed and rubber seed oil biodiesel. Fuel 285, 119255. https://doi.org/10.1016/J.FUEL.2020.119255
15. Khan, O., Yadav, A.K., Khan, M.E., Parvez, M., 2021. Characterization of bioethanol obtained from Eichhornia Crassipes plant; its emission and performance analysis on CI engine. Energy Sources, Part A: Recovery, Utilization, and Environmental Effects 43, 1793–1803. https://doi.org/10.1080/15567036.2019.1648600
16. Kumar, V., Singh, A.P., Agarwal, A.K., 2020. Gaseous emissions (regulated and unregulated) and particulate characteristics of a medium-duty CRDI transportation diesel engine fueled with diesel-alcohol blends. Fuel 278, 118269. https://doi.org/10.1016/J.FUEL.2020.118269
17. Li, Y., Gao, W., Zhang, P., Fu, Z., Cao, X., 2021. Influence of the equivalence ratio on the knock and performance of a hydrogen direct injection internal combustion engine under different compression ratios. Int J Hydrogen Energy 46, 11982–11993. https://doi.org/10.1016/J.IJHYDENE.2021.01.031
18. Mat Yasin, M.H., Yusaf, T., Mamat, R., Fitri Yusop, A., 2014. Characterization of a diesel engine operating with a small proportion of methanol as a fuel additive in biodiesel blend. Appl Energy 114, 865–873. https://doi.org/10.1016/J.APENERGY.2013.06.012

19. Mukherjee, M., Goswami, G., Mondal, P.K., Das, D., 2020. Biobutanol as a potential alternative to petroleum fuel: Sustainable bioprocess and cost analysis. Fuel 278, 118403. https://doi.org/10.1016/J.FUEL.2020.118403

20. Niculescu, R., Clenci, A., Iorga-Siman, V., 2019. Review on the Use of Diesel–Biodiesel–Alcohol Blends in Compression Ignition Engines. Energies 2019, Vol. 12, Page 1194 12, 1194. https://doi.org/10.3390/EN12071194

21. Paulauskiene, T., Bucas, M., Laukinaite, A., 2019. Alternative fuels for marine applications: Biomethanol-biodiesel-diesel blends. Fuel 248, 161–167. https://doi.org/10.1016/J.FUEL.2019.03.082

22. Phoon, L.Y., Hashim, H., Mat, R., Mustaffa, A.A., 2016. Flash point prediction of tailor-made green diesel blends containing B5 palm oil biodiesel and alcohol. Fuel 175, 287–293. https://doi.org/10.1016/J.FUEL.2016.02.027

23. Rai, V.R., Shringi, D., Mathur, Y.B., 2022. Performance Evaluation of Diesel-Jatropha Biodiesel-Methanol Blends in CI Engine. Mater Today Proc 51, 1561–1567. https://doi.org/10.1016/J.MATPR.2021.10.374

24. Renzi, M., Bietresato, M., Mazzetto, F., 2016. An experimental evaluation of the performance of a SI internal combustion engine for agricultural purposes fuelled with different bioethanol blends. Energy 115, 1069–1080. https://doi.org/10.1016/J.ENERGY.2016.09.050

25. Sayin, C., Ilhan, M., Canakci, M., Gumus, M., 2009. Effect of injection timing on the exhaust emissions of a diesel engine using diesel–methanol blends. Renew Energy 34, 1261–1269. https://doi.org/10.1016/J.RENENE.2008.10.010

26. Sayin, C., Ozsezen, A.N., Canakci, M., 2010. The influence of operating parameters on the performance and emissions of a DI diesel engine using methanol-blended-diesel fuel. Fuel 89, 1407–1414. https://doi.org/10.1016/J.FUEL.2009.10.035

27. Thangarasu, V., Anand, R., 2019. Physicochemical fuel properties and tribological behavior of aegle marmelos correa biodiesel. Advances in Eco-Fuels for a Sustainable Environment 309–336. https://doi.org/10.1016/B978-0-08-102728-8.00011-5
28. Vargün, M., Yılmaz, lker T., Sayın, C., 2022. Investigation of performance, combustion and emission characteristics in a diesel engine fueled with methanol/ethanol/nHeptane/diesel blends. Energy 257, 124740. https://doi.org/10.1016/J.ENERGY.2022.124740
29. Wang, Z., Paulauskiene, T., Uebe, J., Bucas, M., 2020. Characterization of Biomethanol–Biodiesel–Diesel Blends as Alternative Fuel for Marine Applications. Journal of Marine Science and Engineering 2020, Vol. 8, Page 730 8, 730. https://doi.org/10.3390/JMSE8090730
30. Yusuf, A.A., Inambao, F.L., 2021. Effect of low bioethanol fraction on emissions, performance, and combustion behavior in a modernized electronic fuel injection engine. Biomass Convers Biorefin 11, 885–893. https://doi.org/10.1007/s13399-019-00519-w
31. Zhang, Z., Tian, J., Li, J., Lv, J., Wang, S., Zhong, Y., Dong, R., Gao, S., Cao, C., Tan, D., 2022. Investigation on combustion, performance and emission characteristics of a diesel engine fueled with diesel/alcohol/n-butanol blended fuels. Fuel 320, 123975. https://doi.org/10.1016/J.FUEL.2022.123975

CHAPTER 7

Conclusions

A two-stage integrated bioprocess was demonstrated for bio-methanol production using *Methylosinus trichosporium* NCIMB 11131 coupled with the sequestration of methane and carbon dioxide. Improved biomass titer, biomass productivity and methane fixation rate of 4.45 g L^{-1}, 0.872 g L^{-1} d^{-1} and 0.476 g L^{-1} d^{-1}, respectively, were achieved through optimization of critical physicochemical parameters, *viz.*, methane concentration, gas flow rate and composition of other limiting nutrients in the growth medium, in a semi-batch stirred tank reactor. Selection of appropriate process design for methanol production from CO_2, and optimization of CO_2 concentration in the headspace and liquid to headspace volume ratio in an air-tight batch reactor led to an improved methanol titer of 0.58 g L^{-1}. Biomass titer in the first stage was constrained by the key challenge of mass transfer limitation of methane from gas to liquid phase. Methanol titer in the second stage was found to be critically dependent on the partial pressure of carbon dioxide in the headspace of batch reactor. A combinatorial process engineering strategy was employed to the two-stage integrated bioprocess for improved biomass and methanol production. Use of micro-sparger, engagement of draft tube and supplementation of mass transfer vector in airlift reactor addressed the key challenge of mass transfer and solubility limitations of methane in the first stage. Maximum biomass titer, biomass productivity and methane fixation rate attained were 7.68 g L^{-1}, 1.459 g L^{-1} d^{-1} and 0.795 g L^{-1} d^{-1}, respectively, exhibiting corresponding improvements of 72.6%, 67.32% and 67.02%, compared with the two-stage process without process engineering strategy. In the second stage, elevation of headspace pressure (up to 4 bar) in high-pressure stirred tank reactor

increased CO_2 solubility, resulting in an improved methanol titer of 1.98 g L^{-1}, which was an increment of 235.6%, relative to atmospheric pressure. Furthermore, the present study aimed to cut-down the time and cost expended towards biomass production in first stage by employing biomass recycling strategy to reuse the biomass for multiple cycles of second stage and achieve a high cumulative methanol titer. Following three cycles of biomass reutilization, a maximum cumulative methanol titer of 3.6 g L^{-1} was achieved, a value significantly higher than other studies reported in literature. Methanol was recovered from cultivation medium using distillation attaining a maximum purity of 94.74%.

M. trichosporium-derived bio-methanol was demonstrated as a potential diesel fuel blend for fuelling internal combustion (IC) engine. The effect of methanol blending on fuel properties and engine characteristics was most prominent with M20 (blend of 20% methanol and 80% diesel, v/v). Under varying engine loads, M20 reduced CO, HC and SO_x emissions by 38.8-48.4%, 39.8-61.6%, and 79.6-91.0%, respectively, and smoke opacity by 21.0-27.5%, relative to D100. Similarly, engine performance improved through reduction in BSFC and enhancement in BTE by 7.92-16.4% and 10.4-21.2%, respectively. Furthermore, M20 reduced AFR by 15.1-23.7%, and equivalence ratio by 5.6-11.8%, making the combustion process leaner. High O_2 content of diesel-methanol blends compensated for the loss in calorific value delivering D100-equivalent brake power and mechanical efficiency. Hence, this study effectively demonstrates the suitability of methanotroph-derived bio-methanol as a potential diesel fuel blend for fuelling IC engine. Moreover, to the best knowledge of the author, this is the first study unveiling the potential of methanotrophic bio-methanol as a renewable alternative transportation fuel.

The present study highlights and answers key solutions to some of the major bottlenecks through:

- Optimisation of critical physicochemical parameters, design of appropriate reactor systems, and application of novel process engineering strategies towards overcoming the challenges associated with limited mass transfer and solubility of methane and CO_2, thereby improving the production of biomass and methanol.
- Improvement in methanol titer facilitating its recovery from fermentation medium, thereby making it suitable for further application, *e.g.*, as a biofuel.
- Demonstration of methanotroph-derived bio-methanol as a transportation fuel, thereby providing an alternative to methanol synthesized via non-sustainable chemical routes, as well as petroleum-based non-renewable fuels.

The two-stage integrated bioprocess reported in the present study possesses potential to be implemented in industries (*e.g.*, refineries, oil-gas extraction industries, gas processing and chemical plants) for sustainable sequestration of CO_2 and CH_4 present in exhaust off-gases and flare gases, offering an eco-friendly biological route for decarbonization, and value-addition through bio-methanol production, a renewable alternate transportation fuel.

Scope for further investigation

- Scale-up of the combinatorial process engineering strategies in the first and second stages to evaluate commercial scale methanol production along with product recovery.
- Techno-economic assessment of the two-stage integrated bioprocess for methanol production coupled with the sequestration of methane and CO_2.
- Evaluation of the strain's potential towards multiproduct biorefinery to develop a sustainable technology.
- Understanding the biosynthesis pathways and appropriate metabolic engineering for improvement in yield of methanol, and sequestration of methane and CO_2.

List of publications

Patent from thesis work

1) **Krishna Kalyani Sahoo**, Ankan Sinha and Debasish Das. Apparatus and method for enhanced production of methanol. (Application No. 202231054522, **Granted on 28 August 2023**, Patent No. 447607).

Research articles from thesis work

1) **Sahoo, Krishna Kalyani**, Swagata Datta, Gargi Goswami, and Debasish Das. "Two-stage integrated process for bio-methanol production coupled with methane and carbon dioxide sequestration: Kinetic modelling and experimental validation." *Journal of Environmental Management* 301 (2022): 113927. https://doi.org/10.1016/j.jenvman.2021.113927. (Impact factor: 8.7).
2) **Sahoo, Krishna Kalyani,** Ankan Sinha, and Debasish Das. "Process engineering strategy for improved methanol production in *Methylosinus trichosporium* through enhanced mass transfer and solubility of methane and carbon dioxide." *Bioresource Technology* 371 (2023): 128603. https://doi.org/10.1016/j.biortech.2023.128603. (Impact factor: 11.4).
3) **Sahoo, Krishna Kalyani**, and Debasish Das. "Enhanced methanol production from recycled methanotrophic biomass for fuelling four-stroke internal combustion engine." *Fuel* (Under review).

Review articles

1) **Sahoo, Krishna Kalyani,** Gargi Goswami, and Debasish Das. "Biotransformation of methane and carbon dioxide into high-value products by methanotrophs: current state

of art and future prospects." *Frontiers in Microbiology* 12 (2021): 636486. https://doi.org/10.3389/fmicb.2021.636486. (Impact factor: 5.2).

2) **Sahoo, Krishna Kalyani**, John Kiran Katari, and Debasish Das. "Recent advances in methanol production from methanotrophs." *World Journal of Microbiology and Biotechnology* 39, no. 12 (2023): 360. https://doi.org/10.1007/s11274-023-03813-y. (Impact factor: 4.1).

List of conferences

1) **Krishna Kalyani Sahoo** and Debasish Das. Two-stage integrated process for bio-methanol production coupled with methane and carbon dioxide sequestration. North-East Research Conclave (NERC)-2022, 20-22nd May 2022, held at Indian Institute of Technology Guwahati, India (Poster Presentation).
2) **Krishna Kalyani Sahoo** and Debasish Das. Optimization of two-stage integrated process for bio-methanol production with concomitant fixation of methane and carbon dioxide. Research & Industrial Conclave Integration 2023, 14-16th May 2023, held at Indian Institute of Technology Guwahati, India (Oral Presentation).
3) **Krishna Kalyani Sahoo** and Debasish Das. Process engineering strategy for improved methanol production in *Methylosinus trichosporium* through enhanced mass transfer and solubility of methane and carbon dioxide. International Conference on Petroleum, Hydrogen & Decarbonization (ICPHD 2023), 03-05th November 2023, held at Indian Institute of Technology Guwahati, India (Oral Presentation).

Vitae

The author was born in an Odia household on 13th March 1995 in Cuttack, Odisha, India. She passed her higher secondary education by qualifying through All India Senior School Certificate Examination (AISSCE) from Kendriya Vidyalaya No.1, Bhubaneswar, in 2012. She completed her Bachelor of Technology in Biotechnology from Odisha University of Technology and Research (formerly College of Engineering and Technology), Bhubaneswar, in 2016. She did her Master of Technology in Biotechnology from National Institute of Technology Rourkela, in 2018.

Krishna Kalyani Sahoo joined the Ph.D. programme in December 2018 under the supervision of Prof. Debasish Das in Department of Biosciences and Bioengineering, Indian Institute of Technology Guwahati, Assam, India. She received Junior and Senior research fellowships from the Ministry of Education, Government of India. She successfully completed all the academic courses with a Cumulative Performance Index of 9.60/10. She presented her Ph.D. synopsis on 06th October 2023 in an open seminar and submitted the Ph.D. thesis in January 2024. She presented her final viva-voce seminar in May 2024.